Addis Ababa University

አዲስ፡አበባ፡ዩኒቨርሲቲ

SEEK WISDOM, ELEVATE YOUR INTELLECT AND SERVE HUMANITY !

# STABILITY ASSESSMENTS ON THE SELECTED RESERVOIR SLOPES OF AJIMA EARTH DAM NORTH SHOA, CENTRAL ETHIOPIA

Demessie Mulu Eneyew

A Thesis Submitted to School of Earth Sciences

Presented in Partial Fulfillment of the Requirements for the Degree of Master of Science in Geological Engineering (Engineering Geology)

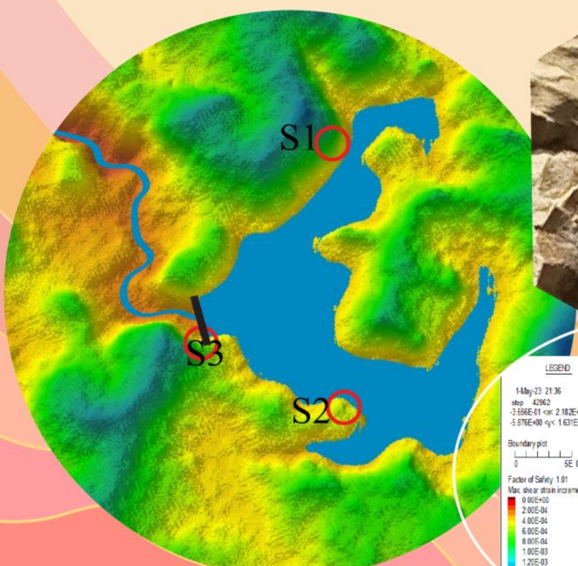


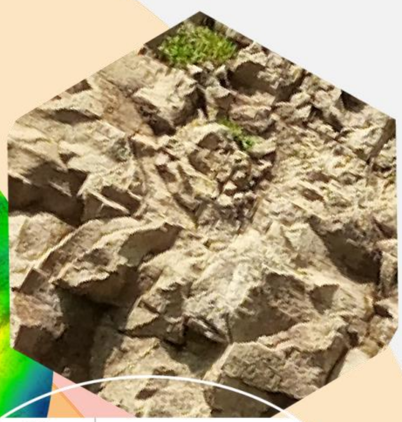

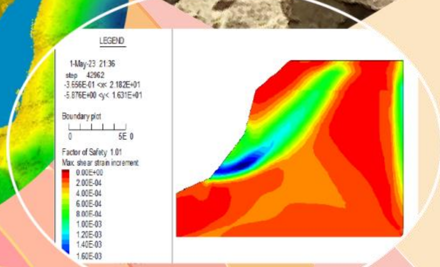


Addis Ababa, Ethiopia

JANUARY, 2024

COLLEGE OF NATURAL AND COMPUTATIONAL SCIENCES

SCHOOL OF EARTH SCIENCE

Thesis Submitted in Partial Fulfillment of the Requirements of the Degree of Master of Science in Geological Engineering (Engineering Geology)

# STABILITY ASSESSMENTS ON THE SELECTED RESERVOIR SLOPES OF AJIMA EARTH DAM NORTH SHOA, CENTRAL ETHIOPIA

A Thesis Presented By:

Demessie Mulu Eneyew

Advisor:

Trufat Hailemariam [PhD]

ADDIS ABABA, ETHIOPIA

JANUARY, 2024

# DECLARATION

I the undersigned, declare that this thesis is my own work and has not been presented for a degree at any other university for the award of any degree program and each and every source of information utilized in the thesis work has been properly credited. The thesis work was carried out under the close supervision of Trufat Hailemariam (PhD).

Engineering Geology, Addis Ababa University

Name of candidate of MSc holder:

Demessie Mulu Eneyew



Signature: ________

This is to certify that the above declaration made by the candidate is correct to the best of our knowledge and it has been submitted for examination with our approval as university advisors.

| Advisor Name: | Signature | Date |
|---|---|---|
| Trufat Hailemariam [PhD] | ________ | Dec 20/2023 |

# SIGNATURE PAGE

Addis Ababa University

School of Graduate Studies

This is to certify that the thesis prepared by DEMESSIE MULU ENEYEW, entitled on: Stability assessments on the selected reservoir slopes of Ajima earth dam North Shoa, central Ethiopia. *Using Numerical Model, Finite Difference Method,* and presented in a partial completion of the criteria for the degree of Master of Science in Engineering Geology (Geological Engineering). The paper complies with university policies and satisfies recognized standards for quality and originality.

**Signed by the Examining Committee:**

Examiner ______________________ Signature ____________ Date ______________

Examiner _____________________ Signature _____________ Date_______________

Advisor _____________________ Signature ______________ Date_______________

________________________________________________

Chair of School or Graduate Program Coordinator

# ABSTRACT

Stability assessments on the selected reservoir slopes of Ajima dam North Shoa, central Ethiopia

This study was conducted in the Ajima Chacha earthen dam area in North Shoa, central Ethiopia. The study aimed to assess the stability of three critical slopes selected in the dam reservoir. These slopes were selected based on their geometry, steepness of slopes, slope material weathering conditions, rockmass discontinuity, and lithology type, which makes them prone to failure. The failure of these slopes can lead to significant problems in the dam reservoir, which is why assessing their stability is crucial for ensuring the safety of the dam.

To conduct the stability analysis, a comprehensive field investigation was undertaken, and rock and soil samples were collected from the selected slopes for testing in the laboratory. The input parameters obtained from these tests were used in the slope analysis carried out using Fast Lagrangian Analysis of Continuum (FLAC2D) and DIP software. However, FLAC2D was mainly used for stability analysis in this research.

The Kinematics analysis was conducted on the upper section of RS-1, which is located on a highly fractured and weathered rhyolite unit and toppling failure type is shown from the DIP analysis. The slope analysis of the entire section of RS-1, RS-2, and RS-3 was done using FLAC2D. The FOS (Factor of Safety) for RS-1, RS-2, and RS-3 was 1.63, 1.42, and 1.32, respectively, under static dry conditions. Under static saturated conditions, the FOS for RS-1, RS-2, and RS-3 was 0.99, 1.12, and 1.24, respectively. Since the FOS (Factor of Safety) for slope one (RS-1) under static saturated conditions was less than one which indicating instability and measures should be taken to stabilize the existing slope. Furthermore, evaluating the dam reservoir slopes' stability under seismic conditions would provide a better understanding of dam safety in the long term.

**Keywords**: Ajima Chacha; Slope Stability; Kinematic Analysis; Finite Difference Method; FLAC 2D; Insitu tests; factor of safety.

# ACKNOWLEDGEMENTS

Glory to the Almighty GOD for his eternal help and allow his spirit to lead me righteousness throughout my life. Basically, thesis work cannot be carried out alone. In this regard, I want to acknowledge the individuals, institutions and organizations which contributed to the completion of this thesis.

I am very much thankful to Dr. Trufat Hailemariam, for his proficient supervision and make this work possible with his fatherly approach and scientific guidance. He had taken efforts in refining my understanding of the research work through constructive comments from the scratch to the better completion of this work in this manner. This has made me confident to independently carry out my future research work in geological engineering.

I would like to give special thanks to Mr. Ahmed Heredin for his assistance in technical issue of geotechnical software during my thesis work. My deepest gratitude also goes to batch MSc candidates Suwalih Nurhusen for his inspiration to have deep focus with time on my thesis work. My sincerest gratitude is to my beloved parents for their constant encouragement, help and support to achieve this goal in all ways. I would not have been able to complete the thesis work, without the helps and encouragements of the above listed persons.

During completion of this study, I came across significant institution and organization, I am grateful in recognizing the following institutions and organizations: Addis Ababa University (for funding the research work), Amhara design and supervision work enterprise (ADSWE) (for providing geotechnical report of the dam investigations). THANK YOU ALL.

# TABLE OF CONTENTS

Contents Page No.

# LIST OF FIGURES

LIST OF PLATES

# LIST OF TABLES

# LIST OF ABREVATIONS AND SYMBOLS

| | |
|---|---|
| *a* | Hoek–Brown material constant |
| ADSWE | Amhara Design and Supervision Work Enterprise |
| ASTM | American Society for Testing and Materials |
| CR | Critical slope |
| D | Disturbance factor |
| DEM | Digital Elevation Model |
| EARS | East Africa Rift System |
| E | Deformation modulus |
| FDM | Finite-Difference Method |
| FEM | Finite Element Method |
| FOS | Factor of Safety |
| G | Shear modulus |
| GIS | Geographic Information System |
| GSI | Geological Strength Index |
| GWC | Groundwater condition |
| GWT | Groundwater table |
| ISRM | International Society of Rock Mechanics |
| Jv | Volumetric Joint, |
| K | Bulk modulus |
| $m_b$ | Hoek–Brown material constant (rock mass) |
| MER | Main Ethiopian Rift |
| mi | Hoek–Brown material constant (intact rock) |
| MRMS | Medium Rock Mass Strength |

| | |
|---|---|
| NMC | Natural moisture content |
| PI | Plasticity Index |
| R | Mean Schmidt Hammer rebound value |
| RQD | Rock quality designation |
| RMR | Rock mass rating |
| RMS | Rock mass strength, |
| s | Hoek–Brown material constant |
| SSR | Shear-Strength Reduction |
| UCS | Uniaxial Compressive Strength |
| Ѵv | Poisons ratio |

# CHAPTER 1 : INTRODUCTION

## 1.1 Background

Slope instability is a complex phenomenon that can occur at many scales and for many reasons. Large and micro dams were constructed in Ethiopia which is very important to improve the economy of the peoples through their multipurpose. However, most of the dams in different parts of the country were constructed in highly weathered, fractured volcanic rocks and sedimentary terrains. These dams have faced engineering geological problems such as leakage, reservoir siltation, and slope instability without giving their desired purposes (Haregeweyn *et al*., 2006; and Berhane *et al*., 2013). Geological weak layer, slope geometries, and high degree of weathering of geologic materials of the slope, human activity, heavy precipitation (saturation) and seismicity which can significantly trigger the slopes movement (Basahel and Mitri, 2018).

Geological factors for slope instability occur through the geological structures such as joints and faults can form slip surfaces which leads to failure of the slope (Fell *et al*., 2005). Hence those factors that will increase the shear stress or reduce the shear strength to have a high possibility of creating the slope failure. Any change of saturation of slope, would result in a reduced factor of safety by reducing shear strength of the slope material (Alex Jacob1 *et al*., 2018). It is a fact that safety of the dam doesn't depend only on the proper design and construction, also monitoring the dam and its surrounding reservoir slopes is important during the life of the dam. Additionally, the shear strength of the rock mass is dramatically decreased by the water and geological conditions of the slope materials, which significantly affect the instability of the reservoir slope (Hou *et al*., 2018). Engineering geological assessments play a great role in the evaluation of the safety of reservoir slope. The finite difference method analyzes the stability conditions of the slopes in terms of factor of safety (FOS), and stress-strain behaviour of the geologic materials (Kanungo *et al*. 2013). It is necessary to analyze and identifying the potential driving forces and triggering factors to avoid dam slope failure casualties (Kaya, 2017; Kumar *et al*., 2017).

The Ajima dam area mainly covered with weathered and fractured rhyolite rock and weak welded tuff rock with moderate to highly weathering degree. In addition, residual clay soil is covering the upper slope surface in some local of the dam rim slopes. Thus, the reservoir slopes failure might cause and possibly trigger by a combination of geological, geomorphological, surface water, presence of weak layers, weathered and friable slope materials like tuff rock and residual soils in the reservoir slopes. The aforementioned conditions have motivated the researcher to conduct this research and evaluate the reservoir slopes of Ajima dam to come up with better understanding and solutions based on the slopes analysis results.

Various techniques have been used to investigate and identify the critical slopes on the Ajima reservoir slopes, and the necessary data were collected. Field investigation on the selected slopes including slopes geometry, geologic structural and slope inclination, rockmass characterizations using GSI method, Schmidt rebound tests, and laboratory tests of soil and rock materials were done to obtain input parameters for the stability analysis. RS-1 has upper section comprising jointed and weathered rhyolite rock underlay by weak tuff rock. RS-2 has moderately weathered tuff rock underplayed by weak highly weathered tuff rock. RS-2 slope sections exist directly below the quarry site. On RS-2 the slope faces slight failure due to the disturbance of upper quarry activity and seepage from quarry logged water directly above the natural slope surface and wetting on the slope face. RS-3 selected critical slope is found on the left abutment of the dam axis comprising residual clay soil underlay by decomposed tuff soil.

In this study, the analysis of slope stability has been done using finite difference method and kinematic analysis which provides better insight for the critical slopes condition. The analyses under different slope condition are highly significant in the evaluation and safety measures of the reservoir slopes. FLAC 2D can give an output to understand the deformation and failure mechanisms of the critical slopes with safety factor value. The results obtained from the slopes analyses provide solutions for practical slopes stability measurements on the sensitive slopes.

## 1.2 Problem Statement

The saturation of the reservoir slopes in the Ajima Chacha zoned earthen dam brings significant changes on the reservoir slope stability of slopes comprising weathered rocks, weak and friable geologic materials. Slope geometry, presence of weak geologic structures, weak layer, leak water through weak zones to the slope face from directly above logged water of quarry site greatly affect the reservoir slopes. Some of the slopes have faced slight failure problem or preexisting slight failure. Moreover, the rain water can change the slope conditions by saturating and reducing the shear strength of the slope materials. Slope failure phenomenon might occur on the reservoir slopes comprising of weak and weathered slope geologic materials.

Compared to other modeling approaches Finite difference method (FDM), FLAC 2D has good capability of showing the deformation behavior and the displacement effect of slope materials that consists of rock and soil properties in the slopes numerical model analysis (Vardakos *et al*., 2007; Young *et al*., 2017). However, reservoir rim slope stability investigations is not done till the completion of this research work in Ajima dam reservoir slopes (ADSWE, 2016). Moreover, previous research works on Ajima dam were on "Characterization and Suitability Analysis of Embankment Material" (Wondirad, 2021), "Geotextile reinforcement possibility on embankment dam" (Hiwot, 2019). Therefore, this research departs from others by emphasizing on rim slope stability and the analyses were carried out by finite difference method, FLAC2D.

## 1.3 Objectives

### 1.3.1 General objective

The primary objective of this research is to assess the stability of the selected reservoir slopes on Ajima dam using kinematic analysis and Finite Difference Method (FDM).

### 1.3.2 Specific objectives

- ✓ Delineate full water level of the Ajima dam reservoir
- ✓ Identify the critical reservoir slopes for slope analysis
- ✓ Characterizing the geologic materials of the critical slopes
- ✓ Estimate the geomechanical properties of the geo-materials through empirical correlations
- ✓ Carryout stability analysis on the selected reservoir slopes
- ✓ Identifying the triggering factors and forward appropriate safety measurements for the sensitive slopes based on the modelling results

## 1.4 Scope of the study

This study is a step towards assessing slope stability. This study has geographically focused on Ajima dam reservoir slopes, conceptually on slope stability analysis. Methodologically it employed finite difference method, FLAC 2D and kinematic approaches, DIP software. The field investigation, insitu measurements and laboratory tests on the field slopes and samples collected from these critical slopes have been used for slope analysis.

## 1.5 Research relevance

The relevance of this research is manifold. The slope analysis in the present study illustrates the deformation behavior of the slopes with its factor of safety value under static dry and saturated conditions. The analysis outputs on the critical slopes are highly relevant to insight safety condition and to respond problems on the critical reservoir slopes. In addition, this study adds knowledge and information about the dam safety under different slope conditions, in which future researchers can use it as related input references for additional study on the dam area.

## 1.6 Limitation of the Study

Representative input values for FLAC2D software are highly important, but determining Young's modulus and Poison's ratio in triaxial test is very expensive. Thus, empirical correlation has been used based on previous literature works and matching the properties of rock mass and soils with the standard ranged values accordingly. The lack of laboratory test results for these testes has limited the precision of the numerical analysis. Furthermore, the analysis requires a better computer performance for fine mesh generation and large slope section to process quickly with the increase of accuracy of slope safety factor.

## 1.7 Ajima dam status

The Ajima-Chacha earthen dam is designed to have 45 m high and 371 m long. The capability of dam is holding 55 million cubic meter of water and 2.54 km upstream extension of reservoir water (ADSWE, 2016). Currently the dam axis construction is on the stage of 18-20m high from the foundation of the dam.

## 1.8 Conceptual framework for the study

The flow chart shows step wise procedures from the data collection techniques and slope analysis methods to come out on the conclusion approaches for the slope analysis.

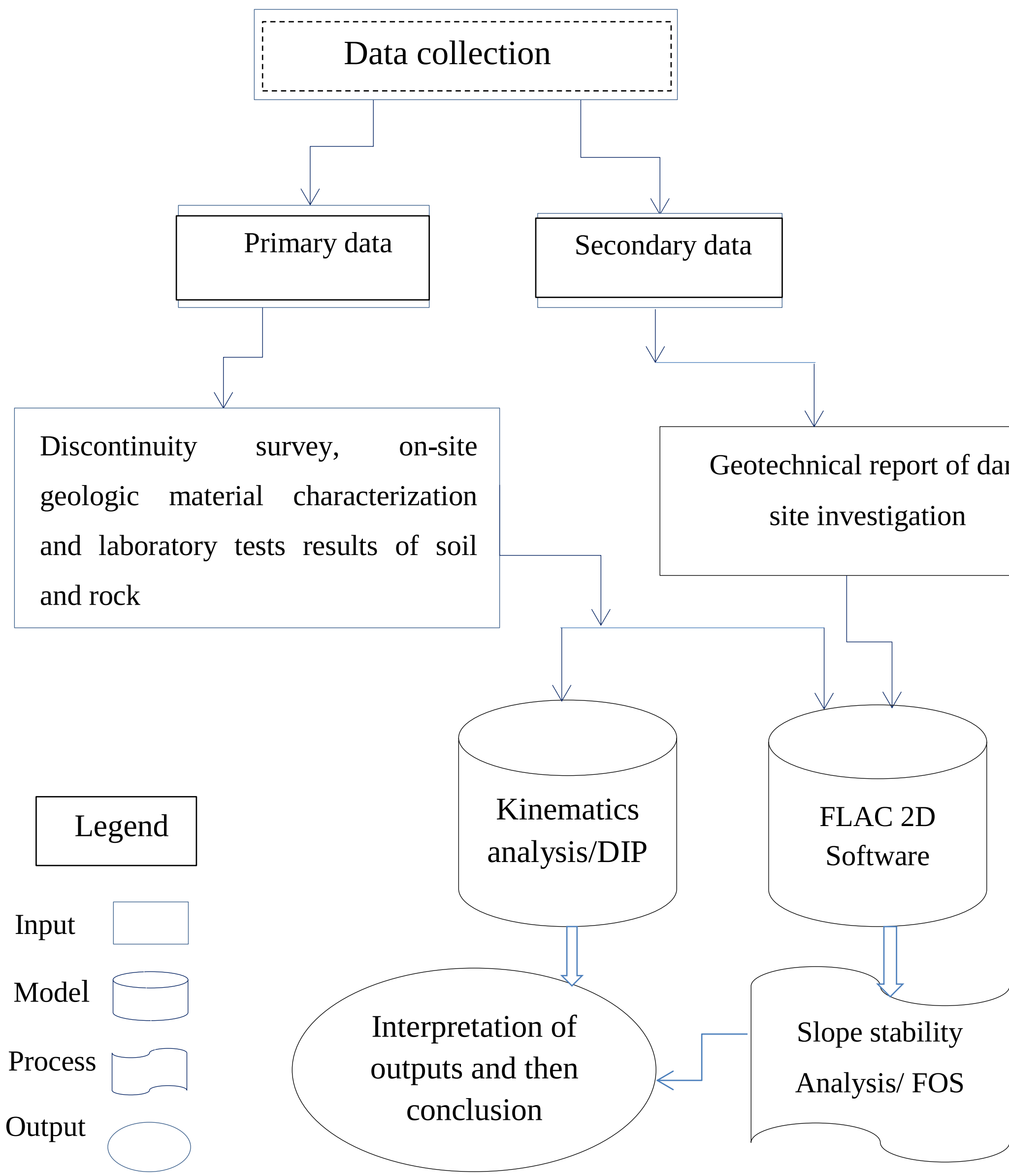


Figure 1-1: Summary of the flow chart for critical slope stability analyses

## 1.9 Organization of the thesis

This thesis is organized into six Chapters. The first Chapter highlights the introduction and justification to the current study in relation with the reservoir slope stability problem and geological and geotechnical conditions of the study area.

Chapter two delves into the description of the study area (accessibility, physiographic setting, geology, climate & rain fail, and seismicity of the area). Present the detail description of regional and local geologic setting, which are important for slope analysis.

Chapter three discusses the relevant literatures by drawing from previously researches on the selection of critical slopes, and rock mass classification, empirical correlation of rockmass geomechanical properties, and methods of stability analysis of the slope.

Chapter four describes the methodology and organization of the synthesized data obtained from on-site field investigation, laboratory works and empirical estimation of the geomechanical properties of rock and soil. Use those parameters as input data of the rock and soil for the slope analysis.

Chapter five has addressed the analysis, presentation of output results, and interpretation of the analysed data obtained from, DIP software, and FLAC 2D software. Moreover, the chapter presents the results of the FLAC 2D contour plot which is sensitive slope materials on the critical slopes.

Chapter six discusses on the conclusions and recommendations draws for possible safety measurements of reservoir slopes based on the results obtained in critical slope analysis.

* * * * * * * * * * *

# CHAPTER 2 : DESCRIPTION OF THE STUDY AREA

## 2.1 Introduction

This chapter deals with the description of study area accessibility and its geology, seismicity, topographic, climatic, topography, drainage density, and geotechnical issues of the study area, which influences the reservoir slope instability.

## 2.2 Location and accessibility

The study area is suited in the northwestern Ethiopian Plateau, located in the western margin of Main Ethiopian Rift (MER) Amhara regional state's north Shoa zone, Angolelana Tera Woreda, specifically at Kitalegn kebele. Chacha is Woreda town in North Shoa which has latitude: $9^{0}31'48''$ North, longitude: $39^{0}27'36''$ East and elevation: 2774m, within a zone of 37P. The geographic coordinate on the dam axis is: latitude: $9^{0}29'15''$ and longitude: $39^{0}31'49''$ with the elevation: 2810m a.m.s.l. (see Figure 2-1**).** The study area is accessible through Addis Ababa - Debre birhan main asphalt road, then turning to the East direction from Chacha town, and then driving about 15km along the concrete road from the Woreda town of Chacha to the dam site (ADSWE, 2016).

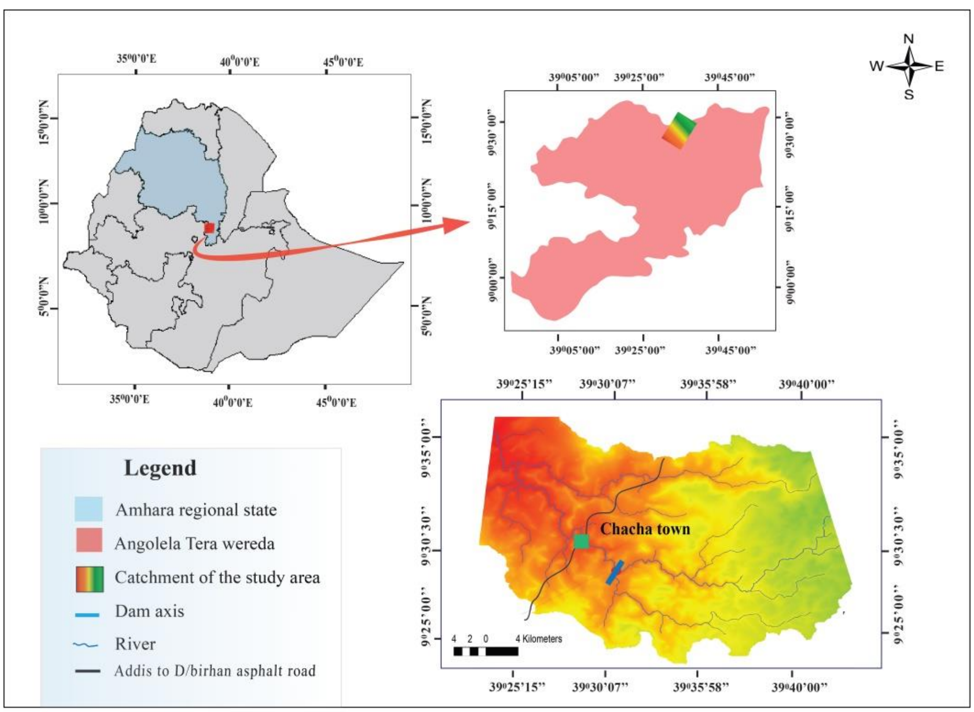


Figure 2-1: Location map of Ajima earthen dam site

## 2.3 Climate of the study area

The north western plateau of the country is characterized by having relatively heavy rainfall. Ajima dam area is situated far away around 15km in the East direction from Chacha town. The dam area has approximately similar physiographic feature and elevation (town: 2774 m, and dam site: 2810m a.m.s.l) (ADSWE, 2016). There is no meteorological station within the catchment region, thus the climate data of Chacha station was used to illustrate the temperature and rainfall conditions to the dam area (locality).

The kiremit season (June15 to Sep15) has intensive rainfall, with monthly rainfall 290mm precipitation in August, and in bega season there is low rainfall in (November to January) (5 mm precipitation in December). In addition, the maximum and lowest temperatures referring from Chacha meteorological stations are 22.3 in June and 7.4 degrees Celsius in December, (Source: Climate data: Chacha, Ethiopia - Climate & Monthly weather forecast (weather-atlas.com)). The wettest month (highest rainfall) is August (290mm). The driest month (least rainfall) is December (5mm accumulation of precipitation). The month with the highest number of rainy days is August (29.9 days). The month with the least rainy days is December (5.3 days) (Source: Climate data: Chacha, Ethiopia - Climate & Monthly weather forecast (weather-atlas.com)) (see Figure 2-2).

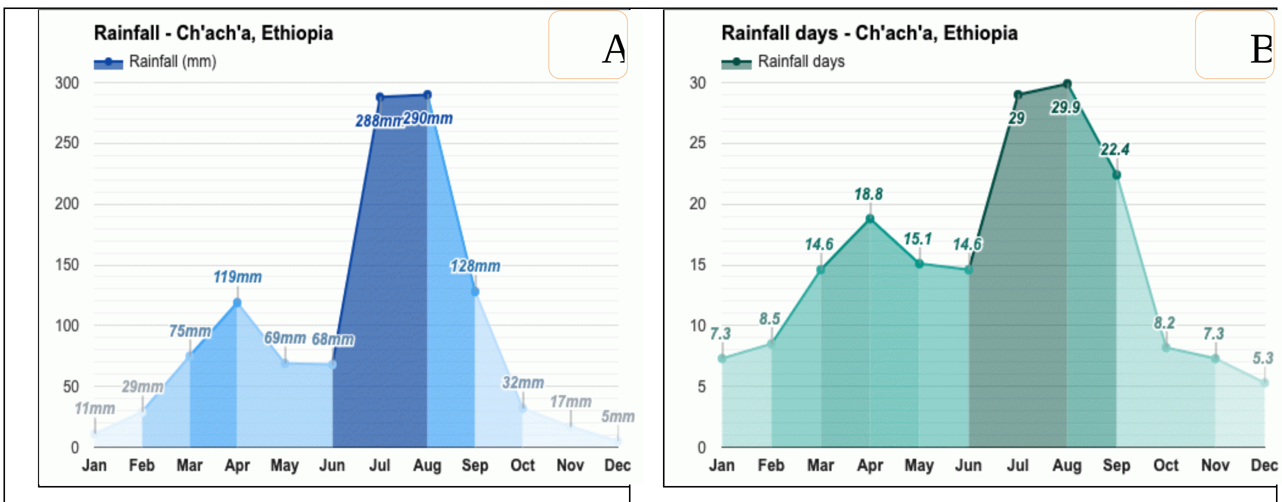


Figure 2-2: A) monthly average rainfall value of Chacha, B) number of rainfall days in each month for Chacha town and its neighboring area.

## 2.4 Topography of the study area

The study area situate on the northwestern plateau adjacent with the western margin of Main Ethiopian Rift. These are the results of plume related volcanism, and the area is dominated with gentle to moderate slope. Around 70% of the dam's catchment is located between 2850 and 2786 meters above sea level. Around 83.22 percent of the upper catchment has a slope value of less than 15 degree (ADSWE, 2016). As a result, unlike other predisposing factors, moderately steep topography has less effect on large slope failure in the study area. The physiography of the dam region is illustrated below (see Figure 2-3).

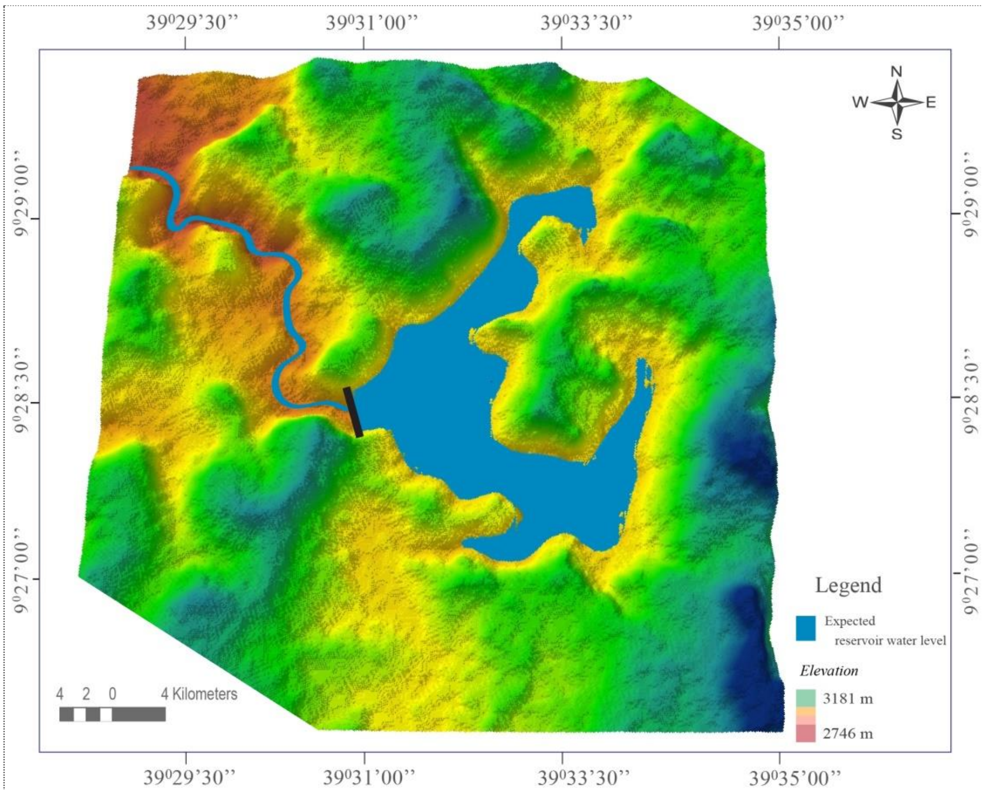


Figure 2-3: Physiographic maps of the dam reservoir area 3D maps (Arc Scene 10.8).

## 2.5 Drainage of the study area

The drainage system of the area is dominantly contributing to the Abay river basin though there is minor portion of the Awash basin in the extreme east (ADSWE, 2016). There are two major drainage lines above the dam site, which generally shows dendritic patterns (see Figure 2-4). The study area has a stream catchment area of about 83km$^2$ (ADSWE, 2016). Drainage of the river is southward for a length of around 150 km into plains of central plateau and finally joins the river Abay (Blue Nile).

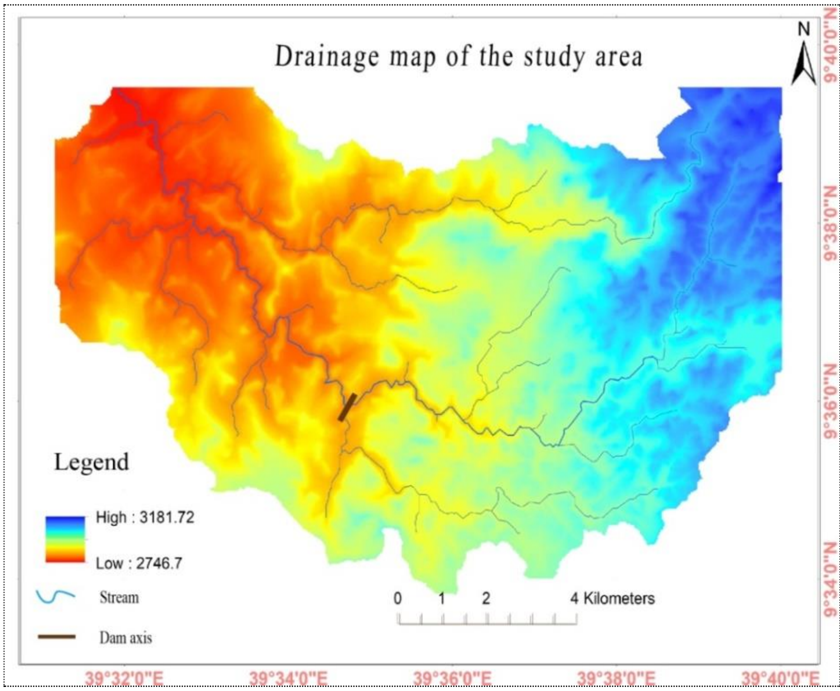


Figure 2-4: Drainage of whole catchment with in the study area

## 2.6 Soil formations

Predominantly two types of soil formations cover the extent of the study area. These include medium plastic clay alluvial soil, and residual soil, which is deposited from weathering of volcanic rocks of rhyolitic and tuff rock formations (ADSWE, 2016). In the dam region landslide movements become low due to relatively thin soil formation on the steep slopes of the dam reservoir slopes.

## 2.7 Geology of the study area

Regional geology of the dam area has been illustrated based on the previous research works and reports. Local geological information in the Ajima dam site is necessary. Acquiring such local geologic data has been done during the site survey and the local geology was elaborated based on the rock formations, lithologic type, rockmass discontinuity, and degree of weathering.

### 2.7.1 Regional Geology and tectonic setting

The East African Rift System is a Miocene-Quaternary intracontinental extensional system composed of several interacting rift segments. The Main Ethiopian Rift is the northernmost sector of the East African Rift System; connecting this continental rift to the oceanic spreading centers of the Red sea and Gulf of Aden (Bonini *et al*., 2005, and Corti *et al*., 2009). The Paleozoic rocks in the Ethiopian geology were removed by a large-scale uplift and subsequent erosion in most areas. Then during the Mesozoic era a regional epeirogenesis sinking of the crust commenced on most part of the land that is currently occupied by Ethiopia and Somalia. This crustal sinking was followed by two major transgression and regression cycles (Kazmin *et al*., 1980) from the Indian Ocean in a general north westerly direction, resulted in the deposition of thick successions of detrital and chemical sediments directly over the Precambrian basement rocks.

Following the late Mesozoic - early Tertiary transgression of the Indian Ocean, a large-scale epierogenic uplift of the Afro Arabia was commenced (Kazmin *et al*., 1980). This regional uplift and thermal erosion of the Tertiary period caused deep rooted fracturing of the crust accompanied by long lasting volcanic activity that produced the Ethiopian continental flood basalt province. The upraised and up arched crust fissuring under tension permitted the ascension of voluminous basaltic magma estimated as 300,000 $km^3$ to form the trap series of the Ethiopian Plateau (Mohr, 1983). Theses basaltic rocks overlie the Mesozoic sediments and at places the Precambrian rocks depending on the level of erosion. It is therefore believed that the Ethiopian plateau is underlain at depth by Precambrian rocks of the Afro-Arabian Shield (Mohr, 1983).

### 2.7.2 Tarmaber-Megezez Formation

Megezez formation is one of the Mid Miocene age volcanic centers in western Ethiopian plateau formed as shield volcano, northwestern sector of main Ethiopian rift (part of Tarmaber formation). Megezez shield has age of 10.5 Ma (Wolfendene, 2004 and Kieffer *et al*., 2004).

According to Mohr & Zanettin (1988) and Merla *et al*., (1979; the first significant volcanic activity in the north western plateau was represented by the Ashangi (TASB) and Tarmaber Basalts (TTB2) that cover extensive areas. Trachytic flows commonly containing lath- like feldspar phenocryst that emanated from Megezez volcanic are overlying the flood basalts (Wolfendene *et al*., 2004).

The Ajima drainage, reservoir and dam axis areas are covered by the Tarmaber series volcanic rocks which were extruded during the Oligocene prior to the initiation of the Main Ethiopian Rift. According to (Merla *et.al*., 1979) The Tarmaber series consists of typical red paleosoils and laterite soil, as well as lenticular basalts with a lot of tuffs, scoriaceous lava flows, and lenticular basalts. A thick series of rock called Tarmaber basalt, which can reach a thickness of 1,000 meters, is what gives volcanic sites like "Megezez Terara" its distinctive appearance. The termination of the other smaller volcanoes found in the northern portion of the basin is the Tarmaber basalts, which directly overlie the Ashangi basalts (in northwest Ethiopia)..

The lava flow from the main rift source is toward south whereas lava form Megezez in this basin is toward north. Here the river follows the area of confluence. At the end of Ajima (near Rift Margin) the area is completely overlain by recent flood. There is a major formation in the study area, i.e., Tarmaber formation (Megezez subdivision) (Mohr, 1983). Figure 2-5 shows the regional geologic setting of Tarmaber formation.

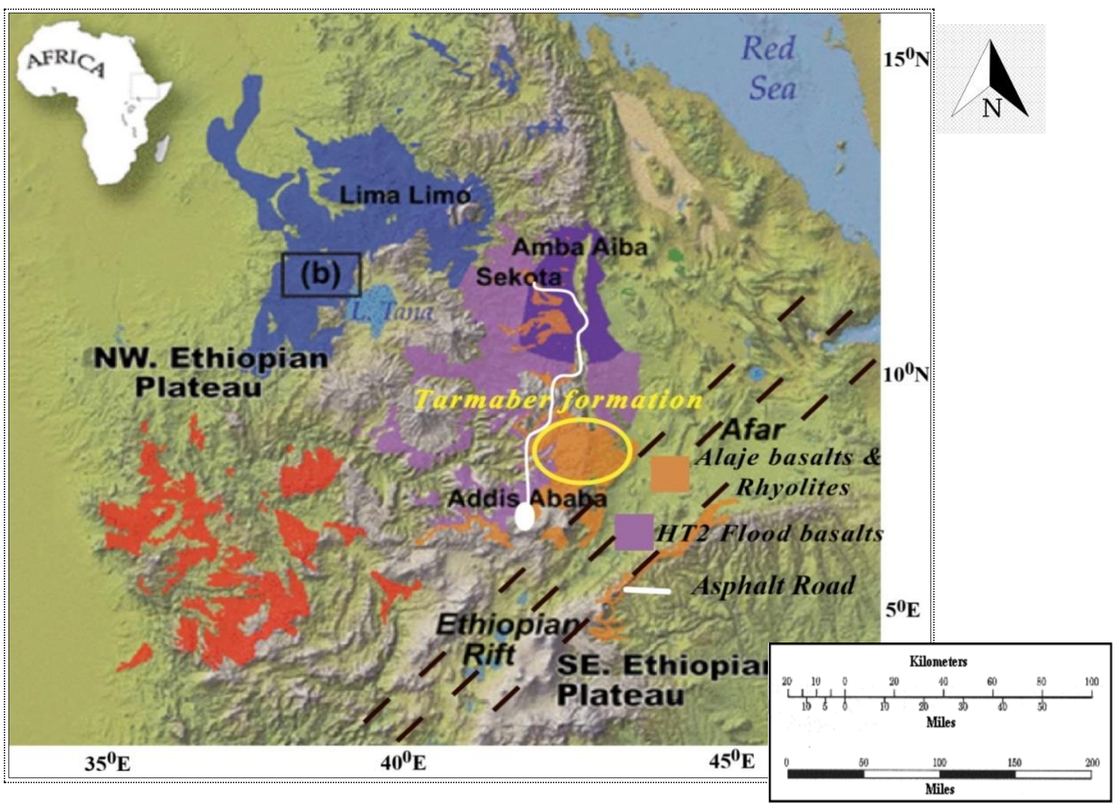


Figure 2-5: Magmatic activity in East Africa during the Early Miocene resurgence phase (26.9–22 Ma) (Rooney, 2017)

## 2.8 Local geology of the dam area

The geology of the study area was investigated using actual field traverses and borehole data for subsurface geologic units on the dam axis from the ADSWE report. Outcrops of rocks slopes and soil slopes have been visually examined during field investigation. The project area located within the Tarmaber series volcanic rocks. Basalts rocks, moderately welded tuff rock, paleosoils intercalation in local area between tuff and rhyolite units, and rhyolite rock units are found on the dam axis of vertical section (ADSWE, 2016). The major formation in the reservoir slope of Ajima dam is dominantly volcanic tuff having various degrees of weathering, fractured and weathered rhyolite unit and residual soils.

### 2.8.1 Residual soil

It covers the upper slope and rim of the reservoir slopes. The residual soils are formed by in situ weathering and decomposition of rocks developed from the underlying local geology through physical and chemical weathering (ADSWE, 2016). It has characteristics of brown to dark color, low plastic behavior, and low to medium permeability which is from dam axis residual soil (ADSWE, 2016).

### 2.8.2 Rhyolite rock

This rock unit shows moderately weathered and fractured behavior. Geologic unit of the reservoir area observed above thick tuff formation, which is attaining a thickness measured between 5 to 10 m on the abutment of Ajima dam (ADSWE, 2016).

### 2.8.3 Paleosoils

The Paleosoils or laterite soil is observed in between tuff and rhyolite rock unit formations at the dam axis and reddish in color, medium to coarse grain in texture and compositionally has aluminum and iron oxide (ADSWE, 2016).

### 2.8.4 Tuff rock unit

This rock unit is light to dull yellowish rock unit and has a moderately degree of weathering. It represents the dominant geologic unit of the reservoir area of the dam which observed in slope exposure and drilling borehole on the dam axis which is attaining a thickness in a range between (10m to 15m).

### 2.8.5 Basaltic rock

The basaltic rock is a dark gray aphanitic texture, having columnar joints on the bed of dam axis (ADSWE, 2016). The rock core reveals some degree of physical weathering defined with highly fractured secondary joint sets. These joints are dominantly developed along the existing primary structure and the direction of joint is perpendicular to the current river direction. The basaltic unit is observed for some limited depth (not more than 10m), especially near to the stream beds (ADSWE, 2016).

### 2.8.6 Alluvial soil

The majority of gentle valley areas along the Ajima river are covered by superficial soils. These are alluvial deposit. It is a soil deposited by the stream during flood times for a long period. It has dark brown color, medium to highly plasticity property (ADSWE, 2016).

Table 2-1 Geological unit description on the dam axis (ADSWE, 2016)

| Geological units (rock & soils) | Description of unit Properties |
|---|---|
| Residual clay soil | _ Brown in color with low plastic behavior<br>_ Fine grained soil (clayey) |
| Rhyolitic rock and tuff rock | _ Moderately weathered and fractured rhyolite rock underlying by tuff rock unit |
| Paleosoils Soil (*Interbedded layer)* | _ Between tuff rock and rhyolite rock unit,<br>Shear parameters of the paleosoils are 13.18KN/m$^2$, cohesion and 20.25$^0$, angle of friction (ADSWE, 2016) |
| Basaltic rock | _ Dark gray aphanitic texture<br>_ jointed and highly fractured |

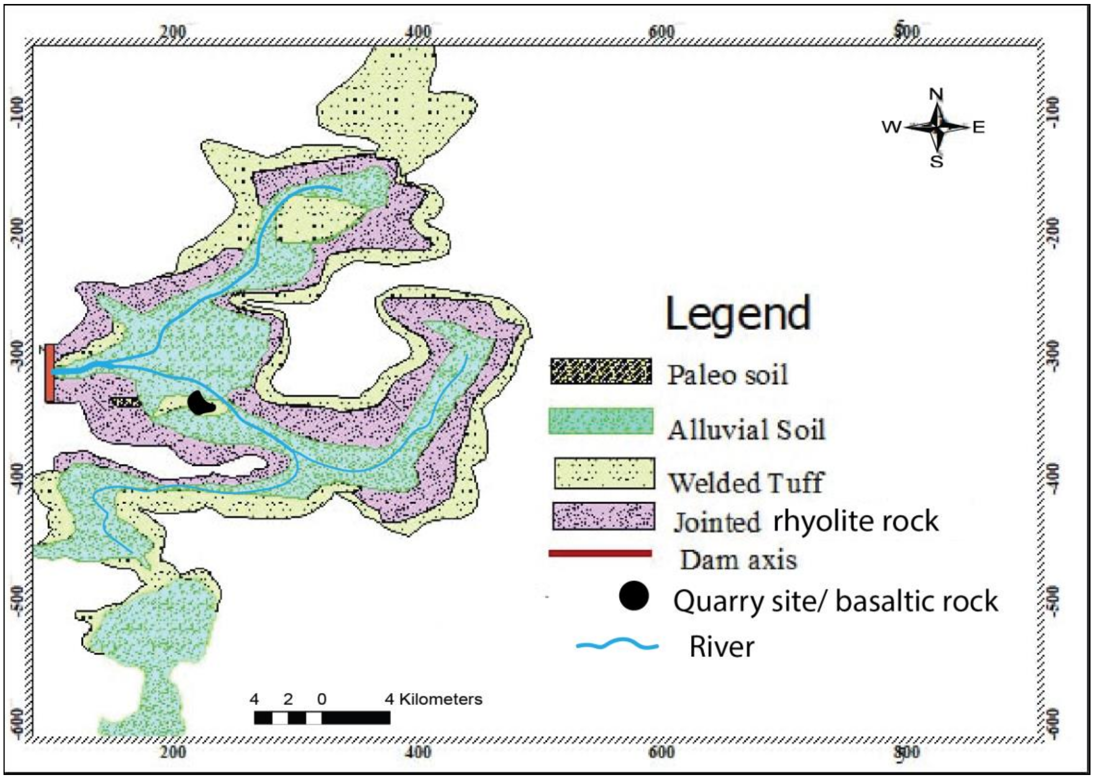


Figure 2-6: Geological map of Ajima dam reservoir area with the elevation of 2850 to 2860m above msl (Adopted from ADSWE, 2016).

Geologic map of the dam reservoir area as shown in (Figure 2-6) has been prepared to show the lithologic distribution in the dam reservoir slopes. The map has been prepared from the scanned map of previous ADSWE work. The local geology was classified based on the rock distributions.

## 2.9 Sub-surface geology on the dam axis

The subsurface geologic investigation has significant value to define, and evaluate the hidden site geologic conditions which affects the design and construction of engineering structures (USBR, 1987). To account for the subsurface conditions of the dam, six boreholes were drilled (see Table 2-2), carried out by ADSWE (ADSWE, 2016). The whole succession are found to be residual soil, highly fractured and weathered rhyolite unit, weathered and less welded tuff rock, paleosoils, moderately welded tuff, fractured aphanitic basaltic rock, and jointed ignimbrite rock at the depth of 20m below the bed of dam axis (ADSWE, 2016) as illustrated in figure below (see Figure 2-7).

Table 2-2: Subsurface exploratory drilling boreholes on the dam axis (ADSWE, 2016)

| Exploratory borehole | Depth (m) | Location | Coordinates |
|---|---|---|---|
| AJFOBHN-1 | 30 | Valley floor | 558120E, 1048538 N |
| AJFOBHN-2 | 30 | RA mid slope | 558122 E, 1048576 N |
| AJFOBHN-3 | 30 | RA feet | 558110 E, 1048663 N |
| AJFOBHN-4 | 30 | LA feet | 558123 E, 1048492 N |
| AJFOBHN-5 | 13 | LA mid slope | 558115 E, 1048453 N |
| AJFOBHN-6 | 19 | LA top slope | 558096 E, 1048421 N |

***Where**, RA is right abutment of the dam, LA is left abutment of the dam*

Test pitting and drilling bore-hole for subsurface explorations at the dam site has been done by ADSWE in 2016. For which about six boreholes were drilled (to a maximum depth of 30m) along the constructed dam axis. In addition, manual test pits were utilized to characterize borrow areas for the impermeable fill soil. A total of seventeen (17) test pits were bored and five borrow areas (1-5) located within the reservoir area of the dam (ADSWE, 2016).

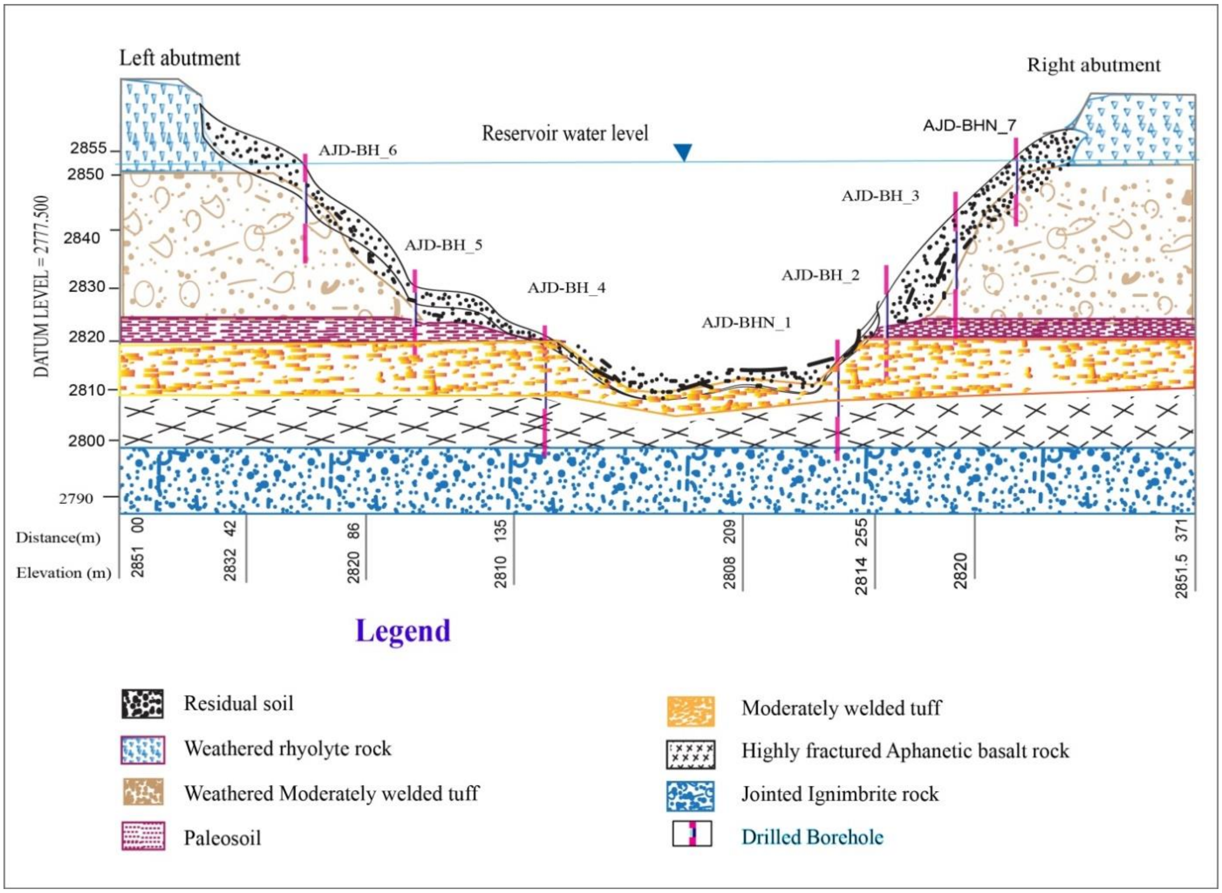


Figure 2-7: Geologic cross-sections of Ajima dam along the dam axis

### 2.9.1 Foundation (bedrock) materials properties on the dam axis

A general foundation rest on bedrock but the top soil shall be removed because of loose or weak compressibility and insignificant thickness (at 2-3m depth). On the area one SPT tests were conducted at the dam site in AJFOBH-1, according to the value of SPT (N=7) has fall in a range of loose to medium (ADSWE, 2016).

Below the tuff rock zones, there is jointed basalt bedrock. The average thickness of this jointed rock is about 9m at (AJFOBH-2) and (AJFOBH -3). Basalt rock underlying on the dam axis at average depth of below 15m are discontinuities, slightly weathered and closely jointed basalt. The RQD value of the unit conducted at certain section is ~65% implying to be good (ADSWE, 2016).
The UCS of intact rock material being 100MPa, the UCS for the rock mass has been calculated and estimated to be 16.6MPa. Deformation modulus, Em of the rock mass is found to be 4.2GPa.

The UCS of Intact rock material being 100MPa, the UCS for the rock mass has been calculated and estimated to be 18.2MPa. Deformation modulus of the rhyolite rock mass is found to be 2.2GPa (ADSWE, 2016).

### 2.9.2 Geophysical investigation along dam axes and reservoir

Geophysical method was usually used at the initial stage of geotechnical investigation to loosely estimate zone of discontinuities, thickness of overburden and lithological contacts on the dam site. Seismic refraction (P-wave velocity and resistivity profiling and vertical electrical sounding (VES) were applied at the Ajima dam sites (including spillway, pick of right abutment and reservoir) (ADSWE, 2016).

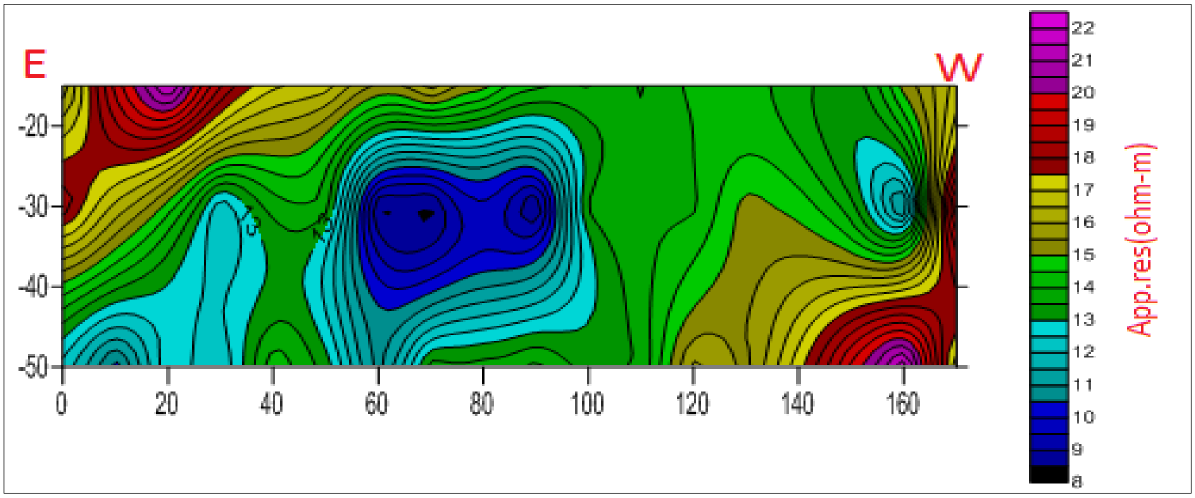


Figure 2-8: Electrical profiling of subsurface map on the dam axis, along the line of stream flow (in E-W direction) (ADSWE, 2016).

The refraction seismic survey's result has been presented in the form of 2D P-wave Velocity tomography (see Figure 2-9).

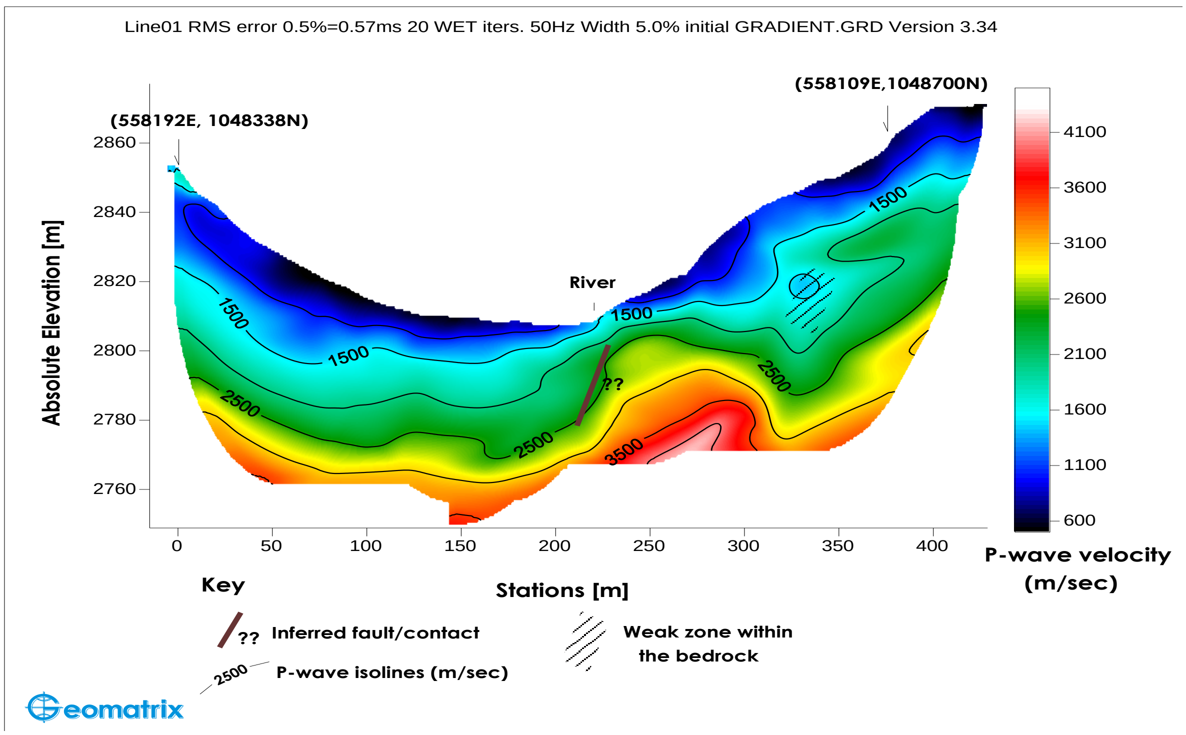


Figure 2-9: refraction seismic survey's result from (ADSWE, 2016) report.

This line extends from UTM geographic coordinates of 558192E, 1048338N and 558109E, 1048701N respectively with ground elevations between 2806m a.s.l and 2853m a.s.l. along the dam axis (ADSWE, 2016).

According to the 2D P-wave velocity tomography (see Figure 2-9), the uppermost part of the section with p-wave velocities below 1000m/sec is mostly related with clay associated with rock fragments and silt with sand (ADSWE, 2016). According to BH-6 bore data the unit also comprises highly weathered and decomposed tuff and rhyolitic rock in the elevated sloppy parts of the line. The thickness of this top unit varies widely from about few centimeters to a maximum value of 12m (ADSWE, 2016).

## 2.10 Hydrogeology of the area

Ground water occurrence in the dam axis is encountered at shallow depth (21m) during the test drilling and discharge 3 L/s. So that the ground water is affected the dam structure and has been solved the problem at a time of construction through pumping (ADSWE, 2016).

Groundwater inflow has strong negative effect on the instability condition in the rock mass excavation. The groundwater sources of the surroundings of the dam area are governed by geology and geological structures of the region. The Cenozoic volcanic rocks, especially the Tarmaber formation that mainly consists of basalt rocks does not have primary porosity that allows groundwater movement and storage. It may develop secondary porosity along fracture and joint openings and weathered sections. However, the clay material that forms in the weathering processes of the volcanic rock usually fills in the secondary openings and decreases the transmissivity and ground water storage of the rocks (ADSWE, 2016). The volcanic rocks of the region and their physical features that control the groundwater movement and storage are not homogeneous. There are several volcanic episodes that took place in the region and these have formed rock beds that are heterogeneous in their physical characteristics and gave time for formation of paleosoil layers between the different volcanic formations (ADSWE, 2016).

The prevailing volcanic rock units due to crevices (a narrow opening or fissure), formed along cracks & weathering that enhance development of open water bearing layers; the open and interconnected porous spaces including discontinuity planes that are without secondary infill material can be considered as potential infiltration and water bearing layers in the dam area (ADSWE, 2016).

## 2.11 Seismicity

Based on the recent conducted study (Atalay, 2017), the country is divided with a partition of five zones which have approximately equivalent seismic threats in a base of previously defined earthquake distribution. The classified zones are: none damaging zone (0 zones), less degree of damaging zone (zone 1 and 2) and major damaging zone (zone 3 and 4). The research area is located in seismically active zone which is under the major region of seismic hazard (zone 4). Based on this seismic hazard zone distributions the ground acceleration fall in a range of (0.15 to 0.20) (Atalay, 2017).

### 2.11.1 Seismic hazard and ground acceleration time-histories

The strength of the seismic activity may be related to ground acceleration. The study area has an estimated ground acceleration fall in a range of (0.15 to 0.20) as per Atalay (Atalay, 2017) (see

Figure 2.10), and (PGA) of 0.18g is the suitable average value of ground motion for the dam area. Ajima earthen dam is not found in a far distance from the margins of (MER), which is found within the influence zone where earthquake occurrences frequently happen.

The site specific seismic hazard didn't indicate which duration will be appropriate for the dam project. In most cases, shorter intervals are taken into account when determining the peak amplitude for concrete dams and dam-appurtenant structures. However, in previous engineering design exercises, a considerably higher period was taken into account because of the adaptable character of embankment dams. Because adopting a shorter period for the embankment designs will result in a more careful design that is not cost-effective. When choosing the dam type for construction, the site of the dam, material behavior, and dam height are crucially considered (according to the Army Corps of U.S Engineering manual).

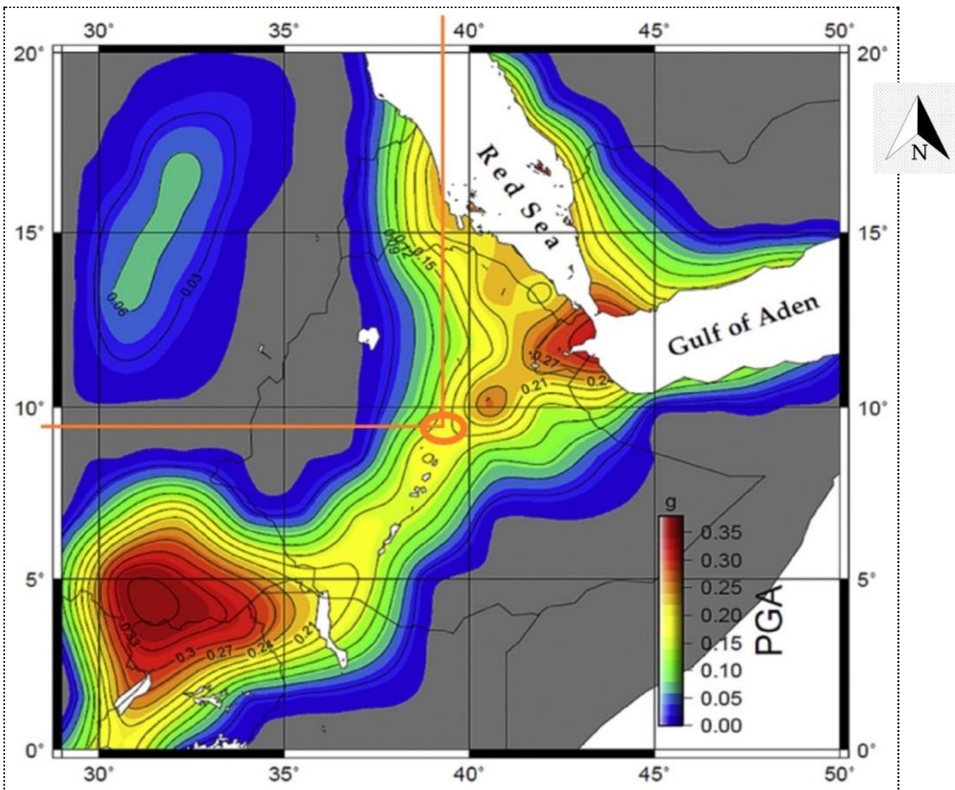


Figure 2-10: For Ethiopia and the surrounding area, seismic hazard map for horizontal peak ground acceleration. This shows a rock site condition exceedance rate of 2% (two percent) within years of fifty (Atalay, 2017).

In conclusion, Ajima dam is not far from the rift margin of MER which needs more investigation. Damaging earthquakes are possible occur along the plateau margin and any potential failure might affect the dam structure its reservoir slopes also, important infrastructure near and on the downstream of the dam area. Therefore, this calls for adapting very conservative values of ground motion for the analysis and design purposes.

## 2.12 Geotechnical issues on the Ajima dam reservoir slopes

The present study area is situated on the highland area. The dam region is defined by complex a geo-environmental process which includes geological, seismic, meteorological and human influences for slope failure (ADSWE, 2016). While conducting field survey to reach more susceptible slope for failure, some of the most predisposing factors in the reservoir slopes was identified (see Figure 2.11).

The crucial intrinsic parameters for slope instability are slope material (lithology or soil type). However, slope geometry, structural discontinuities, rockmass degree of weathering, seismicity, and intensive rainfall are the responsible external predisposing factors for the instability of selected critical reservoir slopes (Kumar and Anbalagan, 2016).

### 2.12.1 Structural discontinuities

The stability characteristics of rock slopes are mostly influenced by the weakened structures of the rockmass (Hoek and Bray, 1981). Discontinuity orientation, joint spacing, rock mass degree of weathering, and the type of filling material inside the discontinuity surfaces can significantly affects the stability of the rocky slopes (Karaman et al., 2013).

If the discontinuities are spaced tightly, the rock mass is more vulnerable to the instability of rock slopes (Dawit and Trufat, 2021). According to Raghuvanshi *et al*., (2014), the continuity of discontinuity can affect the stability conditions of the rock masses and discontinuity orientation of the rockmass is important in kinematic analysis to determine the mode of slope failure.

The state of the discontinuities and the slopes orientation has a significant impact on the stability of rock slopes that have experienced structural control failure. According to Li and Xu (2015) and Hack (2002), the shear strength of the slope rock mass, and slope height has major effects on the stability of rock slopes and which are prone for non-structural control failure.

Seepage of water through cracks and weak zones of discontinuity potentially increase in lateral pressure, resulting decrease in shear strength across the discontinuity surface leading to slope instability. Furthermore, the groundwater lubricates the discontinuity surfaces, promoting the rock sliding. A leaked water manifestation on the slope surface was examined like wetness and pouring as indirect interventions (Karaman *et al*., 2013).

### 2.12.2 Weak and friable rock units in a slope layers

The geology of dam reservoir slope comprises mainly very soft and weathered volcanic rocks overlain by variable thicknesses of residual soils. Mostly tuff rock unit and residual soil are susceptible to failure due to reservoir water saturation and shear strength reductions. The prominent lithology along the reservoir slope of the Ajima dam is covered with weak pyroclastic rock and jointed rocks. These rock units are highly exposed on the moderately to steep hill reservoir slopes.

### 2.12.3 Saturation of critical slopes

The surface water from rain fall has significant effects on the instability of reservoir slopes, which saturate the overburden slope materials. The rain water possibly saturates the slope materials and reduces its shear strength, if there is seepage through the weak zone of slope layers and discontinuity. The response of saturated slope materials for the slope failure problems have different which are depending on the topography, slope gradient, type of the slope materials and its degree of weathering on the slope materials.

Seepage/spring with insignificant discharge has been observed at the upstream of the reservoir slopes from the natural hill slopes (ADSWE, 2016).

### 2.12.4 Pre-existing failure surface

If a slope sits contains pre-existing failure surfaces, there is a large possibility that progressive failure will take place if another failure surface were to cut through them. The way of failure on this situation is that movement has along the previous failure zones.

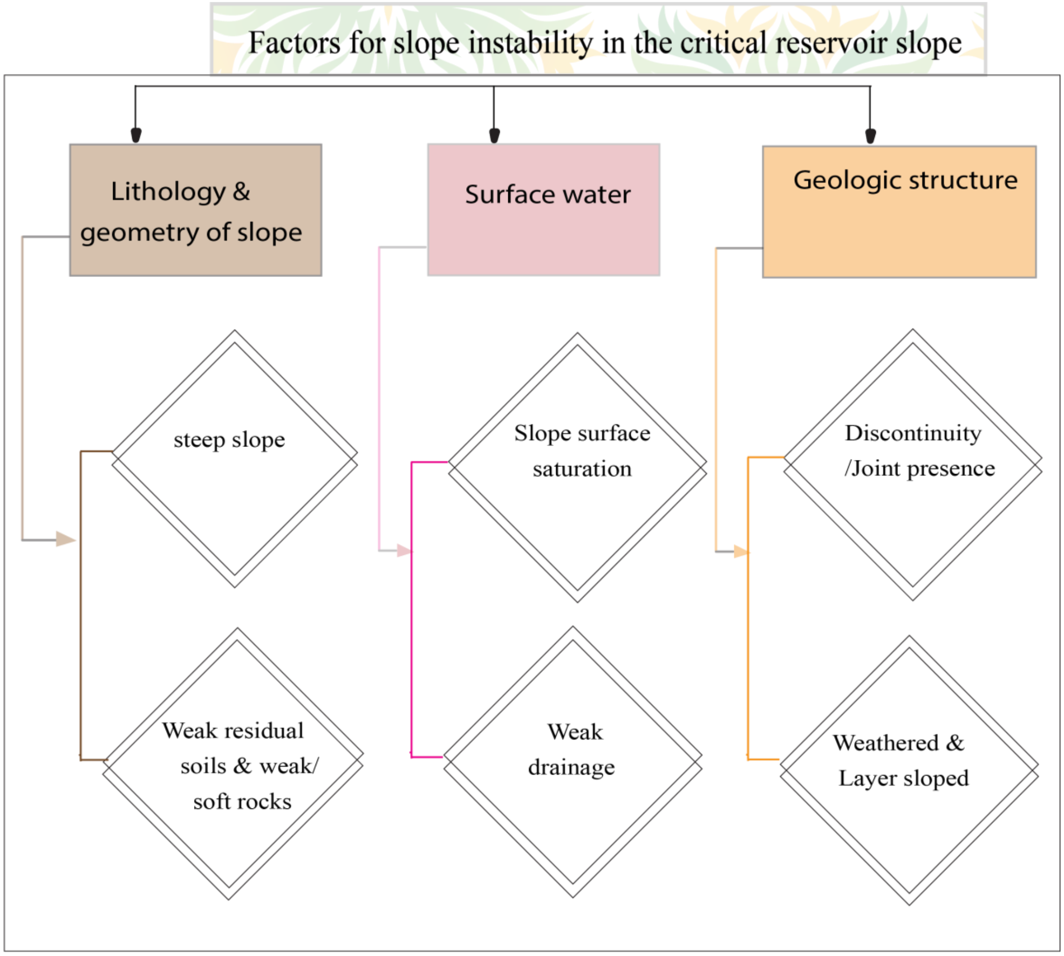


Figure 2-11: Identified predisposing factors for the instability issues on the selected critical reservoir slopes of the Ajima dam

In general, most Ajima dam reservoir slopes are covered by weak geological materials and discontinuous rockmass, and also the dam is located in a high rainfall region. The selected critical slopes are situated in cliff gradient with less strength and highly friable lithology. These all listed predisposing factors possibly control the shear strength of slope materials on the selected critical slopes and which causes for slope failure. There are also evidences of slight slope movements in the reservoir slope which is triggered by surface water seepage from quarry site on RS-2 the quarry is found above the critical slope, RS-2. These failure features is localized and not a significant threat to the dam structures however, may concern for the sedimentation of the dam reservoir and may cause overtopping of reservoir water on the dam structures during flood seasons when the slope failure is not in a creep movement.

# CHAPTER 3 : LITERATURE REVIEW

## 3.1 Introduction

This chapter presents the theoretical bases which used in instability analysis of slope. Currently, there are many approaches to perform slope stability analysis. From these methods the one which is Finite Element Method is elaborated from the theory and practical application on the design and analysis of slope safety in various geotechnical problems.

## 3.2 Delineation of dam reservoir level

Accurate delineation of watershed and reservoir water level is essential for reservoir slope analysis and flood risk management (Elhag & Eljack, 2016), and (Ajibade *et al*., 2020). GIS techniques are used to delineate different topographical site. Full water reservoir level can be delineated using Google Earth, Arc GIS and ARC Scene tools.

## 3.3 Critical slope

Critical slope selection is a major and important first step to determine triggering factors for the detail analysis of the slopes. Critical slopes can be selected by collecting data on the slopes comprising geologic units like, geometric properties of rock mass and soil properties, geologic structure, degree of weathering, and effects of water saturation (Casagli *et al*., 2023), (Tenalem and Bariebri, 2005), and (Soeters and Westen, 1996). Slope instability zone as critical slopes can be identifying using methods of GIS and field investigations.

## 3.4 Causes for slope failure

Slope failures are one of the most common geologic hazards in civil infrastructure. Identifying the causes of slope failure is helpful in assessment of slope safety and in providing appropriate protection measures. The main possible causes for natural slope instability are primarily caused by highly weathered rock units in the slope surface, ground water condition, slope geometry and slope gradients, preexisting discontinuities such as faults, sheared zones, and undercutting support the toe of slope (Abramson, 2002).

Soft rock is a kind of rock mass that has softer lithology and is more prone to being affected and softened by water absorption. It is simple for rainwater infiltration to alter soft rock on a natural slope and cause slope instability factors because of its special physical characteristics. The soft rock softens and deteriorates when it meets with water. The shear strength decreases with the increase of softening time of water, which accelerates the evolution process of soft rock slope instability (Neiman, 2009, and Yonathan *et al*., 2012).

Slope failure at the natural cliff is usually continuous if it is not interrupted by mitigation and remediation works, a kind of instability that is quite frequent along the cliff slopes. The weathered and soft material can gradually remove by the action of gravity and river wave action (Neiman, 2009, and Yonathan *et al*., 2012).

## 3.5 Methods of rockmass characterization

Common technique in order to estimate the parameters is to use empirical correlations to rock mass classification methods, since laboratory and especially in-situ test are expensive and time consuming (Farahmand, 2017). Determining the characteristics of rock mass is the major step to conduct the stability analysis of rock slopes. In this context, rock mass characterization is of huge importance for the applications in rock engineering practice. Therefore, it is crucial to obtain the quantitative appearances of the rock masses as well as a qualitative assessment of the rock mass characteristics as input parameters for empirical methods (Bieniawski, 1989).

In-situ data of rock mass can be analyzed to estimate geomechanical properties of rock mass for the subsequent geotechnical model of slope sections by following the compilation of the rock mass data from field inventories, insitu test and laboratory tests. The most widely used methodology for rock mass classification is Bieniawski Rock Mass Raring (RMR) system (Bieniawski, 1989), the GSI system and Q system. These methods can provides geological parameters of rock mass quality.

Systems for characterizing rock masses are a crucial component of empirical methods that have been applied to slope stability studies. Rock mass classification systems aim to characterize the intrinsic characteristics of the rock masses based on previous experience in order to effectively predict the rock mass behavior for different conditions (Milne *et al.*, 1998). Using parameters of rock mass strength and deformation (Hoek and Diederichs, 2006) together, insight with some additive laws of rock mass (e.g., Mohr’s Coulomb or Hoek-Brown material models), empirical rock mass classification method can be used in numerical models to assess stability and deformations conditions of the rock masses (Abbas and Konietzky, 2017).

Uniaxial compressive strength of intact rock (UCS) can be estimated using the device called Schmidt hammer that measures the rebound number during field tests and UCS can determined by convert Schmidt rebound number in to UCS based on relation proposed by (Barton and Choubey, 1977).

$$\log 10\ UCS = 0.00088\ (\Upsilon * R) + 1.01 \qquad (3.1)$$

From this; $UCS = 10^{(0.00088\ \gamma\ R+1.01)}$

Where; UCS stands for uniaxial compressive strength in MPa, for bulk volume weight (KN/m3), and R for the Schmidt hammer's rebound hardness value. The rock mass strength can be classified based on the UCS values (see Table3-1).

Table 3-1: Rock material strength (ISRM, 2007)

| ISRM grade | Terms | UCS (Mpa) | Field estimation of strength |
|---|---|---|---|
| R6 | Extremely | > 250 | Rock materials only chipped under repeated hammer strong blows, ring when struck |
| R4 | Strong | 50 - 100 | Hand held specimens broken by a single blow |
| R3 | Medium | 25 -50 | Firm blow with geological pick indents rock too strong 5 mm, knife just scrapes surface |
| R2 | Weak | 5 - 25 | Knife cuts material but too hard to shape into triaxial specimens |
| R1 | Very weak | 1-5 | Material crumbles under firm blows of geologic hammer |
| R0 | Extremely Weak | 0.25- 1 | pick, can be shaped with knife Indented by thumbnail |

The RQD index has bias for the characterization of rockmass in slope rockmass. The fracture density or fracture frequency cannot considered in two dimensional ways in the slope rockmass exposure (Lowson and Bieniawski, 20 13).

### 3.5.1 Geological Strength Index (GSI)

The GSI can be used to evaluate the rock mass based on its surface conditions, rock mass structure, and discontinuities; it has been the ideal and direct means to estimate Hoek brown strength criteria (Hoek and Brown, 2019), and (Bieniawski, 1989) was used in the Hoek and Brown failure criterion equation in the first approaches to determine the GSI value of the rock masses.

Hoek and Brown recognize field observation and recognition of rockmass failure criterion is significant for classification system (Marinos *et al.* 2005). GSI value is used to estimate rockmass properties that can be input for numerical computation in slope stability analysis. The index value of GSI link with the compressive strength of intact rock (UCS) and its material constant (mi) to calculate the rockmass properties like deformation modulus and shear strength parameters using Roc Lab software (Marinos and Hoek, 2000).

Hoek in 1994 improve the chart of GSI for assessment of rockmass properties and estimation of rockmass strength by making link of Hoek-Brown criterion and its constant with rockmass surface quality conditions (Hoek, 1994)(see in Figure 3.2). Rockmass characterization method in GSI is based on field visual impression of presence of rock structure and joint weathering conditions, alteration and roughness. In a highly weathered rockmass the unconfined strength and rockmass material constant (mi) is reduced, at the same time GSI value also decreased (Marinos *et al*. 2005).

The introductions of GSI chart efficiently removed the inherent limitation in RQD estimation and reduce the error in the incorporation of RMR. The estimation of GSI is important since, the determination of deformation modulus of rockmass in in-situ or in laboratory test is expensive and time consuming. GSI value can correlate empirically to compute modulus of rockmass deformation. Different researcher in their research works can make correlation in between GSI and RMR, namely Hoek and Brown in 1997, Ceballos and Olalla in 2014 and Zhang et al in 2016.

Cosar in 2004, also presented a correlation for GSI and RMR89 (Cosar, 2004),

$$RMR89 = 2.3GSI - 54 \qquad (3.2)$$

General correlation of GSI with RMR89 for rockmass in Himalaya Mountain was also given for all rock types by (Singh and Tamrakar, 2013) as follow Eq. (3.3):

$$RMR89 = 1.3GSI + 5.9 \qquad (3.3)$$

Zhang *et al.*, (2016) obtained the correlation of RMR with GSI at the surface of the tunnel excavation and produced equation Eq. (3.4):

$$RMR89 = 0.827\ GSI + 15.394 \quad (3.4)$$

Recently, an empirical relation of RMR89 and GSI was presented by (Zhang, 2019) as given in Eq. (3.5).

$$RMR89 = 0.8GSI + 15 \quad (3.5)$$

Ceballos and Olalla (2014) made a correlation between GSI and RMR values on different rock units with different outcrops and examine the resulting equation as:

$$GSI = 1.13\ RMR – 11.63 \quad (3.6)$$

GSI value for rock masses having (GSI > 25) can be computed using correlation with RMR value (Hoek and Brown, 2019) as follow (Eq. 3.7):

$$GSI = RMR_{89} - 5 \quad (3.7)$$

Doni *et al*., (2021) used the characterization of rockmass on the intake tunnel of dam, based on GSI method for weak rock on the lithology of volcanic breccia and tuff rocks based on the correlation obtained in the literature works.

The estimation of GSI values directly from RMR values has been proven unreliable, especially for poor rock mass. So, it is highly recommended that the estimation of GSI should be conducted utilizing the charts (Hoek and Marinos, 2000), which is free from RMR values (Hoek and Brown, 2019).

From field observation and characterizations of rockmass discontinuity condition and surface (weathering) condition the GSI value can be predicted by using GSI chart (see Figure 3-2) (Marinos and Hoek, 2007). However, this un-quantitative determinations could be subjective in field geologist to the assessment of the rockmass surface condition and discontinuity condition (Kayabasi, 2017), and the ± of 30% of GSI has less of 6% uncertainty in $E_{mr}$.

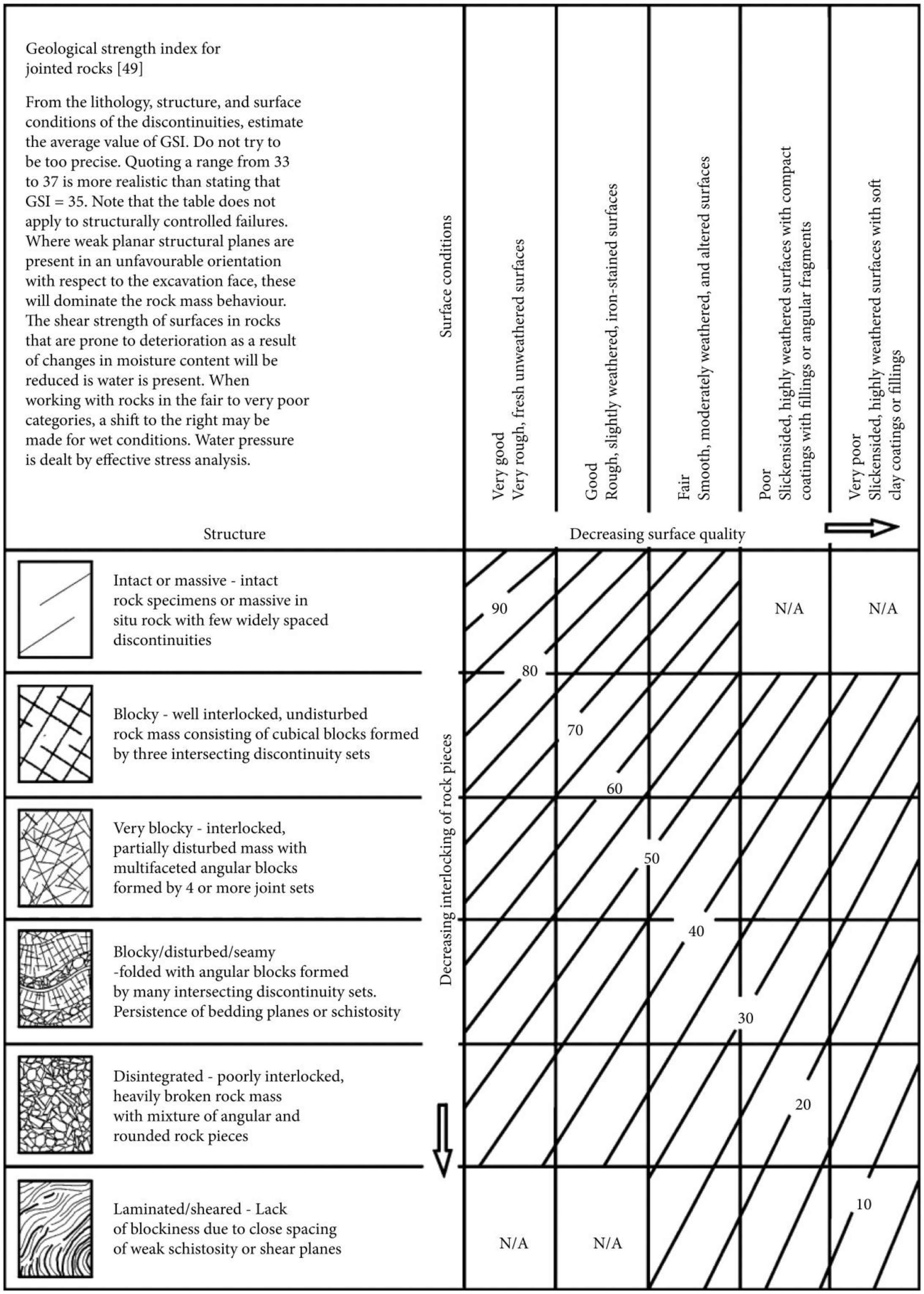


Figure 3-1: GSI chart for jointed rock mass (after Marinos and Hoek, 2000)

## 3.6 The unit weight of geo-materials

Unit weight is one of the input parameter utilized to evaluate slope stability. According to ISRM (2007), the soil and rock unit weight can be taken from the representative materials in the time of field investigation. Dry density ($\rho d$) and bulk unit weights ($\gamma$) of rock and soil sample can be determined using the equations Eq. (3.8) & Eq. (3.9) respectively.

$$\rho d = \frac{Md}{\Delta V} \tag{3.8}$$

$$\gamma = \rho d * \mathrm{g} \tag{3.9}$$

Where, $\rho d$ is the dry density of a rock sample in g/cm$^3$, $M_d$ is the mass of a rock sample after being oven-dried, $\Delta$V is the deference between the volume before and after a rock sample is added into the cylinder water, $\gamma$ is the bulk unit weight of a rock in KN/m$^3$, and g is the gravitational accelerations (m/ s $^2$).

## 3.7 Rock mass shear strength parameters

For the stability assessment of rock slopes, the shear strength properties of the rock mass, including the cohesion and angle of internal friction, must be evaluated. According to Hoek and Brown, 1998), generalized Hoek-Brown failure criteria can be used to estimate the generalized Hoek-Brown failure criteria, like cohesion (C), and angle of internal friction ($\phi$) on the Roc Lab software. This software allows users to easily obtain reliable estimations of rock mass properties and shear strength parameters (Hoek & Diederichs., 2006).

For the sake of simplicity, Rocscience has developed the RocLab window program which can provide Hoek-Brown parameters for the numerical analysis such as; cohesion, angle of internal friction, and deformation modulus of rockmass.

### 3.7.1 Hoek–Brown constants of rock mass

The Hoek-Brown failure criteria was developed as a consequence of Hoek's research on the brittle failure of rock materials in 1965 (Hoek, 1965) and Brown's research on jointed rock masses in 1970 (Brown, 1970). When confining loads are low to moderate and the failure process is driven by block sliding and rotation without a significant amount of entire rock failure, it was intended to be used for rocks comprised of interlocking geometric blocks.

Hoek-Brown failure criterion assumes rock mass consists isotopically and that failure does not follow a preferential direction imposed by the orientation of a specific discontinuity or a combination of two or three discontinuities (Marinos and Hoek, 2007). Once the GSI and disturbance factor have been approximated, the parameters which describe the rock mass strength characteristics ($m_b$, s and α) can be estimated using empirical relations which are originally derived by Hoek & Brown, 1980), these empirical equations are still recommended by Hoek and Brown (2019).

$$\frac{\mathbf{mb}}{\mathbf{mi}} = \exp\left(\frac{\mathbf{GSI-100}}{\mathbf{28-14D}}\right) \tag{3.10}$$

$$S = \exp^{\frac{(\mathbf{GSI-100})}{\mathbf{9-3D}}} \text{ , and} \tag{3.11}$$

$$\alpha = \frac{\mathbf{1}}{\mathbf{2}} + \frac{\mathbf{1}}{\mathbf{6}}\left(\mathbf{e}^{-\frac{\mathbf{GSI}}{\mathbf{15}}} - \mathbf{e}^{-\frac{\mathbf{20}}{\mathbf{3}}}\right) \tag{3.12}$$

Where; Mb is the Reduced value of material constant; mi is Material constant for intact rock, s and a are Material constant for rock masses. When GSI > 25, the quality of the rock masses is good to reasonable, the original Hoek-Brown criterion is applicable with assigning the value of a equals 0.5. For GSI < 25, i.e., rock masses of very poor quality, **s** = 0, and a in the Hoek-Brown criterion is no longer equal to 0.5. The value of **α** can be estimated from GSI by using Eq. (3.12). The value of ***mi*** can be determined by a triaxial test from intact rock pieces. However, if the tests are not available, they can be possibly determined from the table developed by (Hoek and Brown, 1998).

### 3.7.2 Roc Lab software

Roc Lab software used to compute rockmass properties. Rock mass properties can be determined from the estimated input parameters such as: GSI value of rockmass, mean of UCS (intact rock), unit weight and material constant (mi) of intact rock and height of rock slope layer. Therefore, shear strength parameters of rockmass (cohesion (C) and angle of internal friction (ϕ), and UCS of rock masses, and deformation modulus of rockmass can be estimated using the generalized Hoek–Brown failure criteria on Roc Lab software to use the output as input parameters for slope analysis in FLAC 2D software (Hoek and Brown, 2019).

## 3.8 Poisson's ratio of the rock masses

Poisson's ratio is a property that describes the volume change of material to the direction perpendicular to the application of a load. It can be define the ratio of the axial compression to the lateral expansion of soils, and which is the most significant rock engineering factors for engineering designs of the rock mass. Its value is being used mostly for calculating the deformation and stability condition (Sonmez and Ulusay, 2002). Vasarhelyi (2008) presented a simple method for the determinations of rock mass Poisson's ratio value, if the intact rock Poisson's ratio value is known.

$$V_{rm} = -\,0.002GSI + V_i + 0.2 \qquad (3.13)$$

Where, $\nu_{rm}$ and $\nu_i$ is the Poisson's ratio of the rock mass and the intact rock, respectively, and GSI is the Geological Strength Index.

Form Eq. (3.13), to get the $V_{rm}$ value, the value of the intact one is needed. According to Kulatilake *et al*., (2004), if there are known intact rock Poisson's ratio values, the Poisson's ratio for the rock mass could have been 21% higher than the Poisson's ratio for intact rock.

Using Hoek-Brown material constant *mi* and *GSI*, Vasarhelyi (2008) has derived a suitable alternative empirical equation to estimate the Poisson's ratio value of the rock masses when the Poisson's ratio value of the intact rock (Vi) is not available as follow:

$$\mathbf{V}_{rm} = -\,0.002GSI - 0.003mi + 0.457 \qquad (3.14)$$

Note that for mi < 5, Eq. (3.14) can never be applied.

The Poisson's ratio is linearly increasing in case of increasing uniaxial compressive strength (UCS). The Poisson's rate value highly depend on the quality of the rock mass, thus in the increasing if the GSI value is increasing.

The Poisson ratio of rock materials range typically [$0.1 \le v \le 0.4$]. The Poisson's ratio is speculated to rely on how hard the undamaged rock is, and as the brittleness of the rock material increases, the Poisson's ratio should decrease. The Poisson's ratio gradually drops when the Hoek-Brown constant (mi) is increased, it can be assumed, that the Poisson's ratio depends on the rigidity of the intact rock i.e., increasing the brittleness of the rock material the Poison's ratio should be decreasing. High fines contents and/or high moisture contents tend to increase Poisson's ratio and reduce Young's modulus. Poisson's ratio for a completely saturated material will be close to 0.50.

## 3.9 Rock mass deformation modulus from GSI

The Elastic modulus of the rock mass is highly important geomechanical input parameter of rock mass for geotechnical model analysis like settlement and deformation analysis (Hoek and Diederichs, 2006). In many study researchers have tried to develop new meaningful equations besides the most expensive and more time consuming insitu tests such as, (Bieniawski, 1978); (Serafim & Pereira, 1983).

For geotechnical modeling, accurate estimates of the strength and deformation characteristics of rock masses are influenced by the characteristics of intact and discontinuous rock masses, such as the number of joint sets, orientation, spacing, aperture, surface roughness, weathering, and alteration, as well as material parameters (such as compressive strength and modulus of elasticity).
In case, if there are no in situ measurements empirical equations are undoubtedly valuable. Even though many engineering projects prefer in-situ tests, sometimes reputed researchers like (Palmstrom and Singh, 2001) preferred empirical equations concerning different constraints during in-situ measuring of modulus of deformation by saying that taking into account the uncertainties associated with in-situ deformation measurements induced by blast damage, test technique, and test method. Different researchers obtain the correlation of deformation modulus with GSI. These correlations are presented as follow (see Table: 3-2).

Table 3-2: Empirical correlation in Erm and GSI proposed by different authors

| | | | |
|---|---|---|---|
| $\mathrm{E}rm = \sqrt{\frac{\sigma\mathrm{ci}}{100}}\cdot 10^{(\mathbf{GSI-10})/\mathbf{40}}$ | $(GPa)$ | by Hoek et al., (1997) | (3.15) |
| $\mathrm{Erm} = 0.35 * \exp^{0.06\mathrm{GSI}}$ | $(GPa)$ | Majdi et al., (2012) | (3.16) |
| $\mathrm{Erm} = 0.0912\mathrm{e}^{0.0866\mathrm{GSI}}$ | $(GPa)$ | Ghamgosar et al., (2010) | (3.17) |
| $\mathrm{Erm} = 0.1451 * \mathrm{e}^{0654\mathrm{GSI}}$ | $(GPa)$ | Gokceoglu et al., 2003 | (3.18) |

Where, $\sigma ci$ is intact rock compressive strength, and Erm is the rock mass deformation modulus, GSI= Geological strength index.

The bulk modulus (K) and shear modulus (G) of the rock mass for the numerical modeling input parameters can be calculated using (Brady and Brown, 1993), as follow:

$$\mathrm{K} = \frac{\boldsymbol{E}}{\mathbf{3}(\mathbf{1}-\mathbf{2}\boldsymbol{V})} \quad \text{(GPa)} \tag{3.19}$$

$$G = \frac{E}{2(1+V)} \quad \text{(GPa)} \tag{3.20}$$

Where: E is the deformation modulus; V is the Poisson's ratio.

## 3.10 Slope stability analysis

Slope analysis refers to the process of evaluating the stability and behavior of natural or man-made slopes. It involves assessing the factors that can influence slope stability, such as soil and rockmass properties, groundwater conditions, and external loads. The goal of slope analysis is to determine whether a slope is stable or prone to failure, and if necessary, to design appropriate measures to mitigate any potential risks (Wang Lei, 2011).

It is essential to understand basic requirement for the stability of slopes which is the shear strength of the slope materials must be greater than its shear stress which is required for the equilibrium (Duncan *et al*., 2014). Therefore, the most fundamental cause of slope instability is concluded to occur when the shear strength of the soil is less than the shear stress required for equilibrium (Duncan *et al*., 2014). The condition can be reached by two means: (1) through the reduction of soil shear strength and, (2) through the increase of shear stress.

In fact, the vast majority of slope stability evaluations still rely on time-honored limit equilibrium techniques that use methods of slicing. The widely accepted usage of the finite difference approach of slope stability analysis should now be preferred in geotechnical practice since; it is an enhanced substitute for traditional limit equilibrium methods.

The failure surfaces found using the SSR approach can occasionally be very different from those found using the LEM technique. According to Cala and Flisiak (2003), the FS calculated by SSR may be much lower and the unit volume of failing slope significantly more than what is predicted by LEM. Over 3m of soft subsurface layer thickness did not result in a further decline in FOS values. In some circumstances, the use of 2D models may result in a highly cautious course of action. In most situations, the use of SSR in 3D can result in a tolerable FS value. The elastic properties have a significant influence on the computed deformations prior to failure; they negligibly influenced FS (Griffiths & Lane, 1999).

The commonly used deterministic methods for slope stability analysis are Limit equilibrium analysis (LEA) and numerical methods. They compute a factor of safety with different methodologies but share the same definition of FOS (Factor of safety). Limit equilibrium technique was found by Mouyeaux *et al*., (2018) to be more user friendly than the numerical methods in the analysis. For the reservoir slope, it is highly crucial to consider the slope instability assessment in the upstream direction of the dam; since the most critical problems may happens at the phase of the end of excavation or during saturation of the upstream natural or man-made slopes (Chen, M., *et al*., 2021).

## 3.11 Kinematic analysis on rock slope

Kinematic analysis examines based on the attributes of discontinuities such as joints, bedding planes, and shear zones that serve as a potentially failures planes to analyze the modes of rock slope failures (plane, wedge, toppling failures), which occurs due to the existence of unsafe or unfavorable orientation of discontinuities. Measuring the orientation, structures and the main discontinuity sets can be necessary for Kinematic analysis (Hoek and Bray, 1981). DIP software allows for illustration of structural data using graphical Stereonets display.

## 3.12 Slope stability analysis in Finite Difference Method (FDM)

In contrast to the traditional limit equilibrium methods, FLAC 2D can simulating the response of slopes to different factors such as saturation of water, groundwater conditions, and seismic activity. The software provides advanced features and widely used in the field of geotechnical engineering to assess the stability of slopes and design appropriate mitigation measures (Wang Lei, 2011).

In FLAC 2D the slope failure surface is delineated by the concentration of shear strain contours to display deformation of material on the contour plot of the analysis output. FLAC is used in analysing, and designing of any geotechnical engineering project where continuum analysis is utilized in FLAC program for the stability analysis and shows displacements and strains behavior of the slope materials (Wang Lei, 2011).

Limit equilibrium methods cannot provide a lower bound. But sometimes it provides a lower factor of safety than the one computed by using the finite difference (FD) methods. In this case, one should not rely on the LE solution (Eleyas et al., 2017). The stability of the railway embankment was investigated by using finite difference programs (FLAC 2D v 7.0) (Eleyas *et al*., 2017) to simulate the stress distributions in order to investigate mechanisms of high deformation and innovative analysis on strain distributions. The analysis of high rock slopes at the Chuquicamata open-pit mine in Chile has primarily used the FLAC 2D and 3D codes.

Coggan *et al*., (1998) successfully demonstrated the use of both two- and three-dimensional finite-difference analyses in the back analysis of highly kaolinite china clay slopes. Both finite-element and finite-difference models remain in routine use in engineering landslide investigations and are most appropriate in the analysis of slopes involving weak rock/soils or rock masses where failure is controlled by the deformation of the intact material (i.e., continuum) or through a restricted number of discrete discontinuities such as a bedding plane or fault (Wang, D, *et al*., 2007).

FLAC2D (Fast Lagrangian Analysis of Continua in two Dimensions) is numerical modeling software for geotechnical analyses of soil, rock, groundwater, constructs, and ground support. Such analyses include engineering design, factor of safety prediction, research and testing, and back-analysis of failure (Itasca, 2018).

Numerical method is more versatile in detailed analysis with respect to deformations and stresses in slope (Chugh, 2015). This method has the salient feature of derivation of the critical failure surface and a safety factor without the presumption for the shape and location of the failure surface (Liu F, 2020).

Table 3-3: Numerical methods of analysis modified after (Coggan *et al*., 1998)

| Analysis method | Critical input parameters | Advantages |
|---|---|---|
| Continuum modelling [e.g., finite difference method] | Shear strength of surfaces; representative slope geometry; constitutive criteria (e.g., elastic, elasto-plastic, etc.), groundwater properties; in situ stress state. | Modeling material deformation and failure in 2-D, including complex geometry of the slopes. Can evaluate the impact of changing key parameters on the instability mechanisms. Also, include dynamic analysis and creep deformation. |

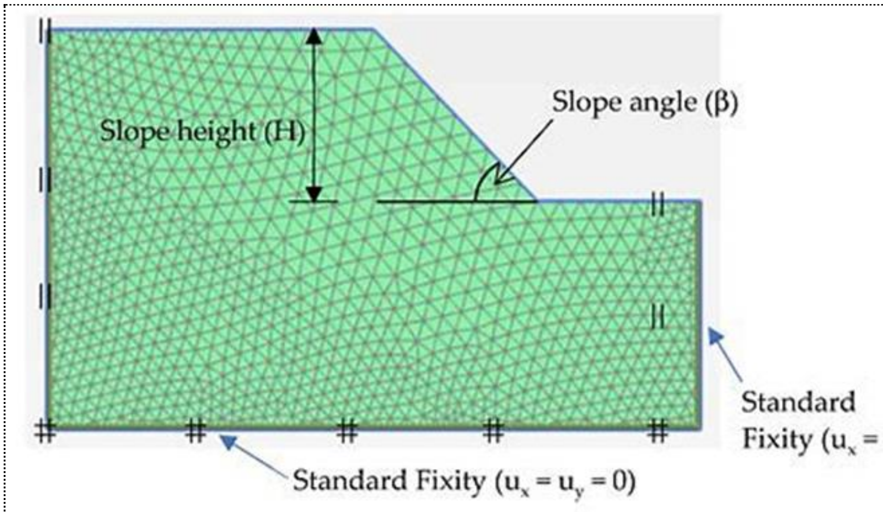


Figure 3-2: Meshing and designing for slope analysis in FLAC program

The following advantages are offered by the FLAC 2D:

1) Multiple failure surfaces (or complex internal yielding) evolve naturally if the conditions give rise to them. Structural interaction (e.g., rock bolt, soil nail, or geogrid) is modeled realistically as fully coupled deforming elements, not simply as equivalent forces (Itasca, 2018).
2) In giving a set of material properties of rock and soils, the system is determined to be stable or unstable, by automatically performing a series of simulations while changing the strength properties, the factor of safety can be found to correspond to the point of stability, and the critical failure (slip) surface can be located (Itasca, 2018).
3) Any failure mode organically arises; there is no need to predetermine a set of trials. There is no requirement for fake input parameters, such as functions for interslice force angles.
4) FLAC can model the slope with variable geometries, numerous layers, diverse soil and rock properties, loads or stress on the surface, and structural reinforcement. FLAC can model the stability issues in a wide range of slope conditions like static and dynamic with dry and saturated state of the slopes.
5) The software calculates FOS with the contour plot to show the displacement, shear strain, and plasticity of the slope materials (Itasca, 2018).

FLAC 2D offers a wide range of capabilities to solve problems in the field of geo-mechanics (Itasca, 20018). The slope analysis of landslide occurrence using FLAC 2D is significantly important for risk evaluation before a landslide and during the rescue stage.

Numerical method is more versatile in detailed analysis with respect to deformations and displacement in the slope (Chugh, 2015). This method has the most noticeable feature of derivation of the critical failure surface without the presumption for the shape and location of the failure surface (Liu F, 2020).

## 3.13 Numerical Model and input parameters for slope analysis

It is difficult to have complete field data of the rock and soil. Since the necessary input data for slope stability analysis are limited, a numerical model in geomechanics should understand primarily to the dominant factors affecting the stability of the slope. The results produced in a FLAC 2D analysis will be accurate when the program is supplied with appropriate direct material data (Itasca, 2018).

The program has built-in material models describing geologic materials properties. In this study Mohr-Coulomb and Hoek-Brown criterion were used to analyse the stress–strain behaviour of the slopes for the soil and rock materials respectively. The basic input parameters of the materials required for modelling are; Young's modulus (kN/m^2), poison's ratio (υs), unit weight (kg/m^3), cohesion (kN/m^2), and internal friction angle Φ (°).Young's modulus (Es) (Itasca, 2018).

Geotechnical parameters which are employed in FLAC 2D software as an input data under the Mohr-Coulomb model are like; cohesion, friction angle, unit weight, modulus of elasticity, and poison ratio. It is recommended to use Poison's ratio of soil in a range between 0.4 and 0.5. For stiff clay and medium to dense cohesionless soil ranges in (0.3 to 0.4) respectively (Bowles, 1996).

### 3.13.1 Mesh Generation

FLAC 2D utilize a mesh to discretize zones in the slope geometry**.** The discretize mesh density can be adjusted to capture critical areas and accurately represent the slope's geometry and slope material heterogeneity (Itasca, 2018).

### 3.13.2 Boundary Conditions

Boundary conditions define the external forces acting on the slope, such as surcharge loads, groundwater level, and seismic loads. FLAC 2D allows users to apply various boundary conditions to simulate different scenarios and study their effects on slope stability (Itasca, 2018).

## 3.14 Analyzing FOS of the slopes

Slope FOS can be compute by following the defined steps and utilizing the software's features. Firstly, the slope geometry must be precisely defined. FLAC 2D provides a user-friendly interface to input necessary parameters such as slope inclination, height, and slope face properties (Liu, 2020). Secondly, assigning material properties, then mesh generation, finally implementation of appropriate boundary conditions. After defining all parameters of the model analysis can be proceed to derive the slope surface with the lowest FOS and also plot strain contour of the modeled slopes (Itasca, 2018).

Numerous failure surfaces with multiple radii and with their centers located in the selected grid are considered. Eventually, the critical surface and its FOS will be selected. The FOS practically defines when a slope is unstable (FOS < 1.0). If the FOS was a deterministic variable then any value higher than 1.0 would be sufficient to classify a slope as stable. However, the uncertainties incorporated in the derivation of the FOS (the method of analysis, the physical and mechanical properties of the ground, the geometry of the ground, the seismic load and others) impose a degree of uncertainty in its final value (Itasca, 2018).

These results are obtained through a series of calculations and simulations in the FLAC2D slope model (Liu, 2020).

Key output parameters:

- Displacement: Indicates the magnitude and direction of movement of the model elements
- Stress: Reflects the forces acting on the model's elements
- Strain: Measures the deformation and distortion of the model's elements
- Pore pressure: Represents the pressure of the fluids within the model

The analysis of FLAC2D output involves examination of the above aforementioned parameters. This analysis is highly important in understanding the slopes' model response and making informed measures and decisions regarding the stability and sustainability of slope safety (Cala and Flisiak, 2003).

### 3.14.1 Displacement analysis

Examining the displacement results allows engineers to identify areas of potential instability or excessive movement (Itasca, 2018).

### 3.14.2 Stress Strain analysis

The stress distribution provides critical information about the forces acting on different areas of the model. Evaluating strain data enables engineers to understand the extent of deformations within the model (Itasca, 2018).

## 3.15 Literature Concluding Remarks

The current literature review highlights the existing facts and methods of slope stability analysis and rock mass characterizations. In each part of the present literature review explains how rockmass and soil properties can be determined, from insitu tests, laboratory tests, and using empirical correlations. The current states of the reviewed literature were found from published articles and reports in different journals.

By utilizing FLAC2D for slope analysis geological engineers can simulate natural or manmade slopes and analyze the stability of different geological formations at different slope conditions. Some key reasons to choose FLAC2D for slope analysis include its ability to model complex geological conditions, also allow for the modeling of complex slope geometry including layered soils, and jointed rock masses.

Slope stability analysis is essential to ensure the long term safety and economic viability of the dam projects, as it helps identify potential slope instability problems in the dam reservoir slopes and determine appropriate stabilization measures for the sensitive layers.

# CHAPTER 4 : METHODS AND DATA ORGANIZATIONS

## 4.1 Introduction

Geological and geotechnical characterization of rockmass and soil has been done to characterize the slope and identify the critical reservoir slopes. Numerical and kinematic methods were used in the current study for the assessment of mode of failure and safety of selected reservoir slopes.

## 4.2 General Methodology

A detailed investigation has been carried out from field surveys to laboratory tests to obtain a necessary geotechnical and geological parameters required for the stability analysis. The field survey was performed by traversing along the reservoir rim slopes to select the critical slopes. Based on slope susceptibility for failure due to the causative factors and slight indication of failures on the existing slope (*see Plate 4.2 to 4.4*), three critical slopes were selected for slope instability analysis.

All the essential data related to geometry of slope, height and slope dipping, rockmass description, joint orientation and weathering conditions of slope materials, and hydrological condition of the area that affects the stability of the selected reservoir slopes has been collected. The input data for the critical reservoir slope analysis were obtained from field investigation and laboratory tests. Field investigations involves marking and characterizing the field critical slopes found on the buffer elevation of reservoir water with the level of filling up to 45m height of the dam (2810 + 45m a.m.s.l). Discontinuity surveying, rock mass characterizations and Schmidt hammer rebound tests has been conducted on the critical slopes. Laboratory tests were performed to determine slopes material properties. Such as; unit weight of rock and soils, UCS test, and direct shear tests for soil samples, compressive tests for rock samples. Based on the determined properties of soils and rock masses which obtained from laboratory and field tests input parameters can be found. The stability analysis on the selected slopes has been carried out using finite difference method FLAC 2D software on all three critical slopes under static dry and static saturated condition. Kinematic analysis has been conducted on the selected upper slope section of RS-1.

## 4.3 Data collection

Geotechnical data collection is the fundamental basis and the first steps adopted for creating a representative geotechnical model that was used for advanced technical assessment and data validation process. A detail on the engineering properties of the soil and rock masses has been obtained from a fully developed and realistic geotechnical model. In the data collections process for slope stability assessment the primary and secondary data were collected. So as to collect all these required data a reconnaissance geological traverse and geotechnical assessment along the reservoir rim were carried out to understand the slope conditions and instability problems along the reservoir slopes due to the slope failure triggering factors.

### 4.3.1 Secondary data collection

Final geotechnical reports containing geology of the area, borehole data, maps and soil laboratory results were obtained from the laboratory of ADSWE. The review of report was made to understand clearly the investigation they carried out on the dam area.

### 4.3.2 Primary data collection

In order to carry out this research essential input data were collected. Field data such as, discontinuity survey (discontinuity data of rock mass), Schmidt hammer rebound test, and sketching actual field slope geometry for the software slope geometry in FLAC 2D. Shear strength tests and unconfined compressive tests were conducted on representative samples of tuff soil and clay soil which were taken from the selected slope section (RS – 3) in the geotechnical laboratory of ECDSWE. Compressive strength tests were conducted for samples taken from upper slope layer of RS- 1 in the laboratory of ADSWE.

## 4.4 Delineating dam reservoir and selecting critical slopes

The analysis revealed that the reservoir water level extracted from 12.5x12.5m pixel resolution Digital elevation model data downloaded from online (ALASKA) source. ArcGIS 10.8 software was utilized for reservoir delineation. The lowest elevation in the dam reservoir is 2810 m a.s.l. on the dam axis.

For reservoir critical slope selection detailed traverse was conducted along the whole rim slope of Ajima dam with the buffer zone of 10 m. Traverses were aimed to identify the critical reservoir slopes due to the expected predisposing factors for the slope instability and the then most susceptible slopes have been identified as a critical slope (see Figure 4-1). The three critical slopes were identified as most susceptible slopes for local failure due to its natural slope geometry and slope gradient, weak and friable lithology, weathering conditions of slope rockmass (see Table 4-1). In addition, high intensity of rainfall is common in the summer season at the dam area, this significantly affect the slope stability by saturating the slope materials and decrease the its shear strength. Which makes the critical slopes susceptible and analysis is necessary to predict the safety of the slopes under different conditions.

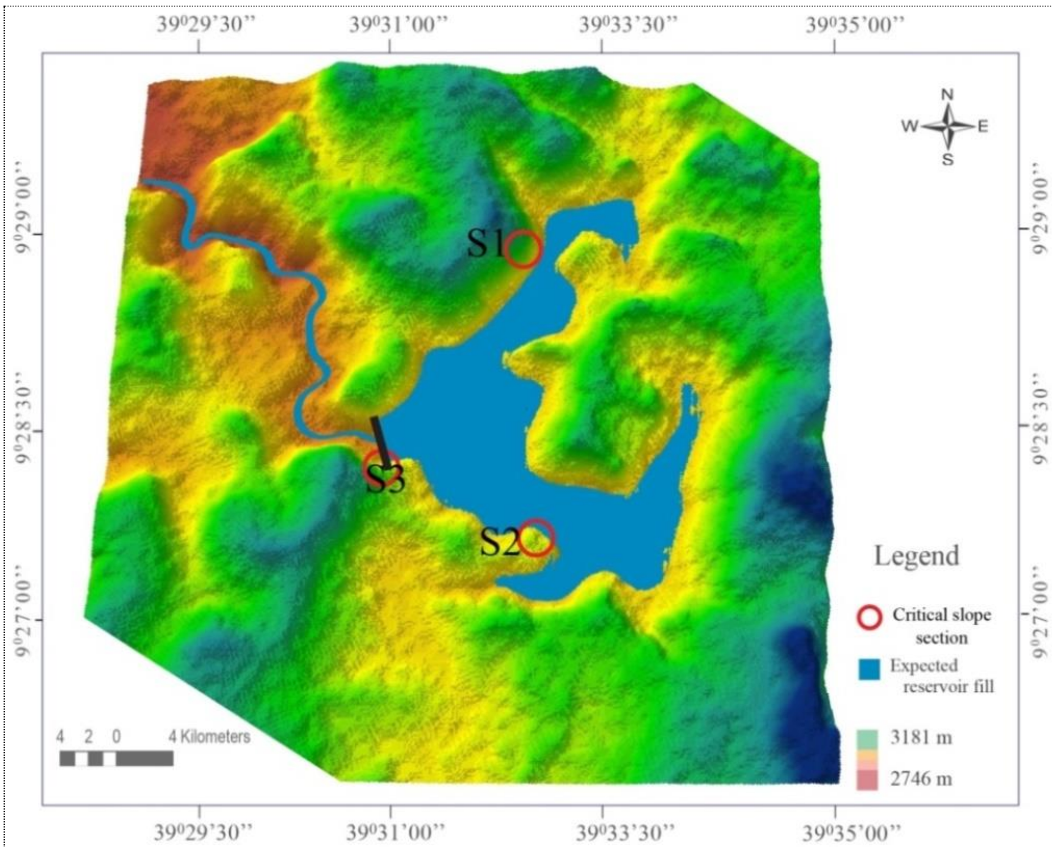


Figure 4-1: S1, S2, and S3 were location of selected slope sections for stability analysis

Table 4-1: The exploratory critical slopes (CR) sections selected from the dam reservoir slopes

| CR | Location CR | Geotechnical units | Expected causative factors |
|---|---|---|---|
| RS-1 | Upstream side of righ abutment around 1.3km from dam axis | Moderately weathered tuff overlay by highly fractured & jointed rhyolite rock | Steep natural hill slope, weak and weathered toe slope material |
| RS-2 | Around 1.2km from le abutment dam axis | Weathered tuff rock underlay by highly weathered tuff rock | Quarry site water seepage and weathered slope materials with steep slope saturate by water |
| RS-3 | On the left abutment o the dam axis | Residual clay soil underlay by decomposed tuff soil | Removal of support and also surface water saturation |

## 4.1 Field investigations and slope geometry on the selected critical slopes

The detailed survey reveals that there are three selected critical slopes in the periphery of the reservoir slopes. It was found that RS-3 slope layer profile consists of residual clay on the top layer of the slope and the bottom layer is a decomposed tuff soil (see Table 4-1). From RS-3 the disturbed soil samples have been taken from both bottom and upper layer to do laboratory tests. In RS-2 the upper slope layer is moderately weathered tuff rock and on the bottom of slope section highly weathered tuff rock unit. The slope geometry and stratigraphy, depth of slopes layer were obtained based on field characterization and measurement. The inclination of RS-3 is in arrange of (40-50) at the bottom layer and (70-80) on the upper slope section. RS-2 has an inclination of (80-85) at the bottom of slope and (30-40) degree at the upper slope section. RS-1 has weathered and fractured rhyolite unit. The inclination of RS-1 is in arrange of (80-85) at the upper layer and (30-35) degree on the bottom of the slope layer.

During the field survey measurements has been made for the depth and inclination of the slopes layer. The maximum height of slope has been taken as 17m, 18m and 14m for RS-1, RS-2, and RS-3 respectively. The slope used in the study consisted of varying heights, H. From this it is inferred that with increasing steepness of slip surface, and height of the slope tends to get more unstable marked by reduction in FOS.

It is divided into different sections of geologic materials and the geometry was built in FLAC 2D tool for analysis. To perform a realistic numerical study to investigate stability of a critical slope, it is very important to build an accurate geological model including all the important material properties. It is not suitable to reflect the original topography since; the slope surface is irregular with many waviness surfaces. However, it was simplified by drawing in guidance with the slope layer depth and inclination measured values on the FLAC 2D slope model based on the field investigations.

## 4.2 Uncertainties from methods of sample tests

Parameters of the slope materials were derived from insitu and laboratory testing. Sources of uncertainties were due to natural variation which is occurrence of heterogeneous material in the slope extent and therefore there can be differences in properties. Natural variation is due to the geological conditions that the slope material is exposed.

The soil taken from RS-3 for laboratory tests was disturbed samples. The shear strength parameters of soil can be affected when the sample has disturbance. Therefore, some uncertainties in the determination of shear strength parameters from disturbed soil samples were expected.

## 4.3 Geotechnical properties of critical slope material for analysis

Insitu tests and laboratory tests were performed to determine the soil and rockmass properties which are used for the input data for software analysis.

### 4.3.1 Unit weight of slope materials

The soil unit weight is an important property in the computation of slope stability. The unit weight of soil can affect the stress conditions of soil meaning that it can affect the shear strength. Soil unit weight is the density times the gravity. The density of soil is obtained by the mass of soil sample divide by volume of a given soil sample, and also the volume of a given soil sample were obtained through buoyancy method by firmly coting with plastic.

### 4.3.2 Shear strength of slope materials

One of the important parameters in slope stability is the shear strength. Therefore the shear strength is evaluated from direct shear test in the laboratory for soil and from roc Lab software for rockmass. Test results can be seen in Appendix part of the thesis.

### 4.3.3 Pore water pressure on the critical slopes

The pore water pressure determines how high the effective stress is in a material. High pore pressure will often imply reduced shear strength. Thus, it has a clear link between soil and rock parameters in with pore water pressure. Since, there is no water table up to the slope's depth, pore water pressures have been set at zero in this study for the selected three critical slopes analysis.

## 4.4 Insitu uniaxial compressive strength measurement on the critical slopes

The Schmidt hammer test determines the surface rebound hardness which is related to the compressive strength. Tests were carried out in accordance with ASTM D5873 (2001) test procedure. A Schmidt hammer was used to gently strike the test surface while being applied perpendicular to it. The Schmidt hammer rebound values were listed in ascending order and the mean of the rebound value (R) was taken for the computation to determine UCS value of the intact rock. The harder the surface, the shorter the penetration time (i.e. smaller impulse) or depth (i.e. lesser work or energy loss) and hence the greater the rebound i.e. smaller momentum change.

For the current research, the test was conducted with N type Schmidt hammer and it was carried out on in-situ outcrops at 10 points with a minimum separation of 50 cm on the tuff rock slope. During the test, a spring-loaded mass impacts the material and the rebound value is read from the sliding mark. Ten values are acquired for each test and took the mean values of the records, and recommend averaging the left rebound values of the Schmidt hammer from at least 10 single impact readings after removing any that deviate by more than 7 units.

## 4.5 Estimated rock mass deformation modulus of critical slopes

Deformation modulus of rock mass is an integral parameter for numerical modeling of rock slopes for the slope failure analysis. The rock mass deformation modulus determination in the actual field slope is a very challenging task, and then questionable results may obtain due to complicated procedures. Thus, in this study rockmass modulus of deformation has been computed using empirical techniques from estimated GSI values (see Table 4-13).

## 4.6 Poison's value of critical slope materials

The poison's value for the rock mass has been determined from empirical relations for the input value in the FLAC2D software. Poison ratio of a given soil sample has been taken in a range between (0.3- 0.4) for residual clay soil referenced from previous scientific literature works.

## 4.7 Disturbance factor D of critical slopes

When slopes are excavated in rock masses the rock results in stress relief which allows the surrounding rock mass to relax and dilate. No blasting results in minimal disturbance to the surrounding rock mass and the Suggested value of natural slope has zero disturbance factors. Disturbance factor can significantly reduce the adopted rock mass strength and possibly the FOS.

## 4.1 Geological Strength Index (GSI) value on the critical slopes

GSI value can vary in different rock masses based on the discontinuity conditions and degree of weathering of the rock exposure. For the moderately weathered tuff rock in RS-1 estimated GSI value fall in a range of [20-25] and 23 has been taken. Rhyolite rock masses in RS-1 encountered as fractured and highly weathered exposure surface. Most blocks in this unit are created by four set of visible joints and the estimated value of GSI has been taken in a range of [30-35]. The estimated GSI value for RS-2 bottom layer was on a range of [10-15] and taken 13, which is a tuff rock mass and has highly weathered slope surface with loss fragment rock unit, and the upper slope layer in RS-2 was moderately weathered and GSI value from the GSI chart fall in a range of [20 – 25] and 23 has been taken for HW tuff rock (see Table 4-11 & Table 4-12).

## 4.2 RS-1 Geological unit properties

The RS-1 is located on the side of right dam axis far of about 1.3km in the upstream. The material constitute of moderately weathered tuff rock overlain by highly weathered and fractured rhyolite rock, the slope is found at the cliff edge of the river bank.

Two samples were taken from slope one (RS-1) to determine compressive strength at the ADSWE laboratory. The samples were tested to determine UCS value, using compressive strength machine.

The rock mass GSI values were taken in the field estimation the rock mass properties. The GSI value of rock unit has reduced value due to the presence of high degree weathering and more fractured surface on the exposed slope.

### 4.2.1 Discontinuity survey on RS-1

Rock data were collected from discontinuity surveys in the fieldwork, which are a crucial part of estimating the quality of the rock mass in the science of rock engineering. The qualities of a rock mass strength, deformability, and permeability are all significantly affected by its discontinuities of rock mass. Scanline surveys are an effective approach that involves tracing a line over an outcropped rock surface and measuring and describing all the discontinuities that cross it. Joint orientation and filling materials, rockmass roughness, and degree of rock weathering have been investigated to estimate GSI value of the rockmass. Upper slope layer of RS-1 comprises of highly fractured rhyolite unit as shown from the slope surface exposure (see Plate 4-2).

### 4.2.2 Uniaxial compressive strength (UCS) for RS-1

Table 4-2: The UCS values of rhyolite rock sample from bottom section (compressive strength test) RS- 1

| Code of sample | Area of compression face (mm2) | Max load at failure (KN) | Compressive strength UCS (MPa) |
|---|---|---|---|
| S- 1 | 96 | 55 | 57 |
| S- 3 | 108 | 14 | 13.2 |
| | | *Average =* | 35.1 |

Table 4-3: The UCS values of RS-1 upper slope section (from compressive strength test)

| Code of sample | Area of compression face (mm2) | Max load at failure (KN) | Compressive strength UCS (MPa) |
|---|---|---|---|
| S- 1 | 104 | 54 | 52.9 |
| S- 2 | 78 | 58 | 76.16 |
| | | *Average value =* | 64.53 |

The reported UCS test result on the sample in RS-1 has significant difference in values this is expected due to the presence of microstructure and weathering degree variation in the tested samples. Thus, the mean values of UCS become recommended as the input parameters for the slope analysis. The average UCS of fractured rhyolite has been determined as 49.8 Mpa from the average minimum UCS value of 35.1MPa, and the average maximum value of 64.53Mpa. The selected rock sample has a medium strength in a range of (25-50) according to the classification by Deere and Miller (1966).

Table 4-4: Schmidt hammer rebound test values for moderately weathered tuff rock on the bottom of slope section one RS-1 and UCS value using empirical equation.

| Slope station | Schmidt hammer Rebound value, R | R. av | γ, dry density in KN/m3 | UCS, (Mpa) |
|---|---|---|---|---|
| RS- 1 | MWT: *21, 22, 23, 21, 21, 20, 20, 22, 21, 20* | 21 | 16 | 17 |

*Where, MWT – Weathered Moderately welded tuff, and*

*R. is average Schmidt hammer rebound values*

Table 4-5: The physical and mechanical input parameters in Roc lab software for RS-1.

| Geologic units | Estimated GSI | UCS (Mpa) | mi | Slope height of each layer | Unit Weight $\gamma(KN/m^3)$ |
|---|---|---|---|---|---|
| Weathered rhyolite (WFR) | 30-35, (33) | 49.8 | 23 | 7 | 24 |
| Weathered tuff rock, MWT | 10-15, (13) | 17 | 11 | 10 | 16 |

Table 4-6: Results of rock mass properties from Roc Lab software for RS-1

| Geologic units | *mb* | *s* | *a* | Cohesion (MPa) | Friction angle (º) | Modulus of deformation *Em* (Mpa) |
|---|---|---|---|---|---|---|
| WFR in upper slope section | *2.101* | *0.0006* | *0.518* | 0.147 | 63.9 | 2652 |
| MWT in bottom slope section | *0.492* | *0.0001* | *0.570* | 0.046 | 41 | 490 |

Where: FWT is fractured and weathered rhyolite rock unit, and MWT is moderately weathered tuff rock.

| | |
|---|---|
| **Hoek-Brown Classification** | **Hoek-Brown Classification** |
| intact uniaxial compressive strength = 49.8 MPa | intact uniaxial compressive strength = 17 MPa |
| GSI = 33 mi = 23 Disturbance factor = 0 | GSI = 13 mi = 11 Disturbance factor = 0 |
| **Hoek-Brown Criterion** | **Hoek-Brown Criterion** |
| mb = 2.101 s = 0.0006 a = 0.518 | mb = 0.492 s = 0.0001 a = 0.570 |
| **Mohr-Coulomb Fit** | **Mohr-Coulomb Fit** |
| cohesion = 0.147 MPa friction angle = 63.90 deg | cohesion = 0.046 MPa friction angle = 41.03 deg |
| **Rock Mass Parameters** | **Rock Mass Parameters** |
| tensile strength = -0.014 MPa | tensile strength = -0.002 MPa |
| uniaxial compressive strength = 1.051 MPa | uniaxial compressive strength = 0.069 MPa |
| global strength = 9.027 MPa | global strength = 1.101 MPa |
| modulus of deformation = 2652.25 MPa | modulus of deformation = 490.03 MPa |
| *WFR rock strength compute using Roc Lab* | *MWT rock strength compute using Roc Lab* |

Plate 4-2: Field photo on critical slope section one (RS-1)

## 4.3 RS-2 rockmass properties determination

The uniaxial compressive strength (UCS) of the intact rock at RS-2 was obtained from Schmidt hammer strength test in the field (Barton and Choubey, 1977).

The Schmidt hammer rebound values are lower for the moderately welded tuff rebound number which ranges from 20 to 24 Schmidt hammer rebound number for welded tuff.

Using these empirical equations, the values of UCS for the geotechnical unit of RS -2 were presented below (see Table 4-7).

Table 4-7: Schmidt rebound values on RS -2

| Critical station | Schmidt hammer Rebound value, R | $R_{av.}$ | γ, dry density in KN/m3 | UCS (Mpa |
|---|---|---|---|---|
| RS-2 | **MWT**: *23, 22, 20, 22, 21, 23, 21, 22, 24, 23* | 22 | 16 | 19 |
| | HWT: *21, 22, 21, 21, 21, 20, 20, 22, 21, 20* | 21 | 15 | 15 |

Where; MWT – Moderately weathered tuff, HWT – Weathered welded tuff,

$R_{av}$**:** is average Schmidt hammer rebound values.

UCS: values were obtained from conversion of Schmidt rebound values.

Table 4-8: The physical and mechanical input parameters in Roc lab software for RS-2.

| Geologic units | Estimated GSI | UCS (Mpa) | mi | Slope height | Unit Weigh $\gamma(kN/m^3)$ |
|---|---|---|---|---|---|
| MWT | 20-25, (23) | 19 | 13 | 14 | 16 |
| HWT | 10-15, (13) | 15 | 11 | 4 | 15 |

Table 4-9: Results of rock mass properties from Roc Lab software for RS-2

| Geologic units | *mb* | *s* | *a* | Cohesion (MPa) | Friction angle (°) | Modulus of deformatic *Em* (Mpa) |
|---|---|---|---|---|---|---|
| MWT | *0.831* | *0.000.* | *0.536* | *0.059* | *51.3* | *921* |
| HWT | *0.492* | *0.000.* | *0.570* | *0.019* | *49* | *460* |

| | |
|---|---|
| **Hoek-Brown Classification**<br>intact uniaxial compressive strength = 19 MPa<br>GSI = 23 mi = 13 Disturbance factor = 0<br>**Hoek-Brown Criterion**<br>mb = 0.831 s = 0.0002 a = 0.536<br>**Mohr-Coulomb Fit**<br>cohesion = 0.059 MPa friction angle = 51.29 deg<br>**Rock Mass Parameters**<br>tensile strength = -0.004 MPa<br>uniaxial compressive strength = 0.194 MPa<br>global strength = 1.959 MPa<br>modulus of deformation = 921.25 MPa | **Hoek-Brown Classification**<br>intact uniaxial compressive strength = 15 MPa<br>GSI = 13 mi = 11 Disturbance factor = 0<br>**Hoek-Brown Criterion**<br>mb = 0.492 s = 0.0001 a = 0.570<br>**Mohr-Coulomb Fit**<br>cohesion = 0.019 MPa friction angle = 49.12 deg<br>**Rock Mass Parameters**<br>tensile strength = -0.002 MPa<br>uniaxial compressive strength = 0.061 MPa<br>global strength = 0.971 MPa<br>modulus of deformation = 460.30 MPa |
| *MWT rock strength compute using Roc Lab* | *HWT rock strength compute using Roc Lab* |

See (Figure 4-3) it shows slight failure of slope materials, wetting of slope surface and leek of water on the weak zone of slope face due to the percolation of logged water on the quarry site. Critical slope two (RS-2) exist below the quarry site one of Ajima dam.

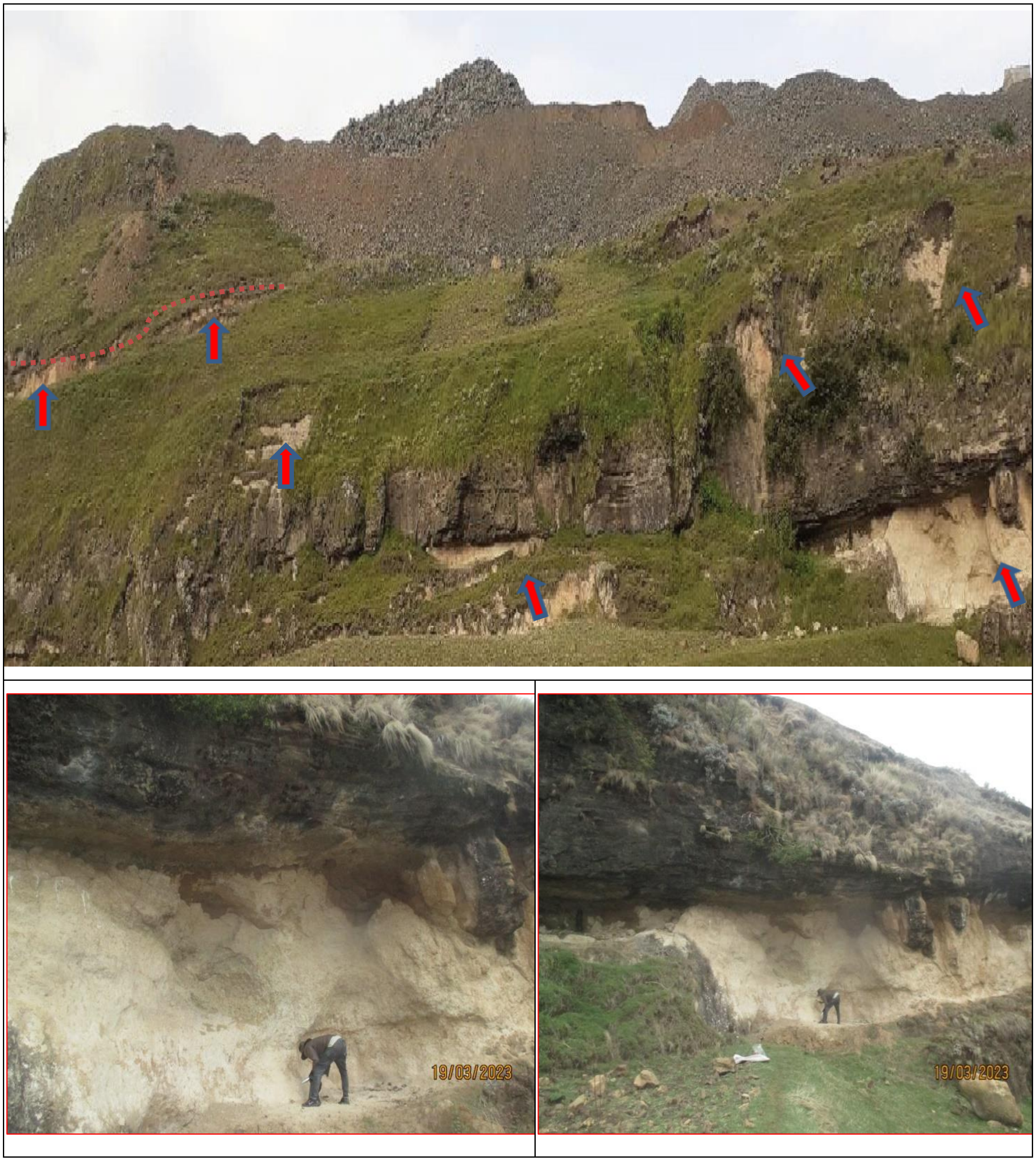


Plate 4-3: Field photo on critical slope section one (RS-2) below the quarry site one

NB: The red dot line and arrows (see Plate 4-3) can show the step down movement of the slope parts due to slight disturbance of the critical slopes.

## 4.4 Estimated Young's modulus of soil on RS- 3

The UCS result presented as 77.25 Kpa for tuff soil, and 177.46 Kpa for clay soils and cohesion and friction angle of tuff soil and clay are shown in (Table 4-10).

Table 4-10: The physical and mechanical parameters of critical slope (RS-3) obtained in lab test

| Lithology | UCS (Kpa) | Young's Modulus (MPa) | Unit Weigh *γ(kN/m$^3$)* | ***C****(Kpa)* | *Angle* ***Φ****(°)* |
|---|---|---|---|---|---|
| Tuff soil | 77.25 | 2.912 | 14 | 13.33 | 34.21 |
| Residual clay | 177.4 | 5.629 | 19 | 28.67 | 12.13 |

Plate 4-4: Field photo on critical slope section one (RS-3) on the left side of dam axis.

The deformation modulus of soil and a rock mass is an important input parameter in any numerical modelling analysis of slope.

The stress strain curve of soil obtained from laboratory tests is the basis to determine soil parameters like: the elastic modules corresponding, in a sense, with Young's modulus E, as in the case of soil the stress-strain relationships.

Young's modulus ($E_d$) of Tuff soil and residual clay soil was generated from the slope of stress – strain graph, using the unconfined compressive strength test data. The result of young's modulus of tuff soil and residual clay soil are presented below (see Figure 4.5 B) and (Figure 4.6 B) respectively.

The laboratory test was conducted at the laboratory facilities at ECDWE. All laboratory test series for this work can be seen in the Appendix part of the thesis.

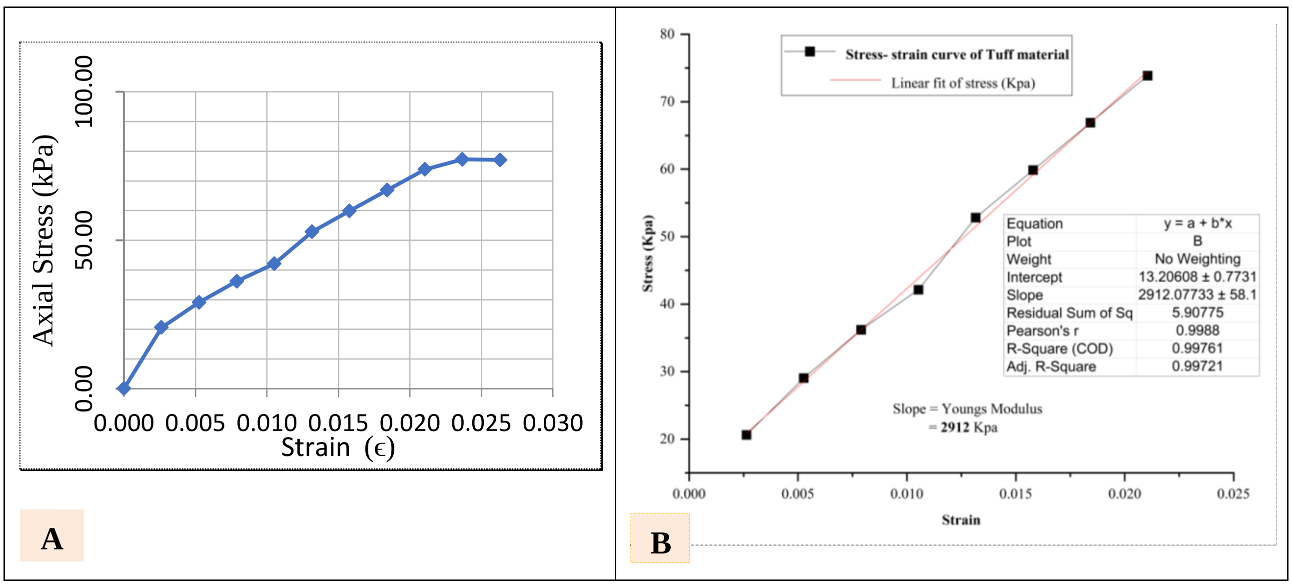

Figure 4-5: **A)** stress-strain graph, and **B**) Young's modulus graph of tuff soil of RS- 3

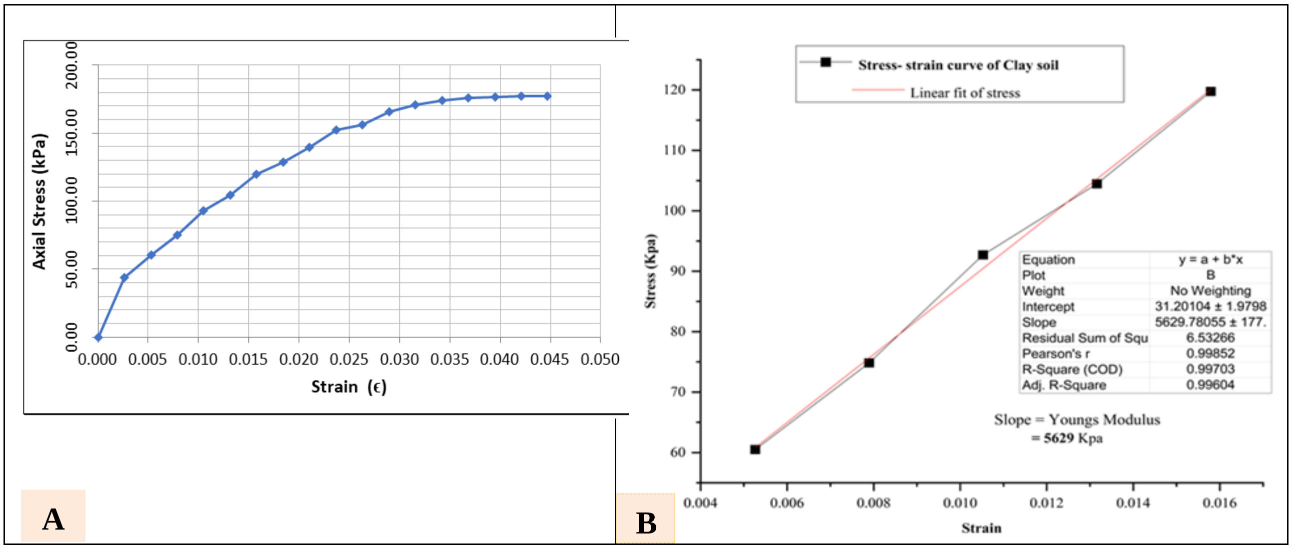


Figure 4-6: **A)** Stress-strain graph, and **B**), Young's Modulus of residual clay soil from RS- 3.

## 4.5 Rockmass characterization on the critical slopes, RS-1 and RS- 2

The joint conditions and weathering conditions of geologic materials on the selected slopes were traced has been done. Based on the GSI chart the value was set for the selected rock slope based on field observation of rockmass conditions (see Table 4-11).

Table 4-11: Summary of rock mass characterization for GSI method on RS-1 & RS-2

| Rockmass Properties | RS- 1 | RS-2 | |
|---|---|---|---|
| | WFR | MW tuff | HW tuff |
| Rockmass surface condition | Highly fractured, gouge < 5 mm infill with clay | Moderately weathered and sheared formation of rockmass surface | Surfaces are rough, highly weathered and sheared fragmental blocks |
| Discontinuity condition | Weathered and four set of jointed block | Joint with weathered surface | Highly weathered joint surface |
| Estimated GSI | 30-35 | 20-25 | 10-15 |

Where; WR- Weathered rhyolite, MW- Moderately welded, WFR= weathered and fractured rhyolite

Table 4-12: Estimated GSI value for rockmass classification in the critical slopes

| GSI | Rockmass quality | Estimated GSI value on the selected critical slope |
|---|---|---|
| < 20 | Very poor | [10-15] for bottom layer RS-2 |
| 21-40 | Poor | [20-25] for upper layer of RS-2 and for bottom layer of RS-1,<br>[30-35] for Weathered and fractured rhyolite unit in RS-1 |
| 41-60 | Fair | -- --- -- -- |
| 61-80 | Good | -- -- --- -- |
| 81-100 | Very good | -- -- -- --- |

## 4.6 Estimated deformation modulus from GSI

Using suitable estimation of rockmass of UCS and GSI, then correlate the deformation modulus with those values to have the critical slopes stability model in FDM modelling. Deformation modulus of tuff rock depends on several factors such as; degree of weathering, composition, internal porosity, and confining applied pressure on the rock. However, the strain rate of soft rock is higher than hard rock under the same stress condition. Pyroclastic tuff rock has a low uniaxial compressive strength which is even more weakly interlocked fragment material in the existing slope rock unit. Field estimation has been taken on the critical slopes rockmass to have of GSI value and empirical correlation has been done using the existing equations from adopted literature works. However, the estimated GSI value in each critical slope directly used in the Rock Lab software as input parameter to compute rockmass modulus of deformation. The empirically computed value of deformation modulus of rockmass has been illustrated below; see (Table 4-13).

Table 4-13: Summary of estimated deformation modulus of rock mass using empirical relations with GSI value.

| Critical Slope | Rock unit | Eq. (3.15) | Eq. (3.16) | Eq. (3.17) | Eq. (3.18) | Average Em (GPa) | Empirical equations proposed by: Hoek et al., (1997)....... *Eq. (3.15);* Majdi et al., (2012) ….. *Eq. (3.16);* Ghamgosar et al., (2010)….. *Eq. (3.17);* Gokceoglu et al., (2003) ….. *Eq. (3.18)* |
|---|---|---|---|---|---|---|---|
| RS-1 | WFR | 1.94 | 3.79 | 2.846 | 1.950 | 2.63 | |
| | MWT | 0.40 | 1.55 | 0.783 | 0.736 | 0.86 | |
| RS-2 | HWT | 0.26 | 1.15 | 0.509 | 0.531 | 0.62 | |
| | MWT | 0.53 | 1.85 | 1.013 | 0.894 | 1.07 | |

From this computation it can be observed that every empirical correlation can estimates the value of modulus of deformation, Em which has different results. The equations proposed by Majdi et al., (2012) and Ghamgosar et al., (2010) indicated very high values compared to other equations. Among rest of the correlations by Hoek et al., (1997) and Gokceoglu et al., (2003) method indicates most conservative estimation with lesser *Em* among the other empirical equations used in this study. However, when compared Em values computed using RocLab, the empirical estimated Em values are still having higher results.

## 4.7 Estimated Poisson's ratio of rockmass for RS-1, RS-2

Poisson's ratio plays an undeniably important parameter in slope analysis in addition to the parameter of deformation of rock masses.

Table 4-14: Hoek- brown constant, minimum and maximum Poisson's ratio of intact rock Gercek (2007), also from the published data by Hoek and Brown (2019).

| Type of the rock | Hoek-Brown constant, mi | Poisson's rate value (v) | | |
|---|---|---|---|---|
| | | min | max | Mean |
| Basalt | 25 ± 5 | 0.1 | 0.35 | 0.225 |
| Granite | 32 | 0.1 | 0.32 | 0.21 |
| Rhyolite | 25 ± 5 | 0.08 | 0.32 | 0.20 |
| Shale | 7 | 0.05 | 0.31 | 0.18 |
| Tuff | 13 ± 5 | 0.1 | 0.27 | 0.185 |

Table 4-15: Estimated Poisson's value of critical slopes rock mass using empirical relations with V*i*, *mi (value of its intact rock)* and GSI value. Eq. (3.13) and Eq. (3.14) for 1 and 2 respectively

| Poisson's empirical equation for rock mass | RS- 1 | | RS- 2 | |
|---|---|---|---|---|
| | WFR | MWT | MWT | HWT |
| 1. V*rm* = -0.002GSI + Vi + 0.2 | 0.32 | 0.33 | 0.34 | 0.32 |
| 2. **V***rm* = **-** 0.002GSI - 0.003mi + 0.457 | 0.29 | 0.36 | 0.36 | 0.35 |
| Average of Poisson's value (Vrm) of rock mass | 0.30 | 0.34 | 0.34 | 0.35 |

Table 4-16: Estimated Shear and bulk modulus of rock mass using Eq. (3.19) & Eq. (3.20)

| Empirical relations | RS- 1 | | RS- 2 | |
|---|---|---|---|---|
| | WFR | MWT | HWT | MWT |
| $K=\frac{\mathbf{E}}{\mathbf{3(1-2V)}}$ (GPa) | 2.26 | 0.94 | 0.69 | 1.11 |
| $G=\frac{\mathbf{E}}{\mathbf{2(1+V)}}$ (GPa) | 1.0 | 0.32 | 0.22 | 0.40 |

Where, WFR is weathered and fractured rhyolite, MWT is moderately weathered tuff rock and HWT is highly weathered tuff rock, K is bulk and G is shear modulus.

In the rockmass characterization of the slope rock materials deformation modulus and poison's ratio were estimated. However, the values estimated using empirical method was much greater than the values computed using Roc Lab software, meaning the more overestimated of elastic modulus of rockmass were observed in empirical correlation using GSI value. In the present study of numerical slope analysis Roc Lab output of rockmass properties has been utilized.

## 4.8 Stability analysis approaches for the selected slopes

The present slope analysis on the selected reservoir slope has been done using conventional kinematic method and numerical modelling. However, for the selected slopes numerical modelling using FLAC2D were important to investigate slope stability and deformation behaviors of slope materials with factor of safety. Thus, in the present study most of the slope analyses were conducted using Finite difference method using FLAC 2D software.

## 4.9 Kinematic approach for upper section of RS-1

In the present kinematic analysis performed to examine which modes of failure can possibly occur in the rock mass of the slope. Analysis requires the detailed evaluation of rock mass structure and the geometry of existing discontinuities contributing to block instability. Program DIP software allows for visualization structural data using Stereonet, determination of the kinematic feasibility of rock mass and statistical analysis of the discontinuity properties based on the geological data of the rock mass structures on the exposed slope. Which is commonly used for determining the modes of rock slope failure by plotting the plane's strike and dip in conjunction with the discontinuity of a plane.

Table 4-17: Input parameters used in DIP 7 software for kinematic modeling for highly fractured and weathered rhyolite rock mass on upper slope section of RS- 1

| Slope layer | Slope face orientation D/DD (°) | | Joint set orientations (dip and dip direction) Respectively, |
|---|---|---|---|
| WFR unit in upper (RS-1) | $80^0/150^0$ | JS1 (°), | 80/310, $83^0$/74, $78^0$/007, $85^0$/248, $87^0$/214, |
| | | JS2 (°), | 80/318, 87/038, 83/112, 85/268, 60/056, |
| | | JS3 (°) | 63/082, 86/190, 85/122, 86/270, 80/250, |
| | | JS4 (°) | 80/326, 88/210, 80/90, 50/170, 70/170 |

## 4.10 Modelling Slopes and Analysis Steeps in FLAC 2D

In the present study to conduct slope stability analysis FLAC 2D of a continuum numerical model has been utilized. The profile of slope is divided into two different geometrical layers. The slope profile is constructed based on the real field geometry, height and inclination of slope sections. Geometry of the slope has to be decided and was built through sketching tool on the modelling work space of FLAC 2D software. After building the geometry of the problem, assigning geotechnical specifications of rockmass and soil layers has been needed. Finally, the computation was performed to generate contour plot of the slope and safety factor in each selected critical slopes. The following procedures have been performed in FLAC2D slope analysis in the present study.

Sketch or build the geometry of slope …, Assign the material properties of soil and rock mass in the selected model type …, Insitu (fix boundary condition, apply stress)..., Setting (gravity)…, Plot to show (displacement contour, stress-strain condition, FOS) in graphical way…, Run (analysis the model) to display graphical output (see Figure 4.7).

**Build/Sketching:** All the geometry of the slopes face and slope layers has been generated to model the existing critical slopes. The geometric creation of slope in FLAC 2D is using sketch or using commands of FISH, however in this study sketching has been used. Selection of the location and type of boundary conditions is very important. If the boundaries are too close to the area of interest, the boundary effects may influence the modelling results. The selected zone size can have a significant effect on key modelling results such as the factor of safety (FOS). A small zone size can produce a large model and longer time to run the slope model.

**Model:** Mesh has been created using automated zoning, the material being modelled (e.g., rock mass or soil) is divided into elements (or a mesh). Each element is assigned a material model and properties and the material models are stress-strain relations that describe the material behavior.

**Initial conditions:** In the FLAC 2D assigning the constitutive model, properties of rocks and soils, assign the roller (side) and fixed (bottom) boundaries has been done. The strength parameters (for the soil, rockmass and discontinuities) are generally very important, and will have a significant impact on the predicted stability/FOS. The adopted elastic properties (Young's modulus and Poisson's ratio) will generally have a great effect on the model displacements but not generally on the FOS.

## 4.11 FLAC 2D Slope Modelling Conceptual Framework

To compute the slope stability under different slope conditions the series of multiple steps from the beginning to the end has been performed with appropriate data entry in each step. The conceptual model has been constructed for FLAC 2D slope analysis. In this case the factor of safety and stress strain behavior of the slopes material can be displayed as an output of FLAC2D after step wise analysis (see Figure 4-7).

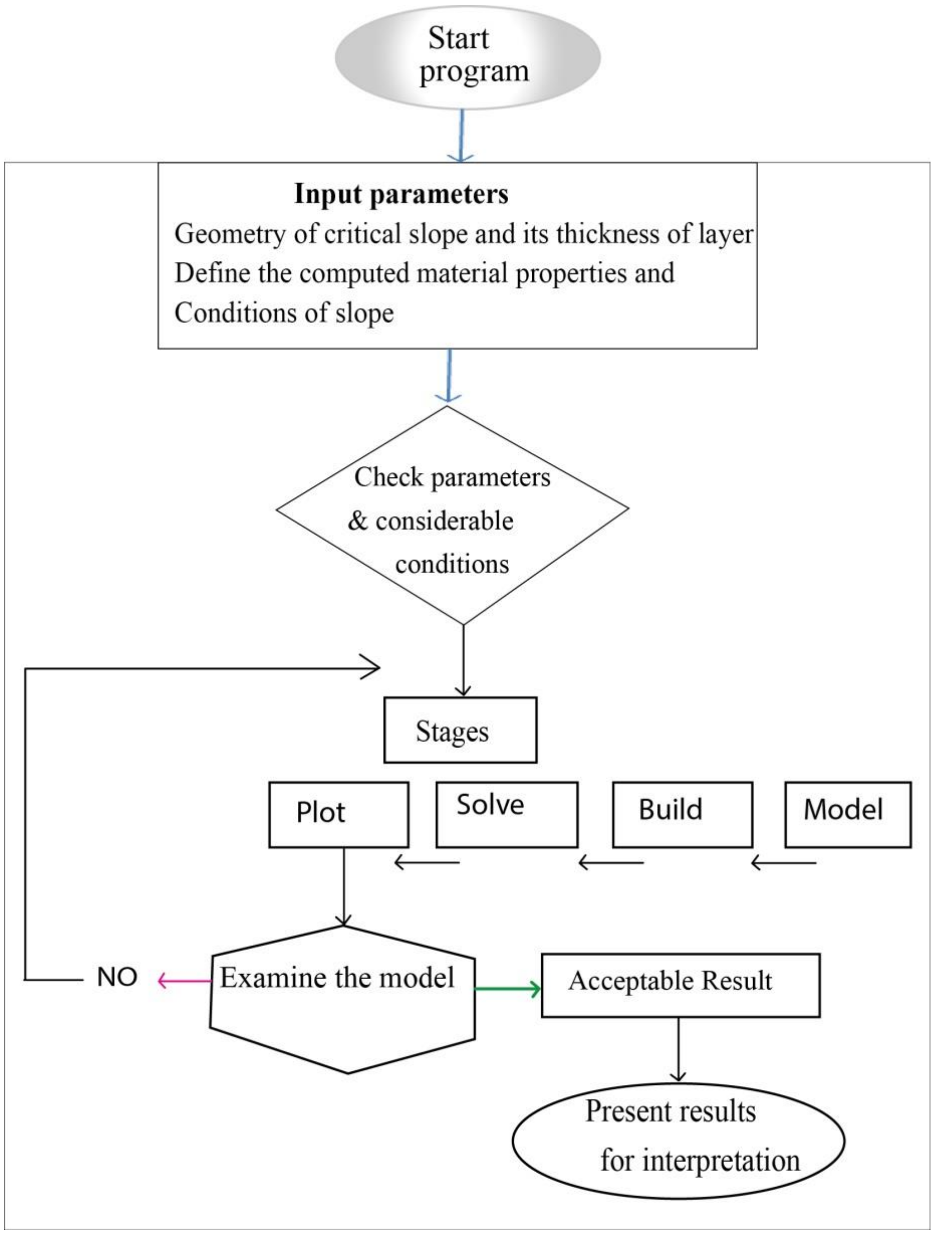


Figure 4-7: Analysis procedure in FLAC 2D program

# CHAPTER 5 : DATA ANALYSIS, RESULTS AND DISCUSSION

## 5.1 Kinematic analysis on RS-1

Their discontinuity orientations were displayed using DIP V7 software and resulting direct toppling of rock mass slope face. The projection of lower-hemisphere in equal-area was selected for DIP software. Determining the magnitude of orientation of potentially unstable block of rockmass in the slope exposure were the primary tasks. As a result, three dominant joint sets were distinguished with their respective orientations which have major joint discontinuity set. The strike of the slope exposure is around $150^0$, dip of $70^0$ and dip direction of slope is $80^0$ (see Figure 5–1).

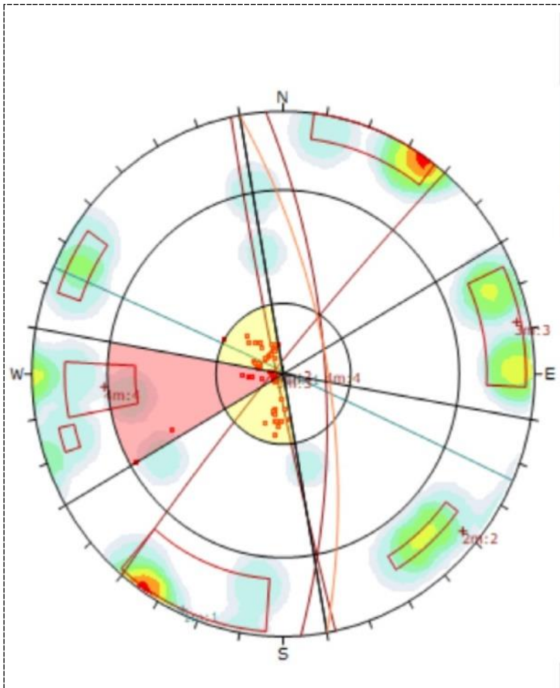


| Color | Density Concentrations |
|---|---|
| | 0.00 - 1.80 |
| | 1.80 - 3.60 |
| | 3.60 - 5.40 |
| | 5.40 - 7.20 |
| | 7.20 - 9.00 |
| | 9.00 - 10.80 |
| | 10.80 - 12.60 |
| | 12.60 - 14.40 |

| | |
|---|---|
| Contour Data | Pole Vectors |
| Maximum Density | 13.14% |
| Contour Distribution | Fisher |
| Counting Circle Size | 1.0% |
| Kinematic Analysis | Direct Toppling |
| Slope Dip | 70 |
| Slope Dip Direction | 80 |
| Friction Angle | 30° |
| Lateral Limits | 20° |

| | Critical | Total | % |
|---|---|---|---|
| Direct Toppling (Intersection) | 13 | 210 | 6.19% |
| Oblique Toppling (Intersection) | 59 | 210 | 28.10% |
| Base Plane (All) | 1 | 21 | 4.76% |
| Base Plane (Set 4: 4) | 1 | 2 | 50.00% |

Figure 5-1: Kinematic analysis indicating failure type and direction (shaded area of the sphere)

### 5.1.1 Mode of rock slope failure in RS-1

The failure mode depends on the geometric interaction of the existing discontinuity orientations in the rockmass of the reservoir slope. The kinematic model of geologic data can identify and shows the possible likely potential failure mode of the rock slope. Thus, the upper section of highly jointed rhyolitic rockmass slope exhibited toppling failure. The failure mode is very familiar in the steep rock slope where, there is steeply dipping joint into the natural reservoir hillside set rotated on the base of the discontinuous block of rockmass.

## 5.2 Numerical model interpretation

Assessing stability condition of the critical slopes was based on the contour plot indicators such as displacements and stress-strain of the slope materials. Numerical model for FOS computation has been modeled and analysed to have deformation contour plots and FOS. In this study the FLAC 2D analysis of critical slopes has been illustrated graphically under dry and saturated conditions.

## 5.3 Stability analysis of reservoir rim slopes using FLAC 2D

In the present study slope analysis results from FLAC2D can clearly shows the maximum shear strain contours for the critical slope using the mean shear strength analysis with FOS.

### 5.3.1 Analysis critical slope section (RS-1) using FLAC2D

The maximum shear strain contours through-out the model is plotted for Hoek - Brown material in (Figure 5-2). Movement of the geologic material concentrated along the bottom side of the slope face. It can be observed that the field slope is stable under static dry condition (FOS=1.63).

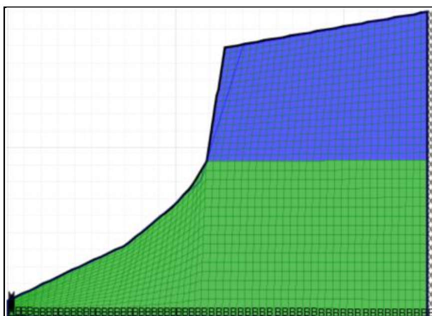

Upper layer is weathered & fractured rhyolite and lower layer is moderately weathered tuff rock with 7m & 10m thickness respectively.

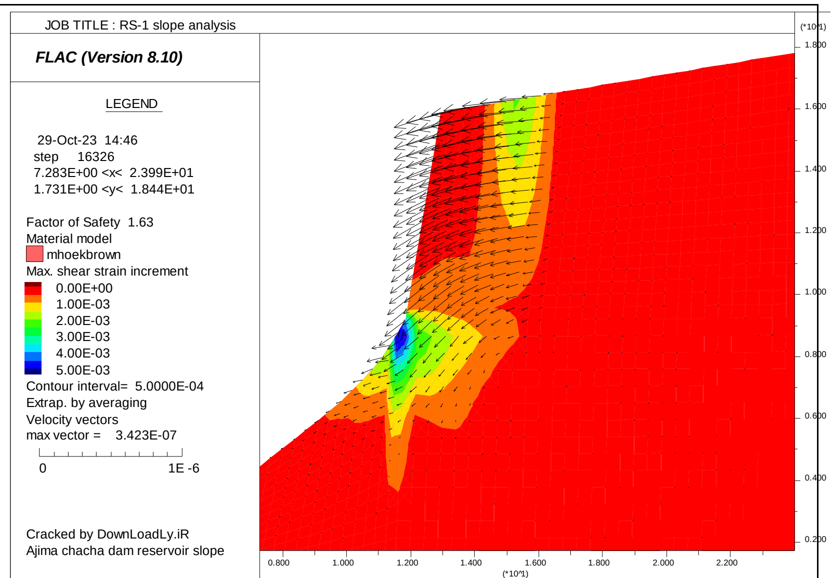


Figure 5-2: Slope displacement contour and factor of safety plot for RS- 1 under static dry condition

The critical reservoir slope (RS-1) was analysed in static saturated condition to have FOS and the contour plot of the model shows the deformation of slope layer (see Figure 5-3).

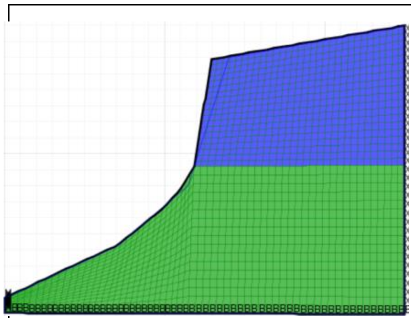

Upper layer is weathered & fractured rhyolite and lower layer is moderately weathered tuff rock with 7m & 10m thickness respectively.

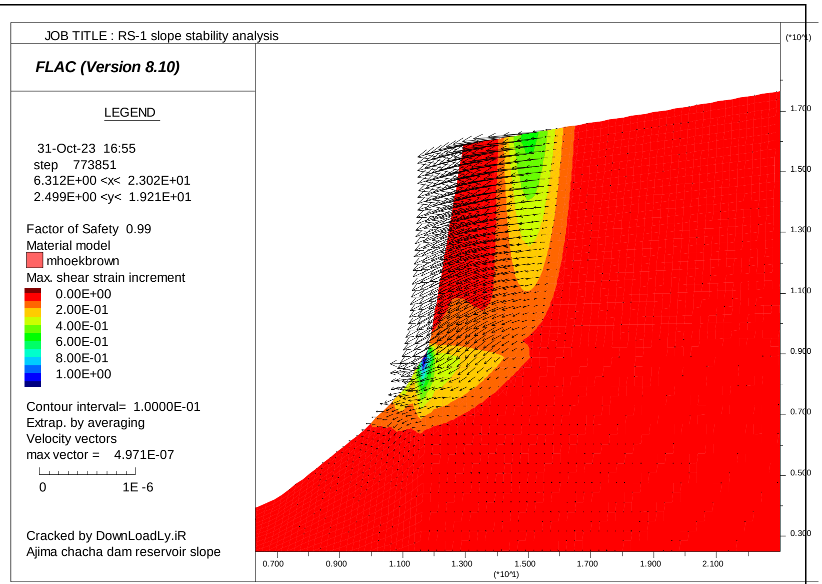


Figure 5-3: Slope displacement contour and factor of safety plot for RS- 1 under static saturated condition

## 5.3.2 Analysis critical slope section (RS-2) using FLAC2D

The maximum shear strain contours throughout the model are plotted for Mohr-Coulomb material model see in (Figure 5-4). Movement of the geologic material concentrated along the mid side of the slope face. It can be observed that the field slope is stable under static dry condition with a safety factor (FOS) 1.42.

The contours for displacement and deformation show a clear failure patterns that goes through the mid of slope materials and extends to the base of the slope face having weak geology.

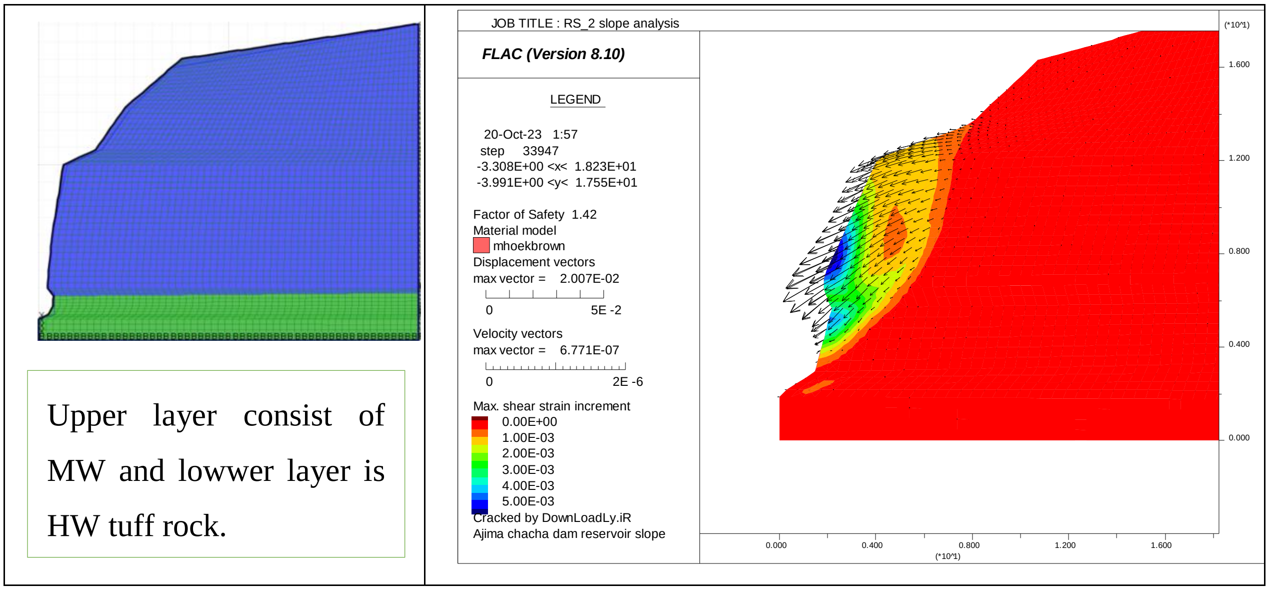


Figure 5-4: Factor-of-safety plot for reservoir rim slope RS-2 in static dry condition

As it can be seen from (Figure 5-4) the FLAC2D model produced noticeable deformations along the weak layer of tuff material on slope RS-2. It can be observed that the field slope is stable under dry condition (FOS=1.42).

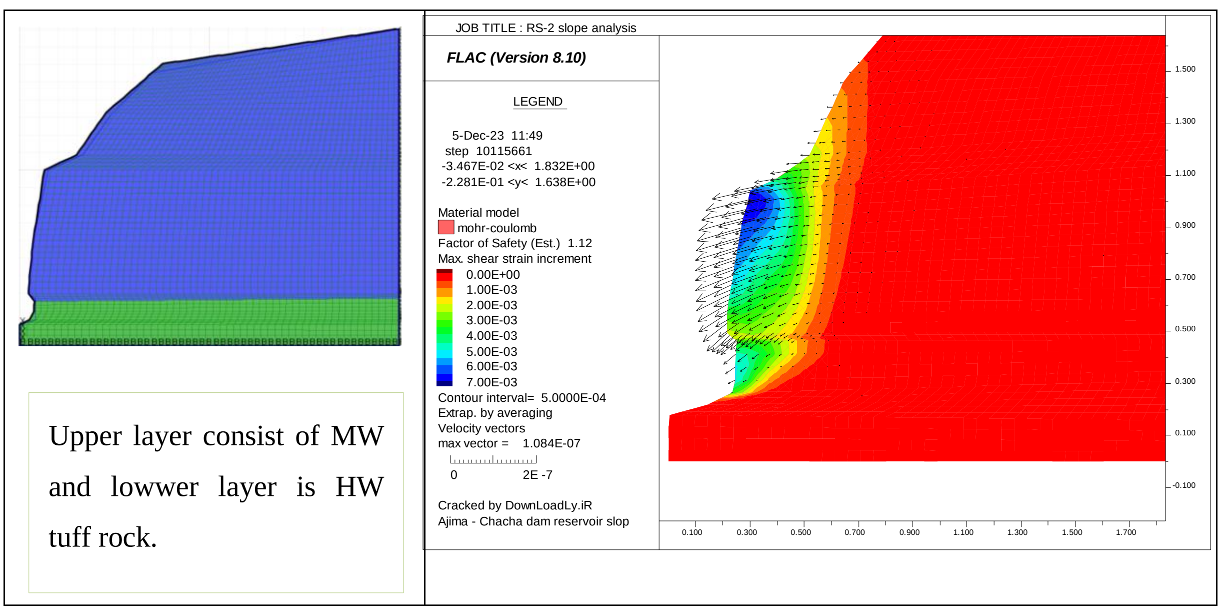


Figure 5-5: Factor-of-safety plot for reservoir rim slope RS-2 in static saturated condition

As it can be seen from (Figure 5-5) the FLAC2D model produced noticeable deformations contour and the slope has (FOS=1.12) under saturated slope condition.

### 5.3.3 Analysis of critical slope section (RS- 3) using FLAC2D

As it can be seen from (Figure 5-5) the FLAC2D model produced noticeable deformations on the foot of slope section. The slope has an inclined semicircular slip surface and of geologic materials has produces high-strain on the weak tuff material at the toe of the slope. It has been observed that the field slope is unstable under static saturate condition (FOS=1.32).

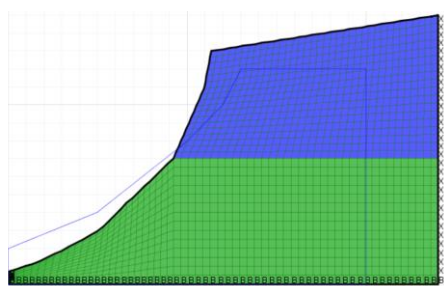

Upper layer consist of residual clay soil and lowwer layer is decompose tuff soil with 6m & 8m thickness of layer respectively.

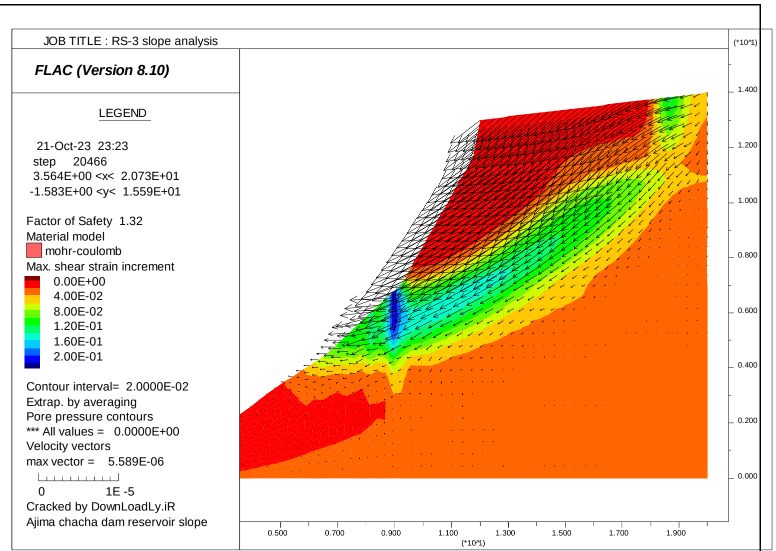


Figure 5-6: Factor-of-safety plot for reservoir rim slope three RS - 3 in static dry conditions

Factor-of-safety calculation has done and stable under the static saturated condition (Figure 5-6). The state of the slope has a FOS of.

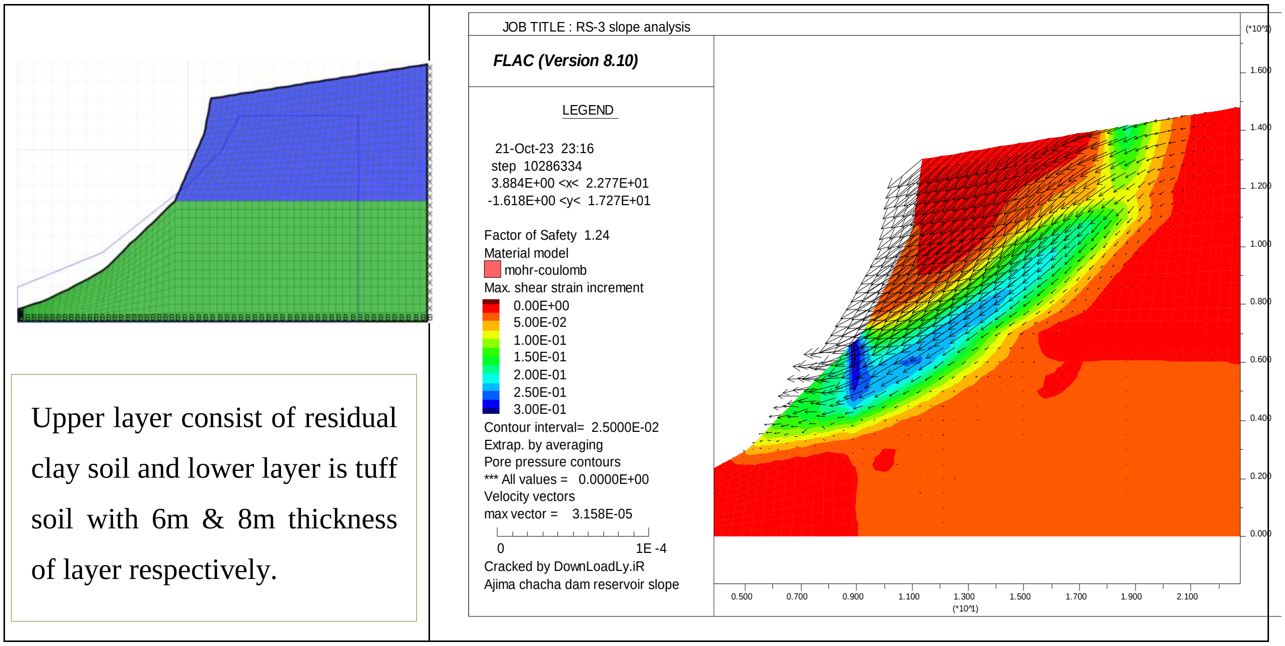


Figure 5-7: Factor-of-safety plot for reservoir rim slope three RS - 3 in static saturated conditions

The factor of safety values indicates that the slopes were critically stable at section RS-2 and RS-3 under the two conditions of dry and wet slopes. RS-1 under dry condition was stable. However, the slope is unstable for saturated conditions which indicate that the slope stabilization measures have to be undertaken at this slope section.

The main thing from the above FLAC 2D output is that the slope having high value of safety factor does not mean the slope is safe. However, evaluation of slope stability can help to get a better understanding and shows the of the stress-strain behavior or deformation rate of slope materials.

## 5.4 Effect of mesh density

Different options of mesh densities were considered in FLAC 2D analysis, the mesh zone may range from very fine mesh to a very coarse size. As the mesh density or size increases, the number of discrete model elements increases. The factor of safety decreases slightly with increasing of mesh density in the slope model. Even though it takes more analysis time and needs a high-performance computer, the accuracy of the analysis increases with increasing the density of mesh. Analysis time is high for large dimensional slope geometry. All in all, the selection of mesh size mainly depends and aimed for accurate work of model analysis.

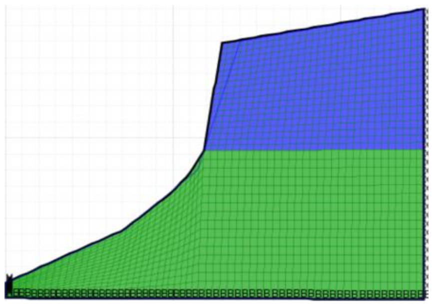

Upper layer is weathered rhyolite with 7 m thickness and lower layer is highly weathered tuff rock layer with 10m thickness.

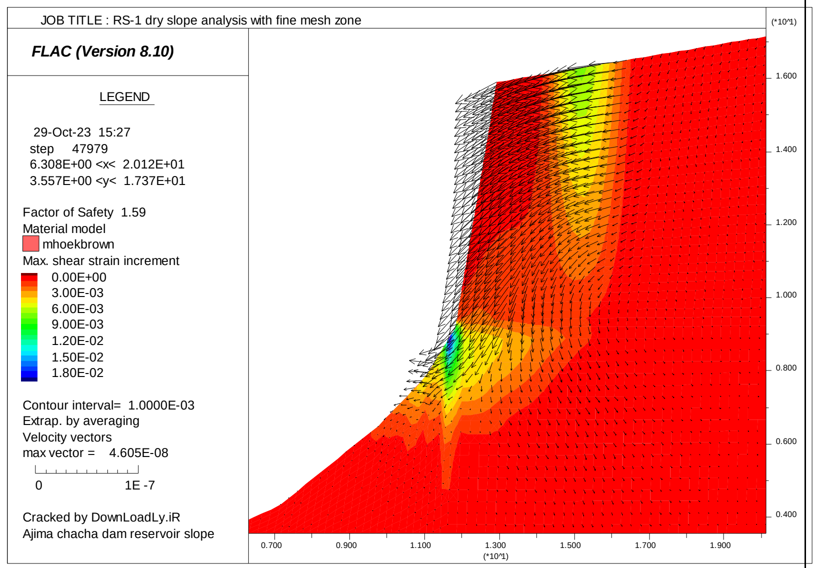


Figure 5-8: Shear strain contour plot of RS-1 under static dry condition with fine mesh zone.

The mesh size can has small variation of safety factor compared with the medium mesh. With same parameters and material properties of the slope RS-1 has a FOS of 1.63 and 1.59 in medium and fine mesh size model respectively.

## 5.5 Effect of the UCS and GSI variations on slope stability

As the weathering degree increases in a rock, it increases the clay content on the weathered rockmass and results the decrease of GSI value. The estimation of the GSI system required better knowledge and skills about collecting and evaluating the field data on the rockmass. However, the quantitative and empirical model approaches are easy to be used for the assessment of exposed rock mass slopes.

Extensive weathering and moisture on the rockmass can play a crucial role in lowering the strength of the rock materials. The major controlling factors for uniaxial compressive strength (UCS) can be: mineral composition in the rockmass, rockmass structure and its texture, jointing and heterogeneity, moisture content in the rockmass and the state of stress on the rockmass. The uniaxial compressive strength (UCS) values of weak and soft rocks are reduced. These the GSI and UCS variation can directly affect the reduction of rockmass deformation modulus and with the values of safety factor of the slopes in the computed output of FLAC 2D.

**In this study,** an attempt has been made to a better understanding of failure mechanism and deformation of slope materials through developing numerical contour model. The contour models were developed to evaluate the distribution of stress within the slope layers. The results show that the vertical stress distribution and a certain distance from the upper slope crest can plays a significant role in the deformation of the lower slope materials.

When a slope consists of a horizontal weak rock or soil overlaid by some vertical strong rock the slope is prone to a secondary toppling failure. In RS-1 the slope rock column impose pressure on the lower continuous weak tuff rock which leads to a differential settlement at the base of lower slope mass. Also, there is initiation of crack on the upper middle part of the RS-1 slope, which may lead to toppling of the upper slope section. The shear or toppling failure of the slope not only depends on the material's strength but also on the geometry and the slope column distance.

**In this study**, a more thorough a finite difference method of slope stability analysis is presented. All the three critical slopes were analyzed in both static dry and saturated condition and the results of analysis are summarized (see in table 5.2). From the result of FLAC 2D analysis, slope of RS-1, RS-2, and RS-3 are stable in static dry condition which is greater than minimum required value of one and has a FOS of 1.63, 1.42 and 1.32, respectively. The FOS for the slope RS-1 has comes out to be 0.99 in case of saturated condition. Therefore, these slopes require stabilization. A typical contour plot of slope RS-1in fine mesh zone under static dry condition is illustrated (see Figure 5.8). On the RS-1 contour plot indicating that the vertical slip surface starts from the top of the slope indicating the toe slope has getting failure or settle.

Table 5-1: Summary of stability analysis of selected critical slopes

| Critical slope sections | FOS in normal conditions | FOS in saturated conditions | Description of FOS result |
|---|---|---|---|
| RS-3 | 1.32 | 1.24 | Safe in all condition |
| RS- 2 | 1.42 | 1.12 | Safe in all condition |
| RS- 1 | 1.63 | 0.99 | Unsafe in saturated condition |

# CHAPTER 6 : CONCLUSION AND RECOMMENDATIONS

## 6.1 Conclusion

The purpose of this study was to evaluate the critical reservoir slopes of Ajima dam in north Shoa, Ethiopia. This was done through slope stability modeling, which involved extensive fieldwork and laboratory testing. During the field study, critical slope sections were identified, in situ measurements were taken, and in rock slope the discontinuity orientation was assessed. In addition, Schmidt hammer testing was carried out on selected rock slope surfaces, and representative rock samples were collected for laboratory testing. The lab tests aimed to determine the index and geotechnical characteristics of the rocks and soil materials, which is essential for the characterization and analysis of critical slope materials.

The critical reservoir slopes in the Ajima dam area consisted mainly of fractured and weathered rhyolite units and medium to highly weathered tuff rock units. UCS value of the slope rock has been measured using Schmidt hammer. The rhyolite rock mass had a high degree of weathering and fracturing in RS-1, which had a medium strength between 25-50MPa with a UCS value of 49.8Mpa measured in uniaxial compressive test. The moderately weathered tuff rock unit in the lower slope section of RS-1 had a low strength of 17 Mpa (5-25MPa). A tuff rock unit in RS-2 had a UCS value of 19MP and 15Mpa for the upper and lower slope layers respectively. Highly varied compressive strength occurred depending on the degree of weathering on the exposed slope. The deformation modulus was computed through empirical correlation with the GSI value of the rock mass and also through Roc Lab software. However, the value computed through Roc Lab was lower than that of the computed values from empirical correlations. The computed moduli of deformation of rock mass through Roc Lab were utilized as input parameters for numerical analysis of the critical reservoir slopes.

Kinematic modeling was performed on the upper rock slope layer of RS-1, which showed toppling failures. FLAC2D modeling was done under static dry and static saturated slope conditions. The FLAC 2D result showed that RS-1, RS-2, and RS-3 are stable under static dry conditions. However, RS-1 was found to be unstable under static saturated conditions. RS-2 and RS-3 were stable in all conditions. The stability condition in the three critical slopes was determined by the FOS for FDM (stable if FOS >1 and unstable if FOS <1).

FLAC 2D provided more useful information about the deformation and displacement at any point of the slope layer. The deformation contours of the analyzed slopes on the FLAC 2D showed the nature of the deformation of the slope materials on the output of the contour plot. The maximum deformation and displacement occurred at the weak and steep slope layers. Less deformation of slope materials occurred at the strong layer and on a less steep gradient of the slope layer. It was observed that the main reasons for the failure of natural slopes were the presence of weak and weathered geologic materials in the slope layers. Additionally, the slope analysis of the selected slope showed that water saturation in the reservoir slopes was a cause for slope safety reductions.

In conclusion, stress-deformation analysis and factor of safety prediction in finite difference method can demonstrate the behavior and mechanism of failure at dry and saturated conditions of the slopes. This can help to identify the sensitive slope layers for slope failure and provide appropriate safety measures.

## 6.2 Recommendations

Based on the findings of the study, the following recommendations have been made for the slopes of the Ajima Dam reservoir. It is usually challenging to stabilize slopes due to their complex geological and geomorphological nature. However, it is essential to consider safety measures to reduce driving forces and increase the resisting forces or shear strength of slope materials. This can help maintain the slopes in a safer condition for a longer period. Therefore, based on the identified predisposing factors for slope failure, mitigation mechanisms should be implemented.

Some of the slope safety measures in the critical slopes includes, providing adequate surface drainage to enhance the shear strength of slope materials on critical reservoir slopes. Moreover, a significant amount of quarry-logged water above RS-2 can seep through the fractured and weak zone to the RS-2 slope face, leading to slope failure. Thus, it is recommended to use either blanket the quarry excavation with clay soil or divert the logged water to the other side of the existing slope. On RS-1 the slope is unstable in saturated condition, thus avoiding surface water saturation on the existing slope.

The study strongly recommends further assessment of the effect of water level fluctuation or drawdown on the instability of the reservoir slopes. Additionally, dynamic reservoir slope analysis should be conducted to fully understand the dam slopes for longer dam safety. This is crucial because the Ajima dam is located near the margin of the MER system.

# REFERENCES


Abramson L.W., (2002). Slope stability and stabilization methods. Published by John Wiley & Sons Inc, Hoboken. LINK [ ]

Abbas, S.M., & Konietzky, H. (2017). Rock mass classification systems. Introduction to Geomechanics, 9(2017), 1-48. LINK [ ]

ADSWE, (2016). Geological and geotechnical feasibility study and detail design of Ajima earth dam and large scale irrigation project final report *Volume II;* pp149.

Alex Jacob1 et al., (2018). Slope stability analysis using plaxis 2D, International Research Journal of Engineering and Technology (IRJET), Volume: 05 Issue: 04. LINK [ ]

Ajibade, T.F., Nwogwu, N.A., Ajibade, F.O. *et al.* Potential dam sites selection using integrated techniques of remote sensing and GIS in Imo State, Southeastern, Nigeria. *Sustain. Water Resour. Manag.* **6**, 57 (2020). LINK [ ]

Ali Sadeq Abass, Asmaa Dheyauldeen Najeeb. (2018). Analysis of Seepage through Embankment Dams as Case Study (Al-Shahabi Dam) in Iraq, International Journal of Sciences: Basic and Applied Research (IJSBAR), Volume 40, No 2, pp 7-17. LINK [ ]

ASTM, (2001). Standard test method for determination of rock hardness by rebound hammer method. ASTM Stand. 04.09 (D 5873-00).

Atalay Ayele. (2017). Probabilistic seismic hazard analysis (PSHA) for Ethiopia and the neighboring region, Journal of African Earth Sciences 134 (2017) 257e264. LINK [ ]

Barton, N. and Chobey, V. (1977). The shear strength of rock joints in theory and practice. Rock Mech., 10, 1–54. LINK [ ]

Basahel H and Mitri H (2018). Application of rock mass classification systems to rock slope stability assessment: A case study Journal of Rock Mechanics and Geotechnical Engineering Application of rock mass classification systems to rock slope stability assessment: A case study. Journal of Rock Mechanics and Geotechnical Engineering, 9(6), 993–1009. https://doi.org/10.1016/j.jrmge.2017.07.007. LINK [ ]

Berhane et al,. (2013). Water leakage investigation of micro-dam reservoirs in Mesozoic sedimentary sequences in Northern Ethiopia. Journal of African Earth Sciences, 79, Springer, pp.98-110. LINK [ ]

Bieniawski, Z. T. (1978). Determining rock mass deformability: experience from case histories. In International journal of rock mechanics and mining sciences & geomechanics abstracts (Vol. 15, No. 5, pp. 237-247). LINK [ ]

Bieniawski, Z. T. (1989). Engineering rock mass classifications: a complete manual for engineers and geologists in mining, civil, and petroleum engineering. John Wiley & Sons. LINK [ ]

Bonini, M., Corti, G., Innocenti, F., Manetti, P., Mazzarini, F., Tsegaye Abebe, and Pecskay, Z. (2005). Evolution of the Main Ethiopian Rift in the frame of Afar and Kenya rifts propagation. Tectonics 24(1): 1-25.

Bowles, J. E. (1996). Physical and Geotechnical Properties of Soils, McGraw-Hill College. LINK [ ]

Brady, B. H. & Brown, E. T. (1993). Rock mechanics: for underground mining. Springer science & business media. LINK [ ]

Cala, M. & Flisiak, J. (2003). Complex geology slope stability analysis by shear strength reduction. In Brummer, Andrieux, Detournay & Hart (eds.) FLAC and Numerical Modeling in Geomechanics – 2003, Proceedings of the 3rd International Symposium, Sudbury, Ontario, Canada, 21- 24 October. pp. 99-102. Lisse: A.A. Balkema. LINK [ ]

Casagli, N., Intrieri, E., Tofani, V. *et al.,* (2023). Landslide detection, monitoring and prediction with remote-sensing techniques. *Earth Environ* **4**, 51–64. LINK [ ]

Ceballos F., and Olalla C., (2014). Relationship between RMR and GSI based on in situ data. Technical University of Madrid, Spanyol.

Chatterjee and Choudhury, (2014). Seismic analysis of soil slopes using FLAC2D and modified Newmark's approach, Geo-Congress 2014 technical papers, pp: 10. LINK [ ]

Chen, M., *et al.* 2021). Hydraulic response and stability of a reservoir slope with landslide potential under the combined effect of rainfall and water level fluctuation. *Environ Earth Sci* 80, 25: (https://doi.org/10.1007/s12665-020-09279-7. LINK [ ]

Chen, Q., & Yin, T., (2020). Modification of the rock mass rating system ($RMR_{mbi}$) considering three-dimensional rock block size. *Bull Eng Geol Environ* 79, 789–810; https://doi.org/10.1007/s10064-019-01596-x. LINK [ ]

Chugh, Yoginder & Sinha, Sankhaneel. (2015). Numerical Modeling of Roof Support Plans at 4-Way Coal Mine Intersections. LINK [ ]

Coggan, J.S., Stead, D. and Eyre, J.M. (1998) Evaluation of techniques for quarry slope stability assessment. Transactions of the Institution of Mining and Metallurgy Section B-Applied Earth Science, v.107, pp. B139-B147. LINK [ ]

Corti, G., Manetti, P., Mazzarini, F., Bonini, M., and Tsegaye Abebe, (2009). The Volcano tectonic Activity of the Main Ethiopian Rift (East Africa): Insights into the Evolution of Continental Rifting. Acta vulcanologica 20(1/2): 133-144. Link [ ]

Dawit Asmare & Trufat Hailemariam, (2021). Assessment of Rock Slope Stability Using Slope Stability Probability Classification (SSPC) System, Around Alem Ketema, North Shoa, Ethiopia, Scientific African, doi: https://doi.org/10.1016/j.sciaf.2021.e00730. LINK [ ]

Dearman, W. R. (1974). Weathering classification in the characterization of rock for engineering purposes in British practice. Bulletin of the International Association of Engineering Geology-Bulletin de association International de Géologie de l'Ingénieur, 9(1), 33-42. LINK [ ]

Deere DU, Miller RP. (1966). Engineering classification and index properties for intact rocks. Tech Report. Air Force Weapons Lab, New Mexico, No. AFNL-TR 65-116. Kirtland. LINK [ ]

Doni Apriadi Putera1 , Heru Hendrayana and IGde Budi Indrawan, (2021). Engineering Geological Characteristics Based on Rock Mass Rating (RMR) and Geological Strength Index (GSI) in Jlantah Dam Intake Tunnel, Karanganyar District. Link [ ]

Duncan, J. M., Wright, S. G., & Brandon, T. L. (2014). Soil strength and slope stability. John Wiley & Sons. LINK [ ]

Eberhardt, E. (2012). The Hoek–Brown failure criterion; In the ISRM suggested methods for rock characterization testing and monitoring: 2007-2014: pp 233-240) Springer. LINK [ ]

Eleyas Assefa, (2017). Slope Stability Evaluation for the New Railway Embankment using Stochastic Finite Element and Finite Difference Methods. Electronic Journal of Geotechnical Engineering: 22. 33-49. LINK [ ]

Elhag, A. R., & Eljack, I. H. (2016). Dam site selection using GIS techniques and remote sensing to minimize flash floods in east Nile locality (Soba Valley)-Khartoum State. *International Journal of Engineering Science Invention*, *5*(12), 50-61. LINK [ ]

Farahmand, K., (2017). Empirical methods for estimating rockmass strength and deformability properties: an overview. LINK [ ]

Fattahi, Hadi. (2017). Risk assessment and prediction of safety factor for circular failure slope using rock engineering systems. Environmental Earth Sciences. 76. 10.1007/s12665-017-6549-1. LINK [ ]

Fell, R. et al., (2005) Geotechnical Engineering of Dams; Balkema. LINK [ ]

Genevois R, & Ghirotti M (2005) The 1963 Vajont landslide. Giornale Di Geologia Applicata, 1: 41-52. LINK [ ]

Gercek, H. (2007). Poisson's ratio values for rocks, International Journal of Rock Mechanics and Mining Sciences, 44(1), pp. 1–13. https://doi.org/10.1016/j.ijrmms.2006.04.011

Griffiths D.V. & Lane P.A. (1999) Slope stability analysis by finite elements. Geotechnique; 49(3): 387-403. LINK [ ]

Hack, R. (2002). Evaluation of slope stability classification In: ISRM EUROCK'2002, Portugal Madeira Funchal, pp. 3 – 32. Lisbon, Portugal. LINK [ ]

Haregeweyn, N. et al, (2006) Reservoirs in Tigray (Northern Ethiopia): Characteristics and sediment deposition problems. Land Degradation & Development. 17. 211 - 230. 10.1002/ldr.698. LINK [ ]

Hiwot Yeshitila, (2019). Geotextile Reinforcement Possibility the case of Ajima Dam, North shoa Ethiopia; unpublished MSc thesis, Addis Ababa University, Ethiopia, pp112.

Hoek E, & Brown E., (1980). Empirical strength criterion for rock masses. Journal of the Geotechnical Engineering Division 106(GT9):1013e35. LINK [ ]

Hoek E, & Bray JD, (1981). Rock slope engineering. CRC Press, Boca Raton. LINK [ ]

Hoek E, Brown E.T., (1997). Practical estimates of rock mass strength, International Journal of Rock Mechanics and Mining Sciences, Volume 34, Issue 8,pp 1165-1186, ISSN 1365-1609,https://doi.org/10.1016/S1365-1609(97)80069-X. LINK [ ]

Hoek, E., Diederichs, M.S., (2006). Empirical estimation of rock mass modulus. Int. J. Rock Mech. Min. Sci. 43, 203–215. LINK [ ]

Hoek, E., & Brown, E. T., (2019). The Hoek–Brown failure criterion and GSI, Journal of rock mechanics and geotechnical engineering, 11(3), 445-463. LINK [ ]

Hou, X., Vanapalli, S. K., & Li, T., (2018). Water infiltration characteristics in loess associated with irrigation activities and its influence on the slope stability in Heifangtai loess highland, China. Engineering Geology, 234(1), 27–37.https://doi.org/10.1016/j. enggeo.2017.12.020. LINK [ ]

Hudson JA, & Harrison JP (1997). Engineering rock mechanics. Pergamon, London ISRM 1979. LINK [ ]

Hussain S., et al., (2021). Proposing a Viable Stabilization Method for Slope in a Weak Rock Mass Environment using Numerical Modelling: a Case Study from Cut Slopes. Journal of Mining and Environment (JME) Vol. 12, No. 4. LINK [ ]

Hussain G, Singh Y, Bhat G M, Sharma S, Sangra R, and Singh A (2019). Geotechnical Characterisation and Finite Element Analysis of Two Landslides Geotechnical Characterisation and Finite Element Analysis of Two Landslides along the National Highway 1-A ( Ladakh Region, Jammu, and Kashmir ). July; https://doi.org/10.1007/s12594-019-1272-z. LINK [ ]

ISRM, (2007). The complete ISRM suggested methods for rock characterization, testing and monitoring. Kazan Offset Press, Ankara, p 628. LINK [ ]

Itasca Consulting Group, Inc. (2018). FLAC2D Finite Difference Method, version 8. LINK [ ]

Jens Johansson (2014) Impact of Water-Level Variations on Slope Stability, Lulea University of Technology, MSc thesis: pp.136. LINK [ ]

Karaman, Kadir & Ercikdi, Bayram & Kesimal, Ayhan. (2013). The assessment of slope stability and rock excavatability in a limestone quarry. Earth Sciences Research Journal. 17. LINK [ ]

Kanungo D P, Pain A and Sharma S (2013). Finite element modeling approach to assess the stability of debris and rock slopes: a case study from the Indian Himalayas. Natural hazards, v .69(1), pp.1-24. LINK [ ]

Kaya A (2017) Geotechnical assessment of a slope stability problem in the Citlakkale residential area (Giresun, NE Turkey). Bull Eng Geol Environ 76(3):875–889. LINK [ ]

Kayabasi, A., (2017). The Geological Strength Index Chart Assessment for Rock Mass Permeability. Yerbilimleri, 38(3), 295-309. LINK [ ]

Kayabasi, A., & Gokceoglu, C. (2018) Liquefaction potential assessment of a region using different techniques (Tepebasi, Eskisehir, Turkey). Engineering geology, 246, 139- 161. LINK [ ]

Kazmin, V., Seifemichael Berhe, Nicoletti, M. and Petrucciani, C. (1980). Evolution of the northern part of the Ethiopian rift, 47: 275-292.

Kieffer B., Nicholas A., Henriette L., Florenece B., Delphine. B. Arnaud P., Gezahegn Yirgu, Dereje Ayalew, Dominique W., Dougal A.J, Francine K., and Claudine M., (2004). Flood and shield Basalt from Ethiopia magmas from the African super swell. Journal of petrology 45: 793-834.

Kulatilake, P. H. S. W., Park, J., & Um, J. G. (2004). Estimation of rock mass strength and deformability in 3-D for a 30 m cube at a depth of 485 m at Äspö hard rock laboratory. Geotechnical & Geological Engineering, 22(3), 313-330. Link [ ]

Kumar S., Gautam. A., (2017) Reservoir rim stability: a case study of punatsangchhu-IH.E project, Bhutan, INDOROCK 2017: 7th Indian Rock Conference 25-27. LINK [ ]

Kumar, R., Anbalagan, R. (2016). Landslide susceptibility mapping using analytical hierarchy process (AHP) in Tehri reservoir rim region, Uttarakhand. *J Geol Soc India* 87, 271–286; https://doi.org/10.1007/s12594-016-0395-8. LINK [ ]

Legesse A., & Matebie M., (2021) Rock Slope Stability and Water tightness Assessment of Arjo Didesa Dam site, Western Ethiopia, Research square.pp:31. LINK [ ]

Liu F. (2020). Stability analysis of geotechnical slope based on strength reduction method. Geotech Geol Eng. https://doi.org/10.1007/ s10706-020-01243-3. LINK [ ]

Li, X. Z., and Xu, Q. (2015). Application of the SSPC method in the stability assessment of 26 highway rock slopes in the Yunnan province of China. Bull.Eng.Geol.Env. 75(2): 551-562. doi: 10.1007/s10064-015-0792-z. LINK [ ]

Lowson, A. R. and Bieniawski, Z. T. (2013). Critical Assessment of RMR based Tunnel Design Practices: a Practical Engineer's Approach. SME, Rapid Excavation and Tunnelling Conference, Washington DC, pp 180-198.

Marinos, P., & Hoek, E., (2000) GSI: a geologically friendly tool for rock mass strength estimation. In: ISRM international symposium. International Society for Rock Mechanics and Rock Engineering. LINK [ ]

Marinos, P. & Hoek, E., (2007). Geological Strength Index (GSI). A characterization tool for assessing engineering properties for rock masses. Underground works under special conditions, 13-21. LINK [ ]

Merla, G., Abbate, E., Canuti, P., Sagri, M. & Tacconi, P. (1979). Geological map of Ethiopia and Somalia and comment with a map of major landforms (scale 1:2,000,000). Rome: Consiglio Nazionale delle Ricerche 95. LINK [ ]

Milne, D., Hadjigeorgiou, J., & Pakalnis, R., (1998). Rock mass characterization for underground hard rock mines. Tunneling and underground space technology, 13(4), 383-391. LINK [ ]

Mouyeaux A .,et al.,(2018) Probabilistic stability analysis of an earth dam by Stochastic Finite Element Method based on field data, Computers and Geotechnics, Volume 101,Pages 34-47,ISSN 0266-352X,https://doi.org/10.1016/j.compgeo.2018.04.017. LINK [ ]

Mohammadi, Mohammad; Hossaini, & Mohammad Farouq., (2017). Modification of rock mass rating system: Interbedding of strong and weak rock layers. Journal of Rock Mechanics and Geotechnical Engineering, S1674775517300240. doi:10.1016/j.jrmge.2017.06.002. LINK [ ]

Mohr, P. and Zanettin, B. (1988). The Ethiopian flood basalt province. In: Macdougall, J.D.(ed), continental flood basalts. Klwuer Academic Publishers, Dordrecht, PP 63-110. LINK [ ]

Mohr, P. (1983). Ethiopian flood basalt province, Nature 303: 577-584. LINK [ ]

Niemann, W. L. (2009). Lessons learned from rates of mud rock undercutting measured over two time periods. Environmental & Engineering Geoscience, 15(3), 117-131. LINK [ ]

Ocepek, D., (2005). New trends in rock mass characterization for designing geotechnical structures. Acta geotechnical Slovenica, 2(2), 38-51. LINK [ ]

Pain, A., Kanungo, D. P., & Sarkar, S. (2014). Rock slope stability assessment using finite element based modeling - examples from the Indian Himalayas. Geomechanics and Geoengineering, 9(3), 215–230. https://doi.org/10.1080/17486025.2014.883465. LINK

Palmstrom A, Singh R., (2001). The deformation modulus of rock masses—comparisons between in situ tests and indirect estimates. Tunnel Underground Space Technology 16(3):115–131. LINK [ ]

Palmstrom, A. (1982). The volumetric joint count—a useful and simple measure of the degree of rock mass jointing. In International Association of Engineering Geology. International congress. 4 (pp. 221-228). LINK [ ]

Priest, S.D. and Hudson, J.A., (1976). Discontinuity spacing in rocks. Int. J. Rock Mech. Min. Sci. Geomech. Abstract 13, 135–148. LINK [ ]

Qingfa Chen, Tingchang Yin, & Hangyu Jia, (2019). Selection of optimal threshold of generalized rock quality designation based on modified blockiness index, Advances in Civil Engineering, https://doi.org/10.1155/2019/1340549. LINK [ ]

Raghuvanshi TK. (2017). Plane failure in rock slopes–a review on stability analysis techniques. J King Saud Univ-Sci. LINK [ ]

Raghuvanshi TK. (2019). Governing factors influence on rock slope stability–Statistical analysis for plane mode of failure. J King Saud Univ Sci. 31(4):1254-1263 https://doi.org/10.1016/j.jksus. 2019.01.002. LINK [ ]

Read SAL, Richards LR, Perrin ND (1999) Applicability of the Hoek–Brown failure criterion to New Zealand greywacke rocks. In: Vouille G, Berest P, editors. Proceedings of the ninth international congress on rock mechanics, vol 2, Paris, pp 655–60. LINK [ ]

Rooney, T., Furman, T., Bastow, I., Dereje Ayalew, and Gezahegn Yirgu (2017). Lithospheric modification during crustal extension in the Main Ethiopian Rift. Journal of Geophysical Research: Solid Earth 1978–2012. LINK [ ]

Serafim, J.L., Pereira, J.P., (1983) Considerations of the geomechanics classification of Bieniawski. Proceedings International Symposium Engineering Geology and Underground Construction, vol. 1. Balkema, Rotterdam, pp. 1133–1142. LINK [ ]

Sharma, S., Raghuvanshi, T.K. & Anbalagan, R.(1995). Plane failure analysis of rock slopes. *Geotech Geol Eng* 13, 105–111. https://doi.org/10.1007/BF00421876. LINK [ ]

Shaz A, Chala E T, and Rao K S (2019). Rock Mass Slope Stability Analysis Under Static and Dynamic Conditions in Mumbai, India. Springer Singapore; https://doi.org/10.1007/978-981-13-0562-7. LINK [ ]

Singh, B., & Goel, R. K. (2011) Engineering rock mass classification (pp. 1755-1315). Boston: Butterworth-Heinemann. LINK [ ]

Soeters, R. & Westen, C.J. (1996). Slope instability Recognition, analysis and zonation. In: Turner, A.K., Schuster, R.L. (Eds.), Landslide: Investigations and Mitigation. Special Report, vol. 247. Transportation Research Board, National Research Council, National Academy Press, Washington, D.C. LINK [ ]

Sonmez, H., & Ulusay, R. (2002) A discussion on the Hoek-Brown failure criterion and suggested modifications to the criterion verified by slope stability case studies. Yerbilimleri, 26(1), 77-99. LINK [ ]

Tenalem A., & Barbieri, G. (2005). Inventory of landslides and susceptibility mapping in the Dessie area, northern Ethiopia. *Engineering Geology*, *77*, 1-15. LINK [ ]

Tesfaye A., (2013) Engineering Geological Characterization of Volcanic rocks of Ethiopian and Sardinian (Italy) highlands to be used as construction materials. LINK [ ]

USBR, (1987). Design of Small dams, 3rd ed., U.S. Dept. Interior, Bureau of Reclamation, water resources technical publication, U.S. Government Printing Office, Washington, D.C.

Vardakos, S.S., et al., (2007). Back-analysis of Shimizu tunnel no. 3 by distinct element modeling. Tunnel & underground, Space Technol. 22, 401–413. LINK [ ]

Vasarhelyi, B. (2008). Estimating The Poisson's Rate Value of The Rock Masses. In ISRM International Symposium-5th Asian Rock Mechanics Symposium, International Society for Rock Mechanics and Rock Engineering. LINK [ ]

Vinod B. R, et al., (2017). Some of Limit Equilibrium Method and Finite Element Method based Software are used in Slope Stability Analysis, International Journal of Application or Innovation in Engineering & Management, Vol. 6, Issue 9. LINK [ ]

Wang Lei., (2011) Application Study of FLAC in Analysis of Slope Stability, Liaoning Technical University. LINK [ ]

Wolfenden, E., Ebinger, C., Gezahegn Yirgu, Deino, A., and Dereje Ayalew., (2004). Evolution of the northern Main Ethiopian rift: birth of a triple junction. Earth and Planetary Science Letters 224(1): 213-228. LINK [ ]

Woube Wondirad. (2021). Characterization and Suitability Analysis of Embankment Material – A Case Study of Ajima Earth Dam, Central Ethiopia, Unpublished MSc Thesis, Addis Ababa University, Ethiopia, pp115.

Xing, Y., Kulatilake, P. H. S. W., & Sandbak, L. A. (2018). Investigation of rock mass stability around the tunnels in an underground mine in USA using three-dimensional numerical modeling. Rock Mechanics and Rock Engineering, 51(2), 579-597. LINK [ ]

Yang, S. Q., Chen, M., Jing, H. W., Chen, K. F., & Meng, B. (2017) A case study on large deformation failure mechanism of deep soft rock roadway in Xin'An coal mine, China. Engineering Geology, 217, 89-101. LINK [ ]

Yonathan A. et al.,(2012).Evaluating selected factors affecting the depth of undercutting in rocks subject to differential weathering, Engineering Geology, Volume 124, pp 1-11,ISSN 0013-7952,https://doi.org/10.1016/j.enggeo.2011.09.007. LINK [ ]

Zekai Şen; Bahaaeldin H. Sadagah (2003). Modified rock mass classification system by continuous rating. , 67(3-4), 269–280. doi:10.1016/s0013-7952(02)00185-0. LINK [ ]

Zhang, L. (2016). Determination and applications of rock quality designation (RQD). Journal of Rock Mechanics and Geotechnical Engineering, 8(3), 389-397. LINK [ ]

Zheng, J., et al., (2018). A new perspective for the directivity of rock quality designation (RQD) and an anisotropy index of jointing degree for rock masses. Engineering geology, 240, 81-94. LINK [ ]

# APPENDIXES -1

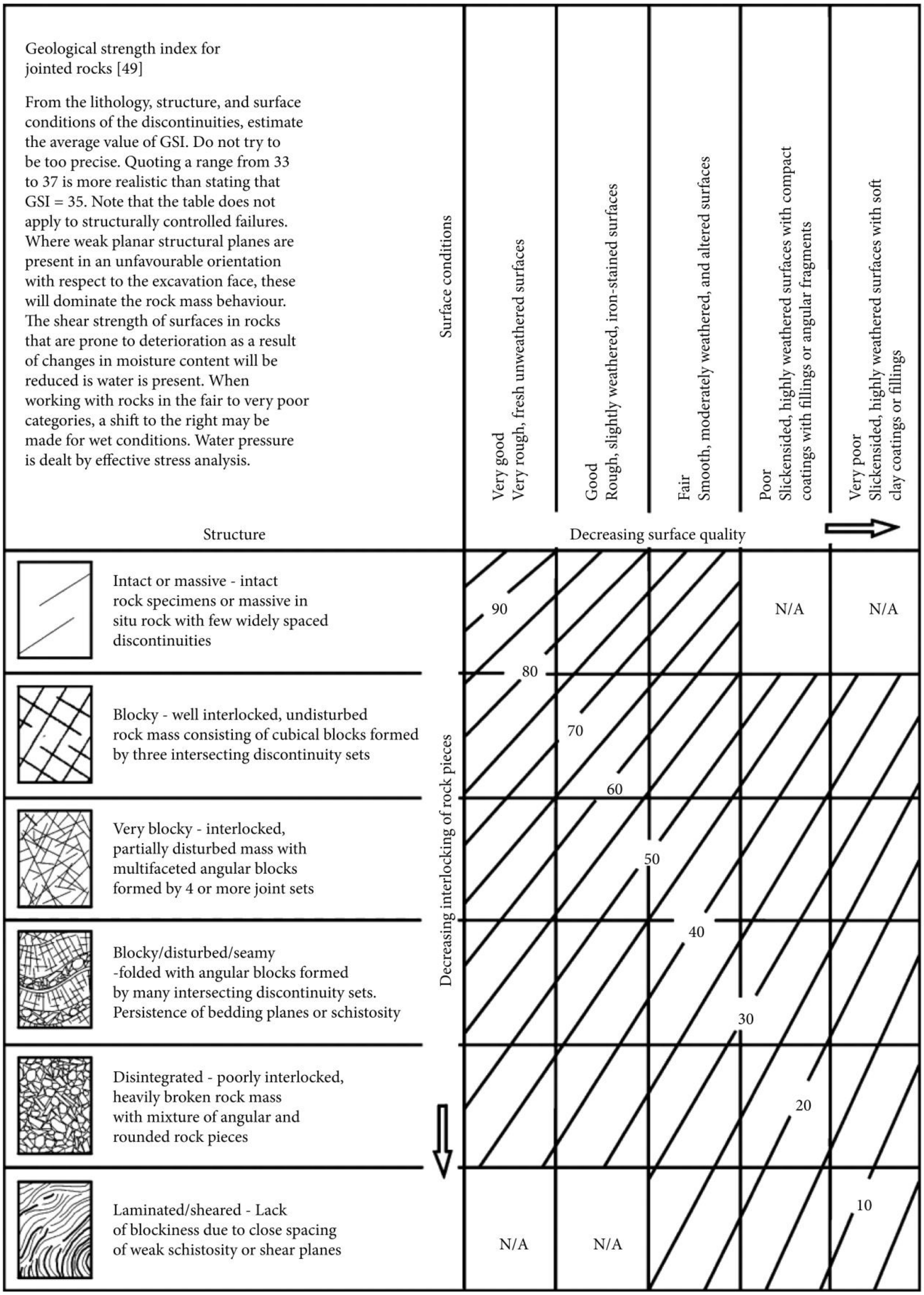

# APPENDIXES -2

| | | | | |
|---|---|---|---|---|
| CDSWC | Company Name: በኢትዮጵያ የኮንስትራክሽን ዲዛይንና ሱፐርቪዥን ሥራዎች ኮርፖሬሽን<br>Ethiopian Construction Design & Supervision Works Corporation | | | |
| Title: | Soil Unconfined Compressive Strength | Document No: OF/ECDSWC/0821 | Issue No. 1 | Page No. 2 of 3 |

**Submitted by :- Demessie Mulu**
**Project :- Thesis**
**Station :- Ajima Chacha**
**Teste Requested :- UCS**
**Reported to :- Demessie Mulu**
Customer Contact Address :- **Demessie Mulu**

| | |
|---|---|
| Test type | UCS |
| Sample type | Disturbed |
| Lab No | 1826/15 |
| Weight of sample | 120.9 |

Moisture content Determination

| | |
|---|---|
| Container No | |
| Wt of Wet Sample + Container(gm) | 120.90 |
| Wt of Dry Sample + Container(gm) | 100.30 |
| Wt. Of Can(gm) | 0.00 |
| Wt. Of Water(gm) | 20.60 |
| Wt of Dry Sample (gm) | 100.30 |
| Water Content(%) | 20.54 |

Specimen Data

| | |
|---|---|
| Dia (mm) | 38.00 |
| Length (mm) | 76.00 |
| Area, $A_0$ ($mm^2$) | 1134.26 |
| Volume, ($mm^3$) | 86203.91 |
| Bulk density($gm/cm^3$) | 1.402 |
| Dry density($gm/cm^3$) | 1.164 |
| Rate (mm/min): | 1.50 |
| (kN/div) | 0.00138 |

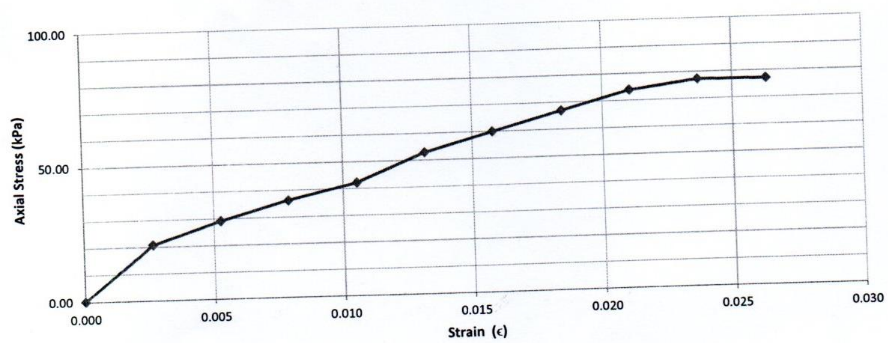


| | |
|---|---|
| UCS (Kpa) | 77.25 |

Tested by : **Mammo.H**
Lab Expert

Processed by : **Getu.M**
Geotechnical Engineer

Checked by : **Biruk.A**
Senior Geotechnical Engineer

Approved by : **Bethlehem.B.**
Geotechnical Lab S/P Manager

Please make sure that this document is the correct version before use

# APPENDIXES - 3

| | | | | |
|---|---|---|---|---|
| CDSWC | Company Name: በኢትዮጵያ የኮንስትራክሽን ዲዛይንና ሱፐርቪዥን ሥራዎች ኮርፖሬሽን<br>**Ethiopian Construction Design & Supervision Works Corporation** | | | |
| Title: **Soil Unconfined Compressive Strength** | | Document No: OF/ECDSWC/0821 | Issue No. 1 | Page No. 3 of 3 |

**Submitted by :- Demessie Mulu**
**Project :- Thesis**
**Station :- Ajima Chacha**
**Teste Requested :- UCS**
**Reported to :- Demessie Mulu**
Customer Contact Address :- **Demessie Mulu**

| | | |
|---|---|---|
| Test type | UCS | |
| Sample type | Disturbed | |
| Lab No | 1827/15 | |
| Weight of sample | 164.2 | |

Moisture content Determination

| | |
|---|---|
| Container No | |
| Wt of Wet Sample + Container(gm) | 164.20 |
| Wt of Dry Sample + Container(gm) | 132.80 |
| Wt. Of Can(gm) | 0.00 |
| Wt. Of Water(gm) | 31.40 |
| Wt of Dry Sample (gm) | 132.80 |
| Water Content(%) | 23.64 |

Specimen Data

| | |
|---|---|
| Dia (mm) | 38.00 |
| Length (mm) | 76.00 |
| Area,$A_0$ ($mm^2$) | 1134.26 |
| Volume, ($mm^3$) | 86203.91 |
| Bulk density($gm/cm^3$) | 1.905 |
| Dry density($gm/cm^3$) | 1.541 |
| Rate (mm/min): | 1.50 |
| (kN/div) | 0.00138 |

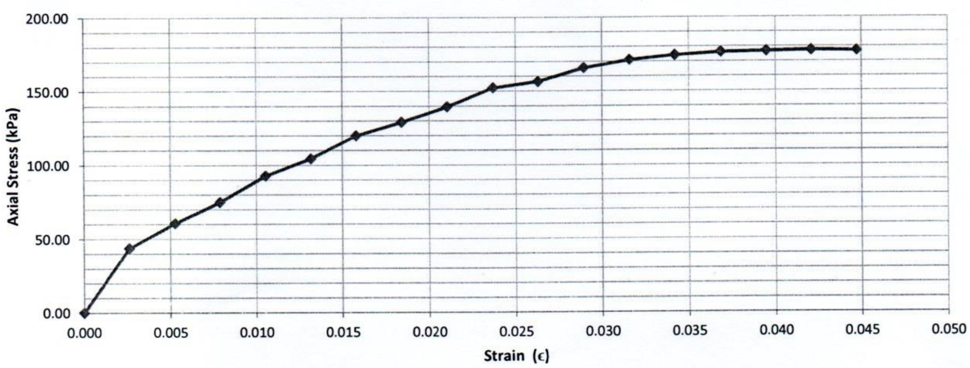


| | |
|---|---|
| UCS (Kpa) | 177.46 |

**Tested by :** **Mammo.H**
Lab Expert

**Processed by :** **Getu.M**
Geotechnical Engineer

**Checked by :- Biruk.A**
Senior Geotechnical Engineer

**Approved by : Bethlehem B.**
Geotechnical Lab T/P Manager

**Please make sure that this document is the correct version before use**

# APPENDIXES - 4

Company Name:
በኢትዮጵያ የኮንስትራክሽን ዲዛይንና ሱፐርቪዥን ሥራዎች ኮርፖሬሽን
ETHIOPIAN CONSTRUCTION DESIGN & SUPERVISION WORKS CORPORATION

ስልክ +251-11-854-7174
+251-11-827-5378
+251-11-849-4199

ፋክስ
Fax
+251-11-661-5371/61-0898
+251-11-661-0898
E-mail: info@ecdswc.com

ፖ.ሣ.ቁ: 2561
P.O.Box
A.A, Ethiopia

| Title: | Document No | Issue No. | Page No. |
|---|---|---|---|
| **Geotechnical Laboratory Testing Report** | OF/ECDSWC/ 0996 | 1 | 1 of 3 |

| | |
|---|---|
| Client Ref.:- | 'GL/171/2023 |
| Date Received:- | 29/03/2023 |
| Reported on:- | 07/04/2023 |

**Lab No.** :- 1826/15 - 1827/15
**Submitted by** :- Demessie Mulu
**Project** :- Research Thesis
**Station** :- Ajima Chacha
**Test Requested** :- As Stated Below
**Reported to** :- Demessie Mulu
**Customer Contact Address:-** Demessie M.

| No. | Testing Date | Test Type | Standard Method | Soil Samples Test Results | |
|---|---|---|---|---|---|
| | | | | Lab. No. :- 1826/15 Sample Id.:- Tuff Depth (m):- Surface | Lab. No. :- 1827/15 Sample Id.:- Clay Depth (m):- Surface |
| 1 | 05/04/2023-07/04/2023 | Direct Shear | ASTM D3080 | | |
| | | C (Kpa) | | 13.33 | 28.67 |
| | | Φ(Degree) | | 34.21 | 12.13 |
| 2 | | UCS (Kpa) | ASTM D2166 | 77.25 | 177.46 |

**REMARK:-** The samples were collected & submitted to the laboratory by student.
:- Sample results relate only to items tested.
:- Samples were remolded by client requirement.

Processed by :- Getu M.
Geotechnical Engineer

Checked By :- Biruk A.
Senior Geotechnical Engineer

Approved By :- Bethelhem B.
Geotechnical Lab S/P Manager

Ethiopian Construction Design & Supervision Works Corporation CDSWC Laboratory Research & Training Center

Among the major services rendered by the Geotechnical and Material Laboratory Testing s/processes of Ethiopian Construction Design & Supervision Works Corporation are:
- *In **Geotechnical Laboratory**:-Testing the engineering properties of Soil Mechanics and Rock Mechanics.*
- *In **Material Testing Laboratory**:- Testing the engineering properties of various Construction materials, such as Aggregates, Asphalts/Bitumen/, Cements, Rocks, Water, Reinforcement steel bars, Hollow Blocks, Bricks, Ceramics, Tiles,Asphalt & Concrete Core Tests, Concrete Mix Designs, Asphalt Mix Designs, Sampling of the soil and construction materials, and so on.*

Please make sure that this document is the correct version before use.

# APPENDIXES - 5

| Client: FDRE Irrigation Development Commission | Consultant: Amhara Design and Supervision Works Enterprise | Contractor: Amhara Water Works Construction Enterprise |
|---|---|---|

PROJECT : Ajima Chacha Irrigation Dam project

| | | | |
|---|---|---|---|
| | | Sub project name | Ajima Chacha Earth fill dam |
| Purpose: | | Reported Date : | |
| Sample source : | | Date Sampling | |
| | | | |

Stone COMPRESSIVE STRENGTH TEST RESULT (rock)

| Codes of stone | Dimension of stone (mm) L | W | H | Area of compressing face(mm2) | Mass(gm) | max-lod at failure(KN) | Correction factor (KN) | Corrected max load at failure | Unit Weight (g/cc) | Compressive Strength (Mpa) |
|---|---|---|---|---|---|---|---|---|---|---|
| Stone1 | 13 | 8 | 9 | 104 | 1416 | 54.00 | 1.026 | 55.03 | 0.03 | 52.91 |
| Stone2 | 13 | 6 | 7 | 78 | 1353 | 58.30 | 1.101 | 59.40 | 0.02 | 76.16 |
| Stone3 | 13 | 12 | 4 | 156 | 677 | 14.10 | 0.266 | 14.37 | 0.05 | 9.21 |
| | | | | | | | | Average(Mpa) = | 0.03 | 46.09 |

| | | Consultant | |
|---|---|---|---|
| | | Test by: Demessie M. | Approved By: ADAMU.M |
| | | Sign : | Sign : |
| | | Date : | Date : 12-07-15 |

Nigus K

Amhara Water works Construction Enterprise Ajima Chacha Dam & Irrigation Project (lot 1 & 3)

Competence Design & Supervision Corporation CDSC

# APPENDIXES - 6

| Client: FDRE Irrigation Development Commission | Consultant: Amhara Design and Supervision Works Enterprise | Contractor: Amhara Water Works Construction Enterprise |
|---|---|---|

PROJECT : Ajima Chacha Irrigation Dam project

| | |
|---|---|
| | Sub project name |
| Purpose: | Reported Date : |
| Sample source : | Date Sampling |

Stone COMPRESSIVE STRENGTH TEST RESULT (rock)

| Codes of stone | Dimension of stone (mm) L | w | H | Area of compressing face(mm2) | Mass(gm) | max-lod at failure(KN) | Correction factor (KN) | Corrected max load at failure | Unit Weight (g/cc) | Compressive Strength (Mpa) |
|---|---|---|---|---|---|---|---|---|---|---|
| Stone1 | 16 | 6 | 5 | 96 | 1004 | 54.00 | 1.026 | 55.03 | 0.03 | 57.32 |
| Stone2 | 15 | 10 | 6 | 150 | 866 | 2.00 | 0.0378 | 2.04 | 0.04 | 1.36 |
| Stone3 | 12 | 9 | 4 | 108 | 677 | 14.00 | 0.264 | 14.26 | 0.03 | 13.21 |
| | | | | | | | | Average(Mpa) = | 0.03 | 23.96 |

| Consultant | |
|---|---|
| Test by: Demessie M. | Approved By: ADANE |
| Sign : | Sign : |
| Date : | Date : 12-07-15 |

Nigus F.

# APPENDIXES -7

**Field traverse GPS location along the reservoir slope of Ajima Chacha dam site**

| Station ID | Easting | Northing | Elevation | Lithology |
|---|---|---|---|---|
| Location- 1 | 558191 | 1048377 | 2842 | MW tuff |
| Loc2 | 558208 | 1048385 | 2843 | MW tuff |
| Loc3 | 558265 | 1048418 | 2842 | MW tuff |
| Loc4 | 558372 | 1048453 | 2840 | MW tuff |
| Loc5 | 558335 | 1048649 | 2824 | MW tuff |
| Loc6 | 558246 | 1048724 | 2843 | MW tuff |
| Loc7 | 558120 | 1048663 | 2847 | MW tuff |
| Loc8 | 558165 | 1048723 | 2855 | MW tuff |
| Loc9 | 558334 | 1048845 | 2842 | MW tuff |
| Loc10 | 558276 | 1049173 | 2855 | MW tuff |
| Loc11 | 558655 | 1049198 | 2849 | MW Tuff |
| Loc12 | 559045 | 1049558 | 2845 | MW tuff |
| Loc13 | 559066 | 1049565 | 2832 | MW tuff |
| Loc14 | 558425 | 1048029 | 2856 | MW tuff |
| Loc15 | 558433 | 1047929 | 2863 | MW tuff |
| Loc16 | 558409 | 1047709 | 2844 | MW tuff |
| Loc17 | 558567 | 1047503 | 2866 | Fractured rhyolite |
| Loc18 | 558847 | 1047552 | 2852 | Fractured rhyolite |
| Loc19 | 558850 | 1047602 | 2840 | Fractured rhyolite |
| Loc20 | 558853 | 1047571 | 2846 | Fractured rhyolite |
| Loc21 | 559215 | 1047509 | 2846 | Fractured rhyolite |
| Loc22 | 559228 | 1047587 | 2832 | Fractured rhyolite |
| Loc23 | 559536 | 1047723 | 2846 | Fractured rhyolite |

| | | | | |
|---|---|---|---|---|
| Loc24 | 559507 | 1047945 | 2827 | Fractured rhyolite |
| Loc25 | 559880 | 1048542 | 2855 | Fractured rhyolite |
| Loc26 | 560084 | 1048706 | 2838 | Fractured rhyolite |
| Loc27 | 559908 | 1048953 | 2846 | Fractured rhyolite |
| Loc28 | 559481 | 1049059 | 2892 | Fractured rhyolite |
| Loc29 | 559388 | 1048839 | 2896 | Fractured rhyolite |
| Loc30 | 559304 | 1048478 | 2904 | Fractured rhyolite |
| Loc31 | 559286 | 1048422 | 2886 | Fractured rhyolite |
| Loc32 | 559206 | 1048291 | 2858 | Fractured rhyolite |
| Loc33 | 559045 | 1048285 | 2838 | Fractured rhyolite |
| Loc34 | 559020 | 1048271 | 2827 | alluvial soil |
| Loc35 | 559186 | 1048175 | 2818 | alluvial soil |
| Loc36 | 559202 | 1047976 | 2828 | alluvial soil |
| Loc37 | 559204 | 1047963 | 2825 | MW tuff |
| Loc38 | 559230 | 1047944 | 2826 | MW tuff |
| Loc39 | 559145 | 1047949 | 2856 | MW tuff |
| Loc40 | 559189 | 1047 | 2842 | MW tuff |
| Loc41 | 559056 | 1047862 | 2858 | MW tuff |
| Loc42 | 558273 | 1048551 | 2825 | MW tuff |
| Loc43 | 558092 | 1048574 | 2826 | MW tuff |
| Loc44 | 558189 | 1048348 | 2855 | MW tuff |
| Loc45 | 558090 | 1048416 | 2838 | MW tuff |
| Loc46 | 557823 | 1048734 | 2840 | MW tuff |
| Loc47 | 557860 | 1048830 | 2840 | Fractured rhyolite |
| Loc48 | 557909 | 1048956 | 2840 | Fractured rhyolite |